Novel Pipe Configuration for Enhanced Efficiency of Vertical Ground Heat Exchanger (VGHE)

by

Adel Eswiasi

B.Sc., Sabratha University, Libya, 1998

M.Sc., University of Tripoli, Libya, 2008

A Dissertation Submitted in Partial Fulfillment of the Requirements for the Degree of

DOCTOR OF PHILOSOPHY

in the Department of Mechanical Engineering

University of Victoria

Supervisory Committee

Novel Pipe Configuration for Enhanced Efficiency of Vertical Ground Heat Exchanger (VGHE)

by

Adel Eswiasi

B.Sc., Sabratha University, Libya, 1998

M.Sc., University of Tripoli, Libya, 2008

Supervisory Committee

Dr. Phalguni Mukhopadhyaya, Co-Supervisor

(Department of Civil Engineering)

Dr. Andrew Rowe, Co-Supervisor

(Department of Mechanical Engineering)

Dr. Rishi Gupta, Outside Member

(Department of Civil Engineering)

ABSTRACT

In this research, a novel U-Tube pipe configuration, consisting of a single U-Tube pipe with two outer fins, was proposed to enhance the thermal efficiency of the vertical ground heat exchanger (VGHE). The ground thermal behavior at and around the VGHE were studied for both conventional single U-Tube and novel U-Tube pipe configurations. The effects of different grout materials and heat injection rates were also studied for the novel U-Tube pipe configuration. To demonstrate superior thermal efficiency, the obtained temperature data from thermal response tests (TRTs) for the novel U-Tube pipe configuration were compared with the result obtained from the conventional single U-Tube pipe configuration.

A small-scale experimental apparatus was designed and built for this research project, including a water supply system, a sand tank, and a data acquisition system to conduct TRTs with various pipe configurations, grout materials, and heat injection rates. The line source model was used in this research to estimate the ground thermal properties.

Two TRTs were conducted for the VGHE with the conventional single U-Tube pipe and with the novel U-Tube pipe configuration, respectively, to find out which pipe configuration had a superior heat transfer rate. The results show the differences between the inlet and outlet water temperatures are 0.4 °C for the conventional single U-Tube pipe configuration, and 0.7 °C for the novel U-Tube pipe configuration, after 60 hours, indicating a superior heat injection rate for the novel U-Tube pipe configuration.

The results indicate that the effective ground thermal conductivity for the novel U-Tube pipe configuration is 4.85 W/ m. K, which is 23.6% higher than that of the conventional single U-Tube pipe configuration. The borehole thermal resistance for the novel U-Tube pipe configuration was 0.680 m. K/ W, which is 29.2% lower than that of the conventional single U-Tube pipe configuration.

The results show that the temperature at the borehole wall had increased by 4.87 °C when the novel U-Tube pipe configuration was used. With the novel U-Tube pipe configuration, at 45 cm radial distance from the center of the borehole and at different depths, the highest temperature had increased by 0.54 °C more than the conventional single U-Tube at a depth of 35 cm from the

top of the sand tank. These observations indicate higher heat injection in the ground when the novel U-Tube pipe configuration was used.

Four TRTs were also conducted in the laboratory to investigate the impacts of grout materials (bentonite and silica sand) and heat injection rates on the thermal efficiency of the novel U-Tube pipe configuration. The results show that the difference between the inlet and outlet water temperatures of the VGHE with silica sand was higher than the VGHE with bentonite as grout, i.e. the borehole thermal resistance for the novel U-Tube pipe with silica sand as grout to be less than that with bentonite as grout. The heat exchange rate also increased with an increase in the inlet water temperature entering to the VGHE.

Based on the experimental results, when the novel U-Tube pipe configuration is used, the number of boreholes required for the conventional single U-Tube is decreased by about 58%, which will in turn decrease the installation and material costs.

Contents

List of Tables

List of Figures

Nomenclature

Acronyms	**Description**
ACWT	Average Circulating Water Temperature
ASHP	Air Source Heat Pump
BHE	Borehole Heat Exchanger
CFD	Computational Fluid Dynamics
COP	Coefficient Of Performance
DTRT	Distributed Thermal Response Test
GHE	Ground Heat Exchanger
GPM	Geothermal Properties Measurement
GSHP	Ground Source Heat Pump
HDPE	High-density polyethylene
LSM	Line Source Model
PCM	Phase Change Material
PVC	Polyvinylchloride
PFA	Pulverized Fuel Ash
TRT	Thermal Response Test
UTES	Underground Thermal Energy Storage
VGHE	Vertical Ground Heat Exchanger

Symbols	**Description**
C_p	Specific heat capacity (J/ kg. K)
d	Borehole diameter (m)
D_{eq}	Equivalent diameter of the pipe (m)
D_g	Outside diameter of the grout material (m)
$D_{p,i}$	Inside diameter of the pipe (m)
$D_{p,o}$	Outer diameter of the pipe (m)
E_1	Exponential integral
H	Boreholes depth (m)

h_i	Convective heat transfer coefficient (W/ m^2. K)
$I_v(x)$	Modified Bessel function of I kind
$K_v(x)$	Modified Bessel function of II kind
L	Fin length (m)
L_g	Grout thickness (m)
L_s	Distance between the center of two U-tube pipes (m)
m	Slope
P	Perimeter (m)
$\dot{m}$	Mass flow rate (kg/ s)
P_r	Prandtl number
Q	Heat injection rate (W)
q	Heating rate per borehole length (W/ m)
q_{fin}	Heat transfer through the fin (W
R_e	Reynolds number
R_b	Borehole thermal resistance (m. K/ W)
R_g	Grout thermal resistance (m. K/ W)
R_f	Fluid thermal resistance (m. K/ W)
R_p	Pipe thermal resistance (m. K/ W)
r_b	Borehole radius (m)
r_i	Inner radius pipe (m)
r_o	Outer radius pipe (m)
t	Time (s)
T	Temperature (ºC)
T_b	Temperature on the borehole wall (ºC)
$T_f\ (t)$	Mean fluid temperature (ºC)
T_g	Grout temperature (ºC)
T_{in}	Inlet of the fluid temperature (ºC)
T_{out}	Outlet of the fluid temperature (ºC)
T_o	Initial ground temperature (ºC)
$\mathrm{T}(r,t)$	Temperature in point (x, y, z) at time t (ºC)

Greek letters	**Description**
α	Thermal diffusivity (m^2/ s)
ρ	Density (kg/ m^3)
γ	Euler's constant
λ	Thermal conductivity (W/ m. K)
θ	Temperature difference (ºC)
λ_{eff}	Effective ground thermal conductivity (W/ m. K)
λ_f	Thermal conductivity of fluid (W/ m. K)
λ_{fin}	Thermal conductivity of fin material (W/ m. K)
λ_g	Thermal conductivity of grout material (W/ m. K)
λ_p	Pipe thermal conductivity (W/ m. K)
τ	Fin width at the base (m)
ω	Fin thickness [depth] (m)

Acknowledgements

I would like to express my deepest gratitude to everyone who helped throughout my stay here at the University of Victoria.

I am thankful to my supervisor, Dr. Phalguni Mukhopadhyaya, who gave me an opportunity to conduct research. Dr. Mukhopadhyaya has continuously conveyed a passion for research and excitement for teaching. Without his guidance and persistent help this dissertation would not have been possible.

I would also like to thank my committee members Dr. Andrew Rowe (co-supervisor), Dr. Rishi Gupta (outside member), and Dr. Mario A. Medina (external examiner) for their support and comments which helped me to understand the subject matter and its importance.

I would like to show my deep gratitude to my family here, and my parents and son in my home country. They have guided and supported me in all aspects of my life. A special thanks to my brothers and all my dear friends who have been supporting me throughout my life with their love, and encouragement.

Finally, I would like to acknowledge the financial support (postgraduate scholarship) I received from the Libyan Ministry of Education for my graduate study in Canada.

Chapter 1

Introduction

This chapter outlines the impacts of fossil fuel based energy generation on the environment and presents the problem description for this dissertation. Thereafter, the objectives and expected contributions of this dissertation are mentioned. In addition, the organization of the dissertation is also described. Finally, the published/under review papers are presented at the end of this chapter.

1.1 Background

Excessive fossil fuel-based energy consumption, due to rapid global development and population growth, has caused environmental damages, global warming and increased the cost of space conditioning in built environment. As a result, researchers around the word are searching for other energy sources which are economical and have the potential to reduce environmental damages. Fossil fuels include coal, oil, gasoline, diesel, and natural gas, and the world depends on these resources for energy production. One of the most significant damages resulting from the use of fossil fuel-based energy is environmental pollution, which results from the combustion of fossil fuels. Another problem is the increase of carbon dioxide emissions in the atmosphere, which contributes to an increase in global warming. In recent years, renewable energies such as solar, wind, ocean, and geothermal are used as clean energies to decrease pollution in the atmosphere. These renewable energies are environment friendly and have less carbon dioxide emissions than other conventional energy sources. The energy generated and/or stored in the Earth (i.e. ground) is called geothermal energy. Geothermal energy is used to produce electricity and heat. Geothermal resources are divided into three different temperatures: high, moderate, and low [1, 2]. Ground source heat pump (GSHP) is used to transfer the thermal energy between the ground and buildings for the purpose of heating and cooling. GSHP consists of a heat pump and a ground heat exchanger (GHE). GHE is a critical component of GHSP that captures heat from and/or dissipate heat to the ground. GHEs can be classified into two types: open and closed systems. GSHPs have three

advantages compared to air source heat pumps (ASHPs[1]). First of all, ASHPs need to be defrosted in winter, unlike GSHPs. GSHPs use water as a heat carrier fluid, which has more suitable heat transfer capacity for this application than air which is used in ASHPs. Another advantage is the constant ground temperature over the year and it is closer to the comfort temperature for human compared to the outside air temperature, which changes significantly depending on the season [3]. The US Environmental Protection Agency reported that the energy consumption and greenhouse gas emission were reduced 44% by using GSHP systems compared to using the ASHP systems, and 72% compared to using standard air-conditioning equipment for heating/cooling of buildings [4].

The ground temperature is approximately constant at depths of 5 to 10 meters, and it is near to the average ambient temperature. GSHP technology exploits the constant ground temperature over the year to extract the heat from buildings and transfer the heat into the ground in summer, as well as to extract the heat from the ground and transfer it into the buildings in winter [5]. GSHPs can be of two types: open and closed systems. In closed systems, there are three types of GHEs, vertical, horizontal, and pond. Recently, vertical ground heat exchangers (VGHEs) are preferred to connect with heat pumps for the GSHP applications because the VGHEs require a small area and have a stronger efficiency. GSHPs is considered as an effective technology to increase the thermal performance and decrease the energy consumption, particularly in building applications. However, designers are still working to improve the design of GSHP with the aim to decrease the installation cost and increase the thermal performance of the GHEs. Due to crude oil predicament in the early 1970's, Europe and North America began scientific search and empirical study about GSHPs. Significant experimental investigations were done to create standard and design methods for VGHEs [6]. More recently, the focus on renewable energy and net-zero constriction practices have increased the research activities related to GSHP. This study focuses on the innovative techniques to enhance heat exchange efficiency of VGHEs.

[1] ASHPs draw heat from the outside air during the winter (i.e. heating season) and reject heat to outside during the summer (i.e. cooling season).

1.2 Problem description

Finding ways to reduce installation cost and optimize the depth of the vertical ground heat exchangers (VGHEs) are among the most important challenges for designers of the ground source heat pumps (GSHPs). Increased depth of the borehole leads to an increase in the installation and material costs, while decreasing the length below the required depth results in the inability to obtain the target fluid temperature. It is very important to predict the accurate temperature of the fluid entering the heat pump in order to design the VGHE. Overall, two types of thermal processes occur in and around the borehole during the heat injection or extraction in the VGHEs. The ground temperature changes rapidly at the borehole. However, it changes relatively slowly around and away from the borehole.

Several past studies focused on improving the thermal performance of VGHEs by inserting different pipe configurations in the borehole. However, there exists further opportunities for researchers to develop new pipe configurations to increase the heat transfer rate in the VGHEs and increase the coefficient of performance of GSHP.

1.3 Objectives

The main objective of this research is to improve the thermal performance of VGHEs. In order to do that a new pipe configuration will be used to increase the heat transfer rate between the ground and the VGHE and decrease the length of the borehole. Also, the heat transfer rates in and outside the borehole will be studied to understand overall heat transfer characteristics of the ground. In addition, the effects of different grout materials and heat injection rates on the thermal efficiency of VGHE will be investigated.

1.4 Expected contributions

Various researchers conducted several studies to improve the thermal performance of VGHEs. A comprehensive literature search was carried out on ways of improving the thermal performance of VGHEs. According to the published literature, several parameters have an impact on the thermal

performance of GSHP systems. However, there is always scope to do more work in this area and suggest a new pipe configuration to increase the heat transfer rate in the VGHEs.

One way to increase the heat transfer rate in VGHEs is to increase the surface area of the pipe configuration. This study suggests addition of two fins in two directions of the outer side of the conventional single U-Tube pipe to increase the heat transfer surface area. The main contributions of this study are:

1) Improvement of thermal performance of VGHEs and decrease the borehole depth, resulting in reduction of installation and material costs.
2) Reduction of installation and material costs would increase the market penetration of GSHP in the building construction sector.
3) Reduction in the consumption of fossil fuels, followed by a reduction in carbon dioxide emission in the environment.

1.5 Organization of the dissertation

This dissertation is organized in seven chapters as outlined below:

Chapter 1 explains the background, problem description, objectives, expected contributions, organization of the dissertation, and publications.

Chapter 2 reviews the efficiency of GHEs in heat pump systems. The main focus of this chapter is to review how different construction and operation parameters (e.g., pipe configuration, pipe diameter, grout, heat injection rate, and volumetric flow rate) impact the thermal efficiency of the vertical ground heat exchanger (VGHE) in a ground source heat pump (GSHP) system. The published literature indicates that thermal performance of VGHEs increases with an increase of borehole diameter and/or pipe diameter. The literature shows that the borehole thermal resistance of VGHEs decreases within a range of 9% to 52% to pipe configurations and grout materials. Furthermore, this chapter also identifies the scope to increase the thermal efficiency of VGHE. The chapter concludes that in order to enhance the heat transfer rate in VGHE, any attempt to increase the surface area of the pipe configuration would likely be an effective solution.

Chapters 3 presents the methodology and it is divided into the thermal response test (TRT) and line source theory. The thermal response test contains the principles and procedures of the TRT, including an estimation of the initial ground temperature, measuring the flow rate, the heat input rate, and the period of the test for VGHEs. This chapter also reviews the derivation of the line source theory that is used to determine the ground thermal properties.

Chapters 4 describes a small-scale experimental apparatus established in the laboratory. The experimental apparatus consists of three main parts: (i) a water supply system, (ii) a sand tank, and (iii) a data acquisition system. The aim of the apparatus was to conduct thermal response tests (TRTs) to characterize the performance of VGHE.

Chapters 5 is divided into two parts. Section 5.1 compares the obtained results from the proposed U-Tube pipe configuration and the conventional single U-Tube pipe configuration, based on the heat exchange rate and the ground thermal properties. Section 5.2 discusses how the ground temperature changed at the borehole wall and around the VGHE during the heat injection and recovery time for the two pipe configurations.

Chapters 6 estimates the effects of two different parameters (two grout materials, and two heat injection rates) on the thermal efficiency of the novel U-Tube pipe configuration. In this chapter, two different grout materials (bentonite and silica sand) and two different inlet water temperatures (50 °C and 60 °C) were used to evaluate the influence of these parameters on the thermal efficiency of the novel U-Tube pipe configuration.

Chapters 7 presents the main observations and conclusions. The suggestions for future research are also provided at the end of this chapter.

1.6 Publications

During writing this dissertation, three chapters from the dissertation have been prepared for publications.

Paper 1 (Published).

Based on Chapter 2 and published in MDPI Journal, Clean Technol. 2020, 2(2), 204-224; https://doi.org/10.3390/cleantechnol2020014, 9 Jun 2020.

Paper 2 (Draft Under Review)

Based on Chapter 5.1: A Novel U-Tube Pipe Configuration for Enhanced Efficiency of Vertical Ground Heat Exchanger.

Paper 3 (Draft Under Review)

Based on Chapter 6: The Influence of Grout Materials and Heat Injection Rate on Thermal Performance of Vertical Ground Heat Exchangers with Novel U-Tube Pipe Configuration.

Note: The number of references in the Chapters does not reflect the number of references in the papers but the number of references in the bibliography.

Chapter 2

Critical review of efficiency of ground heat exchangers in heat pump systems

Abstract

Use of ground source heat pumps has increased significantly in recent years for space heating and cooling of residential houses and commercial buildings, in both heating (i.e., cold region) and cooling (i.e., warm region) dominated climates, to its low carbon footprint. Ground source heat pumps exploit the passive energy storage capacity of the ground for space heating and cooling of buildings. The main focus of this chapter is to review how different construction and operation parameters (e.g., pipe configuration, pipe diameter, grout, heat injection rate, and volumetric flow rate) have an impact on the thermal efficiency of the vertical ground heat exchanger (VGHE) in a ground source heat pump (GSHP) system. The published literature indicates that thermal performance of VGHEs increase with an increase of borehole diameter and/or pipe diameter. The literature shows that the borehole thermal resistance of VGHEs decreases within a range of 9% to 52% to pipe configurations and grout materials. Furthermore, this chapter also identifies the scope to increase the thermal efficiency of VGHE. It was concluded that in order to enhance the heat transfer rate in VGHE, any attempt to increase the surface area of the pipe configuration would likely be an effective solution.

2.1 Introduction

In a world under climate change emergency, the importance of eco-friendly renewable energy as a replacement of fossil fuel based energy cannot be overemphasized. Residential and commercial buildings are considered to be the main consumers of energy in the world, which are responsible for 15% to 30% of the total world energy consumption. Also 15% to 30% of the total

greenhouse gases is produced and emitted to the environment due to fossil fuel combustion [7]. Geothermal energy can be used to produce electricity and heat. Geothermal energy resources are divided into three different categories: (i) high temperature (> 150 °C) resources used to produce electricity, (ii) moderate temperature (< 150 °C) resources used for direct applications, and (iii) low temperature (< 32 °C) resources used to support heat pumps for space heating and cooling buildings [2]. Geothermal is considered as the fifth biggest source of renewable energy and is available across the world [8, 9]. Ground source heat pump (GSHP) systems, consisting of heat pumps and ground heat exchangers, is a source of renewable energy in both cold and warm climates. This technology is employed to extract the heat from buildings in summer and transfer into the ground, as well as in winter to extract the heat from the ground and transfer into the buildings. Ground source heat pump systems can be equipped with two types of ground heat exchangers: (i) Vertical, and (ii) Horizontal. Vertical ground heat exchangers have many advantages over horizontal ones, such as higher energy efficiency and a much smaller area required for installation. However, both vertical and horizontal systems provide a clean energy exchange operation that exploits the thermal energy storage capacity of the underground soil and reduces or eliminates the fossil fuel-based energy consumption in buildings. The amount of heat transferred between the heat carrier fluid and ground determines the efficiency of the ground source heat pump systems. Various researchers used analytical, experimental, and numerical studies to devise ways for improving the heat transfer rate between the VGHE and the ground. The aim of this chapter is to review the published literature on various options, including pipe configurations, to improve the efficiency of ground heat exchangers.

2.1.1 Research background

A ground source heat pump system consists of a heat pump and one or multiple borehole ground heat exchangers that are coupled together to transfer the thermal energy between the ground and buildings as shown in Figure 2.1. The heat pump consists of five major components, including a compressor, an expansion valve, two heat exchangers (evaporator and condenser), and a reversing valve. In addition, there are other accessories, for example pipes, a fan in the air heat exchanger (condenser), and controls [10]. In heating dominated climates, the evaporator heat exchanger is coupled with the vertical ground heat exchanger to exchange the heat while the condenser heat

exchanger exchanges heat with space. Ground heat exchangers generally consist of two types: (1) Open, and (2) Closed systems.

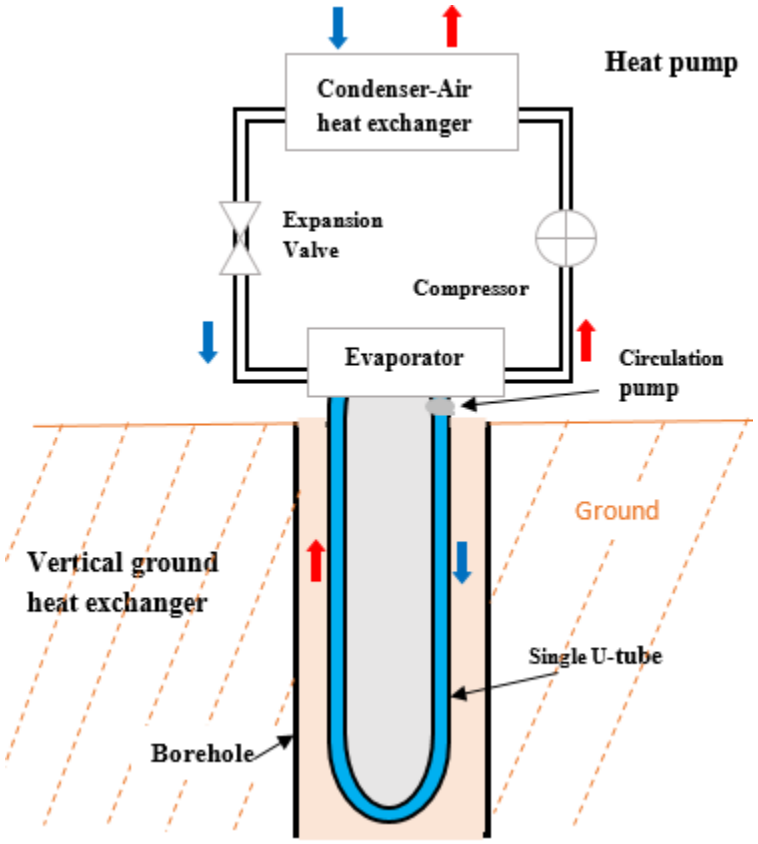

Figure 2.1: Ground source heat pump system (in heating –dominated climate)

- **Open system**

The open system uses a heat source, such as a well, lake, or river as a ground heat exchanger. The groundwater is pumped into the heat pump to exchange the heat and then the groundwater returns to the ground as shown in Figure 2.2.

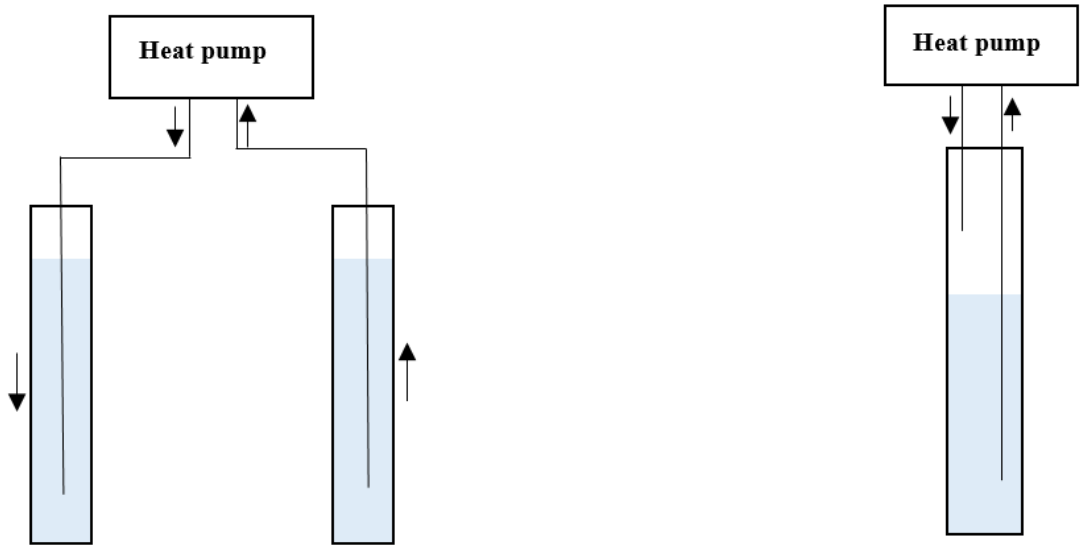

Figure 2.2 Ground schematics of different open ground heat exchanges

- **Closed system**

The closed system can also use heat source, such as a well, lake, or river, as a ground heat exchanger. However, in a closed system, the heat carrier fluid is circulated through a close-loop ground heat exchanger to transfer the thermal energy between the ground and the heat pump unit (Figure 2.3). There are three types of ground heat exchangers (horizontal, vertical, and pond/lake) as shown in Figure 2.3. Figure 2.4 shows the cross section of the commonly used vertical heat exchanger designs.

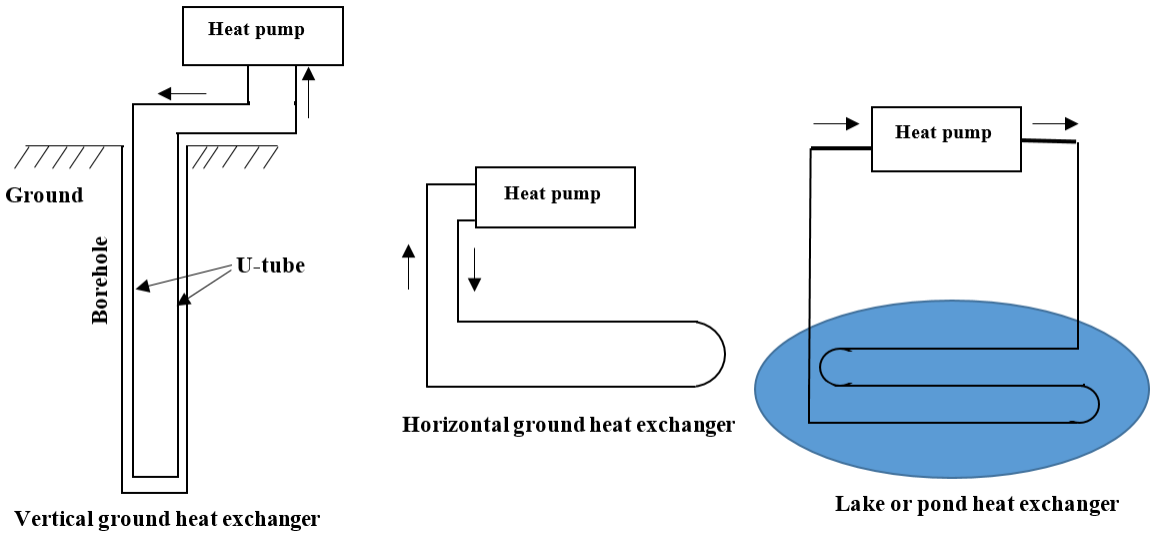

Figure 2.3: Schematics of different closed ground heat exchanges [11]

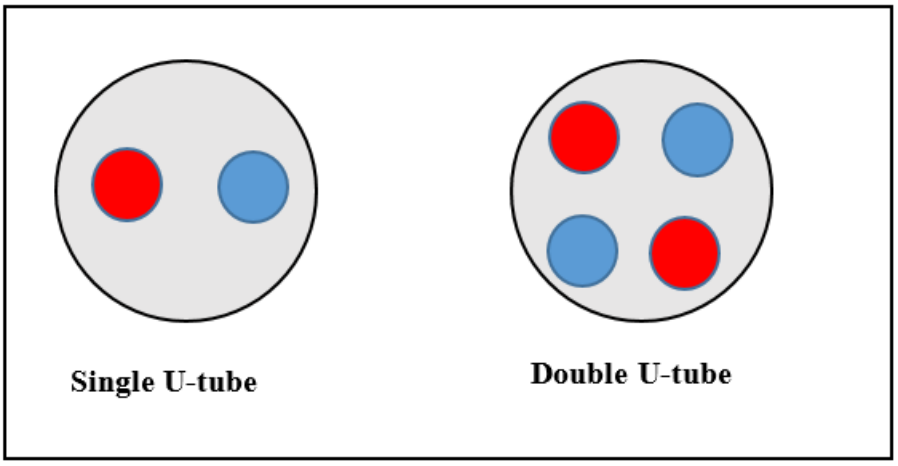

Figure 2.4: Cross section of the commonly used vertical heat exchanger designs

- **Borehole thermal resistance**

A heat exchanger inserted into a vertical or horizontal borehole is termed a borehole heat exchanger, and borehole thermal resistance is an important parameter for both steady state and transient heat transfer analysis. The borehole thermal resistance is a function of the mean temperature of the heat carrier fluid in the legs of the U-Tube and the borehole wall temperature. The steady state thermal resistance of the borehole can be defined by the equation 2.1 [12]:

$$q = \frac{(T_f - T_b)}{R_b} \qquad \textbf{(2.1)}$$

Where T_f is the mean temperature of the heat carrier fluid in the legs of the U-Tube (ºC), T_b is the temperature on the borehole wall (ºC), R_b is the borehole thermal resistance (m. K/ W), and q is a specific heat rate (heat transfer rate per unit length of borehole) (W/ m).

The borehole heat exchanger consists of three components: (1) fluid, (2) pipe, and (3) grout material, as shown in Figure 2.5. The borehole resistance can be expressed as shown in the equation 2.2:

$$R_b = R_f + R_p + R_g \qquad \textbf{(2.2)}$$

Where R_f is fluid thermal resistance (m. K/ W), R_p is pipe wall thermal resistance (m. K/ W), and R_g is grout thermal resistance (m. K/ W).

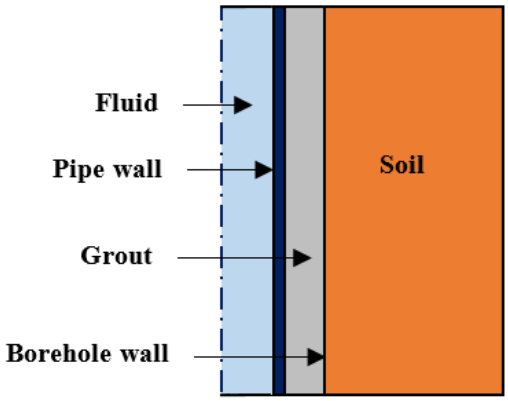

Figure 2.5: Thermal resistance in borehole ground heat exchanger

- **Thermal response test**

Thermal response test (TRT) is the most widely used method to assess the influence of ground properties (e.g., thermal conductivity of the underground soil, thermal resistance of the borehole, etc.) on the performance of the borehole ground heat exchanger [13–16]. In this method, the inlet (T_{in}) and outlet (T_{out}) fluid temperature data are analyzed. The first thermal response test in the field was performed to estimate the thermal resistance of the heat carrier fluid and the borehole wall, and thermal conductivity of the ground [13]. A first mobile thermal response test device was constructed at the Lulea University of Technology, Sweden [14]. In 1996, they also developed a mobile response test device to estimate the thermal conductivity of the ground as well as the impact of natural convection and flow of the groundwater in the boreholes. A similar experimental device

was developed at the Oklahoma State University to estimate the ground thermal properties [15]. In 2000, the first field thermal response test was performed in Germany [16].

2.2 Literature review

Various researchers conducted studies to understand the ground heat transfer behavior in and around the vertical ground borehole heat exchangers. These research studies (numerical and experimental (including laboratory and field studies)) focus on a number of issues related to the measurement and analysis of performance of ground heat exchangers, and could be broadly classified into four different categories:

- Effects of grout materials on the thermal performance of ground heat exchangers.
- Influence of different pipe configurations on the thermal performance of ground heat exchangers
- Effects of borehole depths and diameters on the thermal performance of ground heat exchangers.
- Miscellaneous issues related to performance of ground heat exchangers (e.g., ground heat transfer characteristics calculation methods; recovery time; performance in arctic/cold climate etc.)

2.2.1 Effects of grout materials on the thermal performance of ground heat exchangers

Laboratory and field studies were performed to determine how several variables such as grout thermal conductivity, borehole diameter, pipe size, and pipe configuration could impact the total thermal resistance in the borehole. Laboratory study indicated that an increase in the thermal conductivity of grout reduced the borehole thermal resistance. However, there was very small additional reduction of the thermal resistance produced when grout thermal conductivity was above 1.73 W/ m. K [17]. Laboratory studies were undertaken to study the effects of the thermal conductivity of cementitious grouts with various fillers on borehole thermal resistance. It was reported that decreasing the water-cement ratio and addition of conductive filler significantly increased the grout thermal conductivity. In the dry condition, superplasticizer cement-sand grout had a higher thermal conductivity than bentonites and neat cements. Several grouts were tested to determine how different grouts allow for the decrease of the length of the borehole, resulting in cost savings and improved performance. Theoretical studies predicted that the length of the

borehole decreased by 22% – 37% when the cement-sand grouts were used in the borehole heat exchanger in place of commonly used granular bentonite-water mixes [18]. Four types of soils were tested in the laboratory to estimate the impact of bulk density and moisture content on the thermal conductivity of some Jordanian soils. The four types of soils were sand, sandy loam, loam, and clay loam. The results showed that the thermal conductivity increased with the increase of soil density and moisture content. In addition, it was also observed that the thermal conductivity of sandy soil was higher than the clay loam soil. In this study, the thermal conductivities calculated using the cooling data were found to be lower than the same calculated using the heating data [19]. A number of thermal response tests were conducted to study the impact of different types of grout materials on the thermal performance of double U-pipe ground heat exchangers (GHEs). Figure 2.6 shows the cross section of double U-pipe ground heat exchanger with spacer. Four different types of grout materials: (1) bentonite, (2) bentonite with spacers, (3) 50% sand and bentonite with spacers, and (4) Quartz sand with spacers were used during these thermal response tests. The results showed that the borehole thermal resistance of the double U-pipe ground heat exchanger with quartz sand and spacers was 30% lower compared to when bentonite with spacers was used as grout. It was also noticed that the thermal resistance values for the double U-Tube GHE with and without spacers were 0.141 m. K/ W and 0.143 m. K/ W, respectively [20].

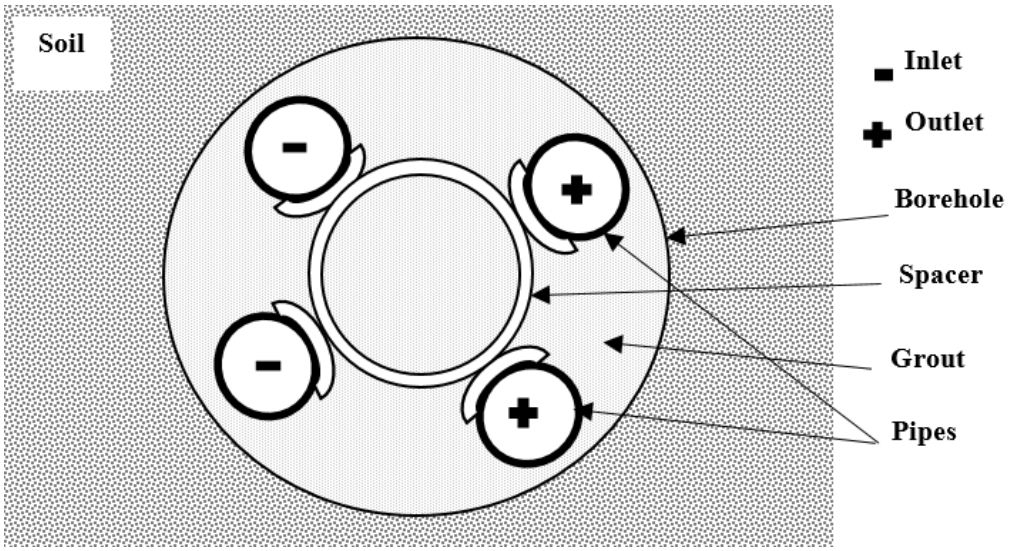

Figure 2.6: Cross section of double U-Tube pipe with spacer to keep space constant

Laboratory thermal response tests were conducted to evaluate the influence of groundwater flow on the heat transfer in the borehole ground heat exchangers. The effective thermal

conductivity increased with an increase of the groundwater velocity [21]. It is a common practice in Scandinavia to use groundwater as grout between the U-Tube and the borehole wall because the borehole is cased at the bottom to solid bedrock. The thermal resistance of groundwater borehole is lower compared to grouted boreholes because the heat transfer is enhanced by buoyancy-driven natural convection. A number of thermal response tests are conducted with different heat flow rates to identify the effect of convective heat flow in groundwater (as grout) on the heat transfer in ground heat exchangers constructed in solid/fractured bedrock. In the borehole heat exchanger constructed in solid bedrock, the convective flow in groundwater affected the borehole thermal resistance. The borehole thermal resistance decreased when the heat injection rate increased. In the fractured bedrock, the heat injection rate influenced the bedrock thermal conductivity. The thermal conductivity of the fractured bedrock increased with the increase of heat injection rate [22]. Six vertical ground heat exchangers were constructed in the field with different construction parameters to estimate the thermal efficiency of the GHEs. The three different construction parameters considered were: (1) grout materials (cement and bentonite), (2) pipe configurations (U-loop and new 3 pipe-type, as shown in Figure 2.7), and (3) additives (silica sand and graphite). It was found that the cement grout has a higher heat transfer efficiency than the bentonite grout. In addition, the thermal efficiency of 3 pipe-type configuration with the cement silica sand grout was higher than that of U-loop with the same grout [4].

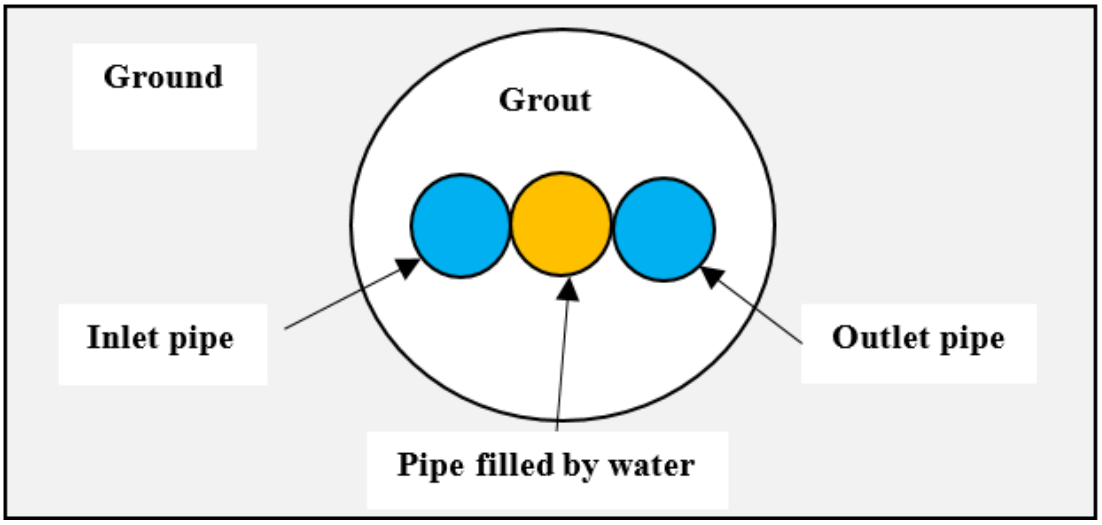

Figure 2.7: Cross section of new 3 pipe-type

Nine thermal response tests were carried out (TRTs) at the Chalmers University of Technology, Sweden to determine the ground properties inside and in the vicinity of the nine boreholes during

heat injection. Groundwater filled the space between the borehole (depth 80 m) and U-Tube. The same heat injection and turbulent water flow rate were used for the nine boreholes, and the minimum test duration was about 48 hours. The mean value of the thermal conductivity of the nine boreholes was 3.01 W/ m. K with ±7% variation. The estimated borehole thermal resistances for nine boreholes were within a range of 0.062 m. K/ W ± 0.012 m. K/ W [23]. New grout mixtures which were produced from industrial waste such as pulverized fuel ash (PFA) were proposed to improve the heat transfer characteristics of the borehole ground heat exchangers. The PFA was mixed with different grout materials such as fine sand, coarse sand, ground glass, and fluorspar. It was found that the heat transfer characteristics of the borehole ground heat exchangers improved when PFA mixed with fluorspar/coarse sand was used as grout material [24]. Laboratory studies were performed for a concentric ground heat exchanger to compare two different grouts (phase change materials (PCMs) and sand soil) to improve the thermal performance of ground heat exchangers. The results showed that the soil temperature oscillates less with PCMs grout than with sand soil grout [25]. A small-scale borehole heat exchanger (BHE) was inserted in the insulating sandbox (length: 1 m; depth: 1 m, and width: 1 m), and two parallel pipes were inserted in 1 m depth of the BHE. The main objective was to estimate the effects of three different grouts (silica sand-based, bentonite-based, and homemade admixture containing natural graphite) on the thermal resistance of the borehole heat exchangers. The results indicated that the homemade admixture with 5% natural graphite was the best option as grout in the borehole heat exchanger [26]. A numerical model was suggested for the BHE in the five-layered subsurface. The influence of groundwater flow was taken into account to minimize the total borehole length. Numerical analysis was used to estimate the performance of heat transfer characteristics of the BHEs with and without groundwater flow. The results indicated that the convection flow in groundwater leads to increased heat transfer between BHE and the ground by 55% [27]. Field studies were performed to estimate the influence of two different grout materials (cement-grout and gravel-backfill) on the borehole thermal resistance of BHEs. The borehole thermal resistance of the BHE with gravel-backfill (0.141 m. K/ W) was lower than the same with cement-grout (0.155 m. K/ W). In addition, use of gravel-backfill reduces the installation cost and time compared to cement-grouted. The space between the U-Tube and the borehole took 2 hours to fill with gravel-backfill, while it needed three days to fill with cement-grout [28]. Field thermal response tests were performed at two different locations to study the effects of the groundwater level on the effective ground thermal

conductivity and heat transfer rate of the borehole heat exchangers. It was reported that the effective ground thermal conductivity and heat transfer rate of the borehole heat exchangers increased with an increase in the level of the groundwater [29]. Field studies were conducted to investigate the effects of different rock types (alluvial deposit, granite, and gneiss) and borehole depths (150 m and 200 m) on the effective ground thermal conductivity. The results indicated that the effective ground thermal conductivity increased by increasing the borehole depth. The results also showed that gneiss was the best option to increase the effective ground thermal conductivity, followed by alluvial deposit and granite [30].

2.2.2 Influence of different pipe configurations on the thermal performance of ground heat exchangers

A novel quasi-three-dimensional model was developed for GHEs to understand the heat transfer processes that occurs in GHEs during the heat injection and rejection. Analytical solutions were used to evaluate the thermal resistance for different configurations of single and double U-Tube boreholes. The obtained results showed that the double U-Tube borehole had 30% – 90% lower thermal resistance than the single U-Tube borehole [31]. A new configuration of coaxial borehole heat exchanger was suggested to improve the thermal performance of a borehole heat exchanger. The coaxial borehole heat exchanger comprises of pipe-in-pipe in which the outer pipe contacted directly with the surrounding bedrock. The goal of this study was to compare the thermal efficiency of a conventional U-Tube borehole heat exchanger with a new coaxial borehole heat exchanger. The temperature of the fluid was measured at specific points by using fiber optic cables installed in the borehole. The heat transfer performance of coaxial heat exchanger was stronger than a common U-Tube heat exchanger [32]. A novel coaxial borehole ground heat exchanger (pipe-in-pipe with external insulation around the central pipe) was suggested to improve the heat transfer rate. The numerical results indicated that the heat extracted from the ground by using coaxial borehole heat exchanger with insulation was 40% higher than the same without insulation [33]. Thermal response tests were conducted to evaluate the thermal performance of GHEs with three different pipe configurations in Oklahoma City. The three different pipe configurations were: (1) coaxial, (2) double U-tube, and (3) single U-tube. The results showed that the best option to reduce the thermal resistance of the borehole was the double U-tube heat exchanger, followed by a single U-tube heat exchanger and a coaxial heat exchanger [34]. Field experiment studies were

undertaken to estimate the impact of different pipe configurations on the thermal borehole resistance of borehole heat exchangers (BHEs). In this study, the three different pipe configurations were: (1) coaxial (115 mm borehole diameter), (2) single U-tube (180 mm borehole diameter), and (3) double U-tube (180 mm borehole diameter), all with the same depth (30 m). The distance between each borehole was 5 m, as shown in Figure 2.8. The results showed the ground thermal conductivity for the coaxial BHE was 2.21 W/ m. K, and the borehole thermal resistance was 0.344 m. K/ W. The thermal resistance of the double U-tube was 0.162 m. K/ W, which represented the best BHE performance, followed by the single U-tube type (0.251 m. K/ W), and coaxial type (0.344 m. K/ W) [35].

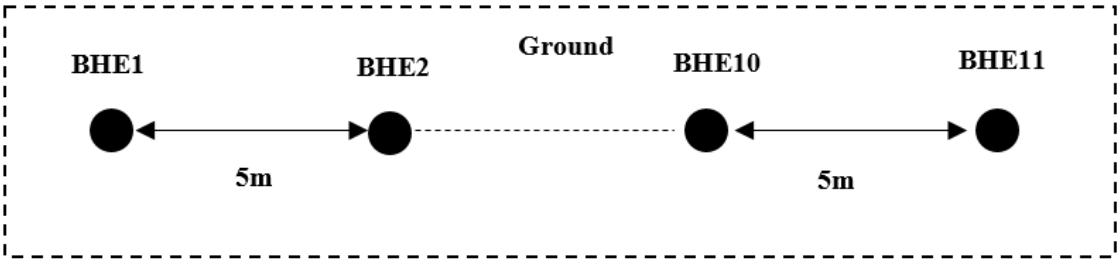

Figure 2.8: Top view of eleven boreholes

Field studies were conducted by using a new method (Distributed Thermal Response Test (DTRT)) to study the effects of different volumetric flow rates (0.13, 0.21, 0.24 L/ s) and pipe configurations (U-Tube, pipe-in-pipe, and multi-pipes) on the ground properties of BHEs. The local borehole resistances were 0.015 m. K/ W and 0.040 m. K/ W in pipe-in-pipe and multi-pipe BHEs, respectively, which were substantially lower than the same for single U-Tube BHE. The results also showed the increased temperature difference between pipes due to the decline of the flow rates, which was followed by decreasing evaporation temperature in the heat pump [36]. Numerical studies were carried out to estimate the influence of two different parameters (volumetric flow rates and pipe configurations) on the heat extraction rate of GHEs. Three different pipe configurations were used for small diameter boreholes: (1) single U-Tube, (2) double cross U-Tube, and (3) double U-Tube, and two different pipe configurations were used for larger diameter boreholes: (1) spiral, and (2) multiple U-Tube. The results showed the thermal performance in GHEs improved by using turbulent flow rate and increasing the flow rate in pipes. The performance of the double U-Tube in small diameter borehole had a range of 8% to 23% higher than double cross U-Tube in the same small diameter borehole. There was little change in

the performance of the spiral and multiple U-Tubes in the larger diameter borehole when the pipe lengths inside the borehole were the same [37]. Experimental studies were conducted to investigate the performance of three different pipe configurations (single U-Tube, double U-Tube, and triple U-Tubes) inserted in GHEs. The results showed the increasing number of U-Tubes in the borehole led to an increase in the performance of the borehole. It was also reported that the performances of triple U-Tube and double U-Tube were 33% and 17% higher than the same for single U-Tube. The drilling cost was also reduced up to 25% with triple U-Tube in the borehole [38]. A numerical analysis (Computational Fluid Dynamics (CFD) code) was used to compare the thermal performance of U-Tube and spiral-tube GHEs in both laminar and turbulent flow conditions. The thermal performance of the spiral-tube GHE was compared with the U-Tube GHE. In the laminar flow, the performance of the spiral-tube increased by 62.7%, and in the turbulent, it increased by 33.5% [39]. Numerical studies were carried out to estimate the internal thermal processes between pipes inside the boreholes and thermal performance of multiple-tube GHEs. In this study, four different ground heat exchangers: (1) single U-Tube, (2) multi-tube, (3) three-tube, and (4) four-tube were used, as shown in Figure 2.9. The thermal performances of multi-tube, four-tube, and three-tube GHEs were compared with the single U-Tube GHE. It increased by 20.1% for multi-tube, 13.6% for four-tube, and 9.1% for three-tube. It was reported that the thermal performance was influenced by the internal thermal processes between tubes in the boreholes. The heat exchange rate increased between the boreholes and the ground due to an increase in the number of inlet tubes in the borehole [40].

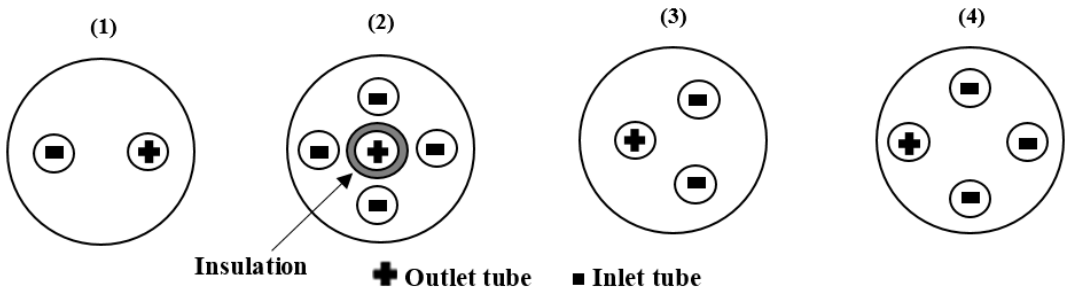

Figure 2.9: Cross sections of four ground heat exchangers (GHEs): (1) single U-Tube, (2) multi-tube, (3) three-tube, and (4) four-tube

Field studies were conducted to estimate the thermal resistance and the average circulating water temperature (ACWT) for three different pipe configurations: (1) new design which has three inlet pipes and one outlet (3I-type), (2) double U-Tube, and (3) single U-tube, as shown in Figure

2.10. The experimental results indicated that the average circulating water temperatures for single U-Tube and double U-Tube were 3.7 °C and 1 °C higher than the same for 3I-type. The results also showed the best option to reduce the thermal resistance of the borehole was the 3I-type, followed by the double U-Tube and the single U-Tube [41].

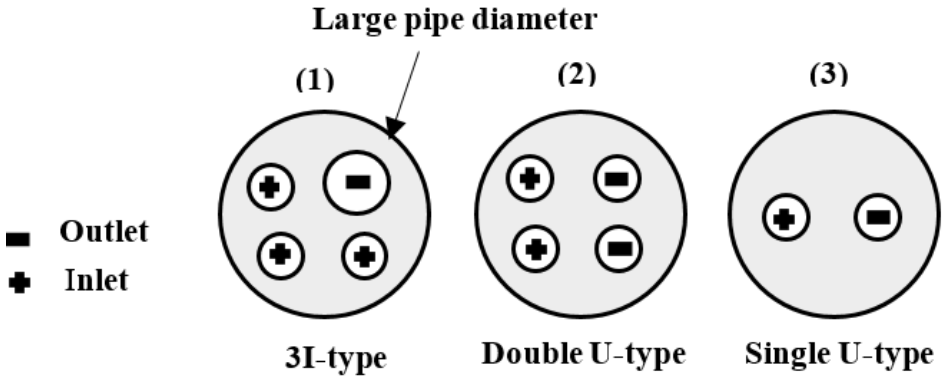

Figure 2.10: Cross section of the 3I-type, double U-Tube, and single U-Tube

Experimental and numerical studies were conducted to estimate the thermal efficiency of two types of GHEs: coil-type and W-type energy piles. There were good agreements between numerical analysis outputs and experimental observations. Numerical analysis was utilized to predict the heat exchange rate in ground heat exchangers (coil-type and W-type energy piles) over a period of three months. The results indicated that the coil-type has higher heat exchange efficiency than the same for W-type but was found to be more expensive than the W-type [42]. An analytical design calculation suggested that the coaxial GHEs at a high flow rate have less borehole thermal resistance (below 0.05 m. K/ W) than a single U-Tube. On the other hand, the coaxial GHEs have higher borehole thermal resistance than double U-pipe GHEs [43]. Two field studies were conducted to evaluate the effects of two different pipe configurations (single U-Tube and double U-Tube) on thermal performance of the GHEs. The results indicated that the ground thermal conductivity values of the double U-Tube and single U-Tube were 31.7 W/ m. K and 3.03 W/m. K, respectively. The borehole thermal resistance values of the double U-Tube and single U-Tube were 0.081 m .K/ W and 0.130 m .K/ W, respectively [44]. Experimental and numerical studies were carried out to estimate the thermal efficiency of four types of energy pile GHEs: double-U, triple-U, double-W, and spiral. The results showed that triple-U type was the best option for thermal efficiency. The results also showed that the highest economic performance was triple-U type, followed by double-U type, spiral type and double-W type [45]. Field studies were

conducted to evaluate the effects of increased number of tubes and tube diameters, as shown in Figure 2.11, on the thermal performance of the GHEs. It was reported that more tubes and larger tube diameter in the borehole led to reduced grout space, followed by decreased water temperature entering into the heat pump [44].

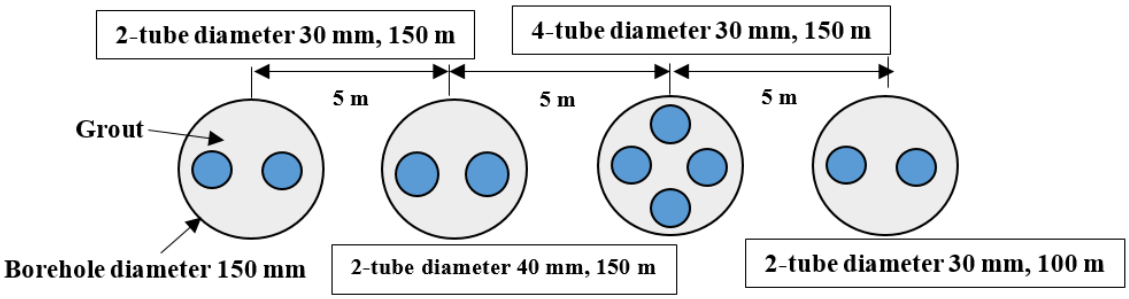

Figure 2.11: Cross section of ground heat exchangers

Small-scale laboratory studies were performed to estimate the influences of different pipe configurations: single and double U-Tubes (with or without spacers), as shown in Figure 2.12, and helical-shaped pipe on the efficiency of GHEs. The best heat transfer rate was found in the helical pipe GHE, compared to both single and double U-Tube (with or without spacers) GHEs. It was also reported that the thermal efficiency of single U-Tube and double U-Tube GHEs with spacers improved by 30%, compared to the same without spacers [46].

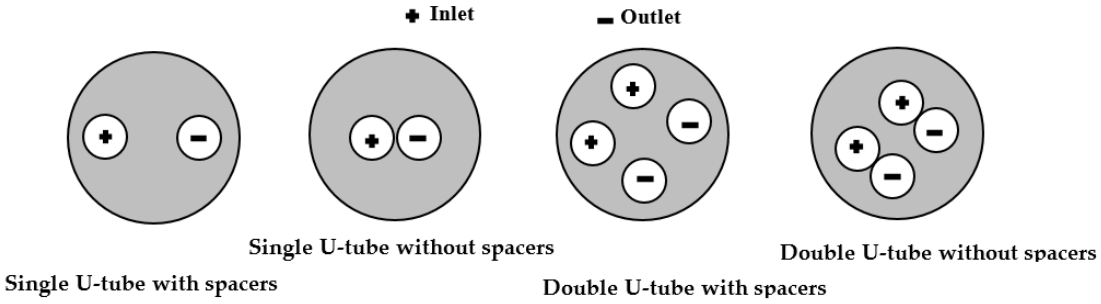

Figure 2.12: The position of the single and double U-Tube with and without spaces

2.2.3 Effects of borehole depths and diameters on the thermal performance of ground heat exchangers

First field studies were carried out, supported by numerical analysis, at a depth of 22 m in Latin America to estimate the borehole thermal resistance and the thermal conductivity of the ground. Thermal conductivity of the ground was calculated by using line source theory [11], which was

lower compared to the same obtained from numerical analysis [47]. First field thermal response test was conducted to evaluate the thermal performance of U-Tube borehole heat exchangers in Cyprus. Line source model was used to evaluate the thermal conductivity of the ground layers composed of clay, silt and sand, and the borehole thermal resistance. Boreholes were of 50 m depth. The thermal conductivity for the ground was 1.61 W/ m. K and the borehole thermal resistance was 0.257 m. K/ W [48]. The first thermal response test in Saudi Arabia was carried out to calculate the ground thermal properties such as the thermal conductivity, the thermal diffusivity, and the borehole thermal resistance for borehole heat exchangers with single U-Tube. The borehole depth was 100 m and bentonite–sand mixture filled the spaces between the borehole and the U-Tube. The mean undisturbed ground temperature was 32.6 °C before the thermal response test started. The thermal characteristics derived from experimental data using line source theory were: thermal conductivity 2.15 W/ m. K, thermal diffusivity $6.252 \times 10 -6$ m^2/ s, and thermal resistance of the borehole wall 0.315 m. K/ W [49]. Three thermal response tests (TRTs) were conducted with different borehole depths (30 m, 60 m, and 90 m), all with a 150 mm borehole diameter in the garden of a village house in Elazing, Turkey to study the temperature distributions in boreholes of a conventional U-Tube borehole heat exchanger. The results from the cooling and heating experiments showed that the 90 m depth borehole heat exchanger had a stronger performance than those with the depths of 60 m and 30 m. The coefficient of performance (COP) of a heat pump is the ratio of energy output to the energy input. However, considering the borehole digging cost, the optimum depth was found to be 60 m with COP = 3.0 [50]. Laboratory experiment in a horizontal sandbox (length: 18 m, depth: 1.8 m, and width: 1.8 m) with a single U-Tube was conducted with GHE to estimate the ground thermal properties. A large number of thermocouples were placed at specific locations in the sandbox to understand the heat transfer process in and around the GHE. Researchers utilized the temperature data collected at the borehole wall to determine the borehole thermal resistance. Temperature data collected during the test within the soil were used to estimate the soil thermal conductivity. The values of borehole thermal resistance and soil thermal conductivity were used to verify the heat transfer in the borehole ground heat exchanger [51]. A novel approach (Distributed Thermal Response Test) was developed to determine the thermal conductivity of the ground and thermal resistance of the BHE at different depths. Figure 2.13 shows the cross section of coaxial borehole heat exchanger. This study showed

that the borehole thermal resistance (local and global) of the coaxial heat exchanger is lower than the same for a single U-tube borehole heat exchanger [52].

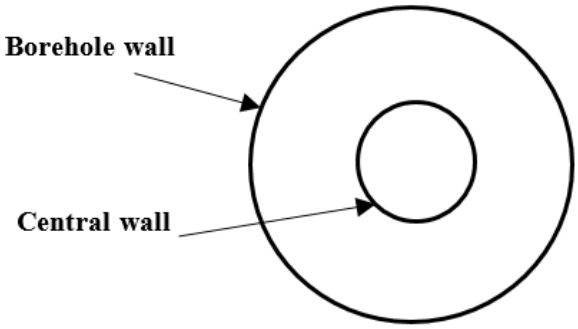

Figure 2.13: Cross section of coaxial borehole heat exchanger

Field studies were performed to investigate the effects of different borehole diameters (121 mm, 165 mm, and 180 mm) (see Figure 2.14) on the thermal efficiency of BHEs. The results showed that the larger diameter led to an increase in the thermal exchange rate. In the seasonal cooling period, the amount of thermal exchange in the180 mm and 165 mm borehole diameters were 7.1% and 3.2% higher than the same for 121 mm borehole diameter [53].

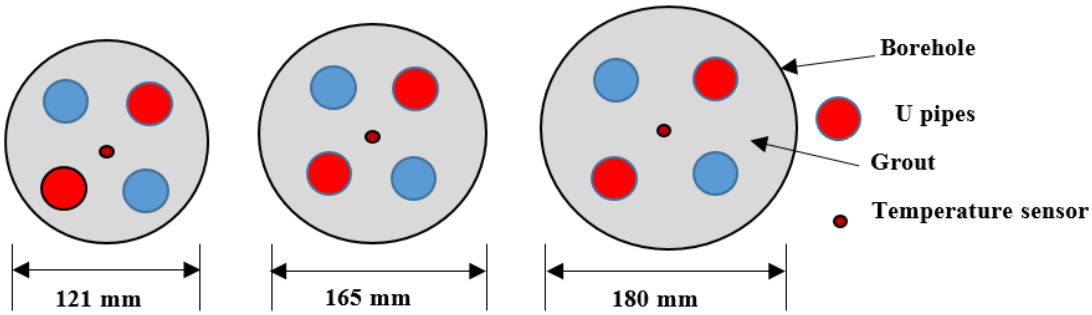

Figure 2.14: Cross section of different borehole diameters

An experimental study was conducted with a single borehole (length: 400 mm) inserted at the center from the top of the sand tank (length: 1.35 m and diameter: 1.4 m) to measure the borehole wall temperature at various depths and different times (1 hour, 6 hours, 12 hours, 24 hours, and 168 hours) during the thermal response test. The results indicated that the temperature at borehole wall increased with the duration of the thermal response test [54]. Field studies were performed to estimate the ground thermal properties at the Technical University of Sofia, Bulgaria. A mobile system was built and used for conducting the thermal response tests. In this study, temperature data were collected during two thermal response tests for single U-Tube borehole ground heat

exchangers in 2011 and 2012 and were compared. In 2011, the ground thermal conductivity was 1.58 W/ m. K and the borehole thermal resistance was 0.187 m. K/ W, while in 2012, the ground thermal conductivity was 1.65 W/ m. K and the borehole thermal resistance was 0.179 m. K/ W [55].

2.2.4 Miscellaneous issues related to performance of ground heat exchangers

Numerical studies were carried out to predict transient ground heat transfer behavior of the vertical U-Tube with different pipe diameters, shank spacing, and borehole sizes. Numerical observations were compared with known analytical case solutions [56]. A three-dimensional unstructured finite volume model for conventional single U-Tube was developed. In this study, Delaunay triangulation method was utilized to mesh the cross section of the borehole field, including inside and around the borehole. In order to characterize the variation of temperature with the depth, the ground was divided into multiple layers. The inlet fluid temperature of the borehole was used as a boundary condition, and the inner and outer surfaces of the two legs of the U-Tube were considered as the conjugated interfaces in the area. Therefore, the conjugate heat transfer processes in and around the pipes could be calculated. There was a good agreement for the outlet water temperature both when measured during the experiment and predicted by the numerical model [57]. A three dimensional numerical computational-fluid-dynamics model was implemented to predict the complex heat transfer process with approximately 3.5% error. Statistical analyses were conducted to show how different design parameters could simultaneously impact the response variables [58]. Rest or recovery period needed was measured for the borehole after the thermal response test to return to the initial ground temperature prior to the test. Thermal response tests were carried out by using many heat injections of different rates and time durations. The recovery time of the initial ground temperature depends on the time and the rate of heat injection throughout the test. The initial ground temperature returned to within 272.85 ºC after 10 days when the thermal response test was conducted for 48 hours and the rate of heat injection was 67 W/ m. There was also a close agreement between the temperatures obtained from the mathematical model and experiment. It was noted that the recovery time increases with the duration of test and rate of the heat injection [59]. It is reported that a number of residential-size GSHPs were installed in cold climates of Alaska to estimate the performance of GSHPs. The

results showed that the ground source heat pumps were effective in cold climates, and the COP was between 2.0 and 3.5 [60]. A residential-size GSHP was installed in Fairbanks, Alaska to study the impacts of the heat extraction over a period of three months on the ground thermal properties and any decline in heat pump system efficiency. The results showed that the surrounding soil temperature was higher than the soil temperature around the ground heat exchanger. The results also indicated that the COP of the circulating pumps and the heat pump was 3.3 [61]. Four field tests on two boreholes (depth 40 m) were performed to evaluate the ground properties of double U-Tube ground heat exchangers used for thermal energy storage in Melbourne, Australia. As the heat injection rate was not constant during the thermal response test, the results were compared by three different methods: (1) conventional slope determination, (2) geothermal properties measurement (GPM) model, and (3) two parameter curve fitting. There was a good agreement between the geothermal properties measurement (GPM) model and two parameter curve fittings. The values of the ground properties were variable while using the slope determination method because the heat injection was not constant during the thermal response test (TRT). The results also showed the difference between the conventional slope determination method and the other two methods, ranging from 2% to 37% [62]. A small experimental apparatus for a single U-Tube ground heat exchanger was established in the laboratory to study transient heat transfer. At the same time, results from an axisymmetric numerical model of the ground surrounding the borehole were compared with the experimental results. There was an agreement between the experimental and numerical results which indicates the accuracy of the data collected from the experimental setup [63]. First field thermal response test was conducted to estimate the soil thermal response in Guayaquil, Ecuador. It was reported that the soil temperature was between 27 °C and 29 °C. The results also showed the thermal conductivity of the soil was 1.13 W/ m. K and the borehole thermal resistance was 0.33 m. K/ W [64]. A field test was carried out to estimate the distribution of undisturbed ground temperature during the period of heat injection in underground thermal energy storage (UTES) system established in Golden, Colorado, USA. The system comprised of five boreholes with a depth of 9 m, and the center to center distance between these boreholes was 2.5 m. It was indicated that during a period of 75 days, a constant heat of 20 W/ m was injected into the ground. The undisturbed ground temperature was increased by 7 °C. Four months later, it was noticed that the heat storage decreased by 60% [65]. A novel transient quasi-3D entire time scale line source model was developed, which studied transient borehole thermal resistance and

examines the heat flux profile along the two legs of the U- tube as a variable. The results were compared with experimental sandbox and maximum relative error was found to be less than 5% [66]. The effect of many variables were analyzed on the GSHPs currently installed in 24 buildings in cold climate zones of the United States. The factors included in the study were: (1) system performance, (2) potential energy savings, (3) cost of system, (4) operational difficulties, (5) purpose of using geothermal system, and (6) owner satisfaction to date. The results showed that 75% of building owners were highly satisfied with the use of GSHP systems, including noise level, cost, and comfort. Approximately 85% of homeowners encouraged other people to use this technology, and about 71% of GSHP systems did not have issues during their operation. Furthermore, the study showed that the overall performance of the real GHP systems used in cold climate regions was 6.1% lower in energy consumption and about 7.2% lower in cost savings than the national energy use and mean energy costs in similar buildings in the United States [67].

A comprehensive list of all the literature discussed in this section is shown in Table 2.1.

Table 2. 1: Summary of the literature

Source	Description	Conclusion/s or Observation/s
Remund C. P (1999) [17]	Investigated the impacts of grout on the borehole thermal resistance.	Increasing the thermal conductivity of the grout from about 0.43 to 0.85 Btu/h.ft.°F reduces borehole thermal resistance by 15.3 to 19.5%.
Allan and Kavanaugh (1999) [18]	Studied how cement-sand, bentonites, and neat cements grout would affect the borehole length.	Cement-sand (grout) more suitable to reduce borehole length than bentonites and neat cements.
Abu-Hamdeh et al. (2001) [19]	Examined the effects of bulk density and moisture content on the thermal conductivity of some Jordanian soils.	Soil thermal conductivity increased with the increase of soil density and moisture content.
Pahud and Matthey (2001) [20]	Estimated the effects of bentonite, 50% sand and bentonite, and quartz sand, with and without spacers.	The quartz sand and spacers was the best option to increase the efficiency. The borehole thermal resistances with spacers was less than without spacers.
Katsura et al. (2006) [21]	Evaluated the influence of ground water flow on the heat transfer in the GHEs.	The effective thermal conductivity increased with an increase in the ground water velocity.
Gustafsson and Westerlund (2010) [22]	Considered the effects of the convective heat flow on the heat transfer in the GHEs.	In the solid bedrock, the borehole thermal resistance decreased when the convective heat flow increased. The heat flow through fractured bedrock increased with increased convective heat flow.
Lee et al. (2011) [4]	Estimated the thermal efficiency of GHEs with U-loop and 3-pipe.	The thermal efficiency of 3-pipe configuration was higher than U-loop.
Alrtimi et al. (2013) [24]	Proposed new grout mixtures which were produced from industrial waste such as pulverized fuel ash (PFA) to improve the heat transfer characteristics of the borehole heat exchangers.	The thermal conductivities of fluorspar and coarse sand, all with 20% of PFA had higher thermal conductivities compared to other grouts.
Lei and Dai (2013) [25]	Compared phase change materials to sand-soil.	The soil temperature oscillates less with PCMs grouts than with sand-soil grout.
Erol and François (2014) [26]	Examined silica sand-based, bentonite-based, and homemade admixture as grout in the GHE.	The homemade admixture with 5% natural graphite was the best option for grout in the GHE.
Luo et al. (2015) [27]	Estimated the performance of heat transfer characteristic of the GHEs with and without groundwater flow.	The convection flow in groundwater led to increased heat transfer between GHE and the ground.

Choi and Ooka (2016) [28]	Studied the influences of cement-grout and gravel-backfill on the borehole thermal resistance of GHEs.	The borehole thermal resistance of the GHE with gravel-backfill was lower than the same with cement-grout.
Luo et al. (2018) [29]	Examined the effects of the groundwater level on effective ground thermal conductivity and heat transfer rate of GHEs.	The effective ground thermal conductivity and heat transfer rate of borehole heat exchangers increased with increasing level of the groundwater.
Lee C (2019) [30]	Studied the effects of different rock types (alluvial deposit, granite, and gneiss) and borehole depths (150 m and 200 m) on the effective ground thermal conductivity.	The effective ground thermal conductivity increased by increasing the borehole depth. The gneiss had the maximum effective ground thermal conductivity.
Zang et al. (2003) [31]	Developed a novel quasi-three-dimensional model to estimate ground properties.	The novel quasi-three-dimensional model was helpful to understand the processes of heat transfer in VGHEs.
Acuña and Palm (2010) [32]	Suggested a new configuration of coaxial (consists of pipe-in-pipe in which the outer pipe contacted directly with the surrounding of bedrock) to improve the thermal performance of GHE.	The thermal performance of the pipe in pipe was superior compared to the single U-Tube pipe.
Guillaume F (2011) [33]	Introduced a new approach of coaxial GHE with external insulation around the central pipe.	The heat extracted from the ground by using coaxial GHE with insulation was higher than the same for without insulation.
Beier and Ewbank (2012) [34]	Performed TRTs for GHEs under various pipe configurations (coaxial, double U-Tube, and single U-Tube).	The thermal resistance of borehole was the lowest when pipe configuration was double U-Tube.
Desmedt et al. (2012) [35]	Estimated the impact of coaxial, single U-Tube, and double U-Tube on the borehole thermal resistance of GHEs.	The thermal resistance of the double U-tube was lower than single U-Tube type, and coaxial type.
Acuña J (2013) [36]	Used a new method (Distributed Thermal Response Test) to study the effects of different volumetric flow rates on the performance of GHEs.	The temperature difference between pipes increased due to the decline of the flow rates.
Bidarmaghz et al. (2013) [37]	Estimated the effects of the fluid flow rate on the thermal performance of GHEs.	The thermal performance in GHEs improved by using turbulent flow and increasing the flow rate in pipes.
Dincer et al. (2014) [38]	Estimate the performance of single U-Tube, double U-Tube, and triple U-Tubes of GHEs.	The performance of triple U-Tube was higher than the double U-Tube and single U-Tube.

Haddada and Miyara (2014a) [39]	Compared the performance of U-tube and spiral-tube GHEs in both laminar and turbulent flow conditions.	In the laminar flow, the performance of the spiral-tube increased by 62.7%, and in the turbulent flow, it increased by 33.5%, when compared with the single U-Tube.
Haddada and Miyara (2014b) [40]	Estimated the performance of different pipe configurations in GHEs.	The heat exchange rate increased between the boreholes and the ground due to increased number of inlet tubes in borehole.
Liu et al. (2015) [41]	Compared the influence of single U-tube, double U-tube, and a new design (3Itype) on the borehole thermal resistance.	The borehole thermal resistance of the 3Itype was lower than for double U-tube and the single U-tube.
Yoon et al. (2015) [42]	Estimated the thermal efficiency of two types of GHEs: coil-type and W-type.	Coil-type had a higher heat exchange efficiency than the W-type.
Raymond et al. (2015) [43]	Preformed analytical models for two coaxial pipe configurations with different borehole diameters to reduce the depth of the borehole.	The borehole thermal resistance of the coaxial GHEs decreased due to an increase in the thermal conductivity of the outer pipe.
Chang and Kim (2016) [44]	Evaluated the effects of increasing number of tubes and tube diameters on the performance of GHEs.	Increasing number of tubes and using large tube diameter in the borehole leads to increased heat transfer in GHEs.
Luo et al. (2016) [45]	Compared the thermal efficiency of four types GHEs: double-U, triple-U, double-W, and spiral.	Tripe-U type was the best option.
Blázquez et al. (2017) [46]	Studied the impact of single and double U-Tube (with or without spacers), and spiral pipes on the efficiency of GHEs.	The performance of the U-Tube VGHEs with spacers was superior to the same without spacers.
Busso et al. (2003) [47]	Conducted a first thermal response test in Latin America to evaluate ground properties.	Both ‘line source model’ and ‘two-variable parameter fitting’ could be considered as quick and reliable evaluation methods. However, the accuracy depends on the amount of care taken while conducting thermal response tests.
Florides and Kalogirou (2008) [48]	Conducted the first thermal response test in Cyprus to evaluate ground properties.	Thermal conductivity for the ground was found to be 1.61 W/ m. K borehole thermal resistance was 0.25 m. K/ W.
Sharqawy et al. (2009) [49]	Conducted the first field study in Saudi Arabia to calculate the ground thermal properties.	The mean undisturbed ground temperature was 32.6 °C.
Esen and Inalli (2009) [50]	Compared the thermal performance of the single U-Tube GHEs with different depths.	The thermal performance increased with increased depths.

Beier et al. (2011) [51]	Designed a laboratory sand tank to verify the heat transfer in and around the GHE.	Independent values of borehole thermal resistance and soil thermal conductivity were calculated from data collected during the test. These independent values were used to verify GHE models.
Acuña and Palm (2013) [52]	Developed a novel approach (Distributed Thermal Response Test) to determine the ground thermal properties of a GHE at different depths.	The borehole thermal resistance of the coaxial pipe was lower than the same for single U-Tube.
Luo et al. (2013)[53]	Preformed field studies to investigate the effects of different borehole diameters on the thermal efficiency of GHEs.	The results showed that the larger diameter leads to an increase in the heat transfer rate.
Cimmino and Bernier (2015) [54]	Conducted laboratory study to measure the borehole wall temperature during the thermal response test. The borehole temperature reached a steady state condition after 168 hours.	The temperature at borehole wall increased with increased duration of the thermal response test.
Georgiev et al. (2016) [55]	Compared temperature data collected during two thermal response tests in the same area and at different times.	Very small difference between temperature data collected during 2001 and 2012.
Yavuzturk et al. (1999) [56]	Developed numerical model to predict the long and short time of the vertical U-tube ground heat transfer behavior with different composition conditions, such as different pipe diameters, shank spacing, and borehole sizes.	The numerical results were compared with the analytical models with an average relative error of ±1% for the inner pipe temperature. During the first hours, the errors were more significant and they decreased with time.
Li and Zheng (2009) [57]	Developed a 3D numerical model to predict the outlet water temperature for single U- tube GHE.	In order to characterize the variation of temperature with the depth, the ground was divided into multiple layers. The inlet fluid temperature of the borehole was used as a boundary condition. The results obtained from experimental and numerical models showed close agreement for the outlet water temperature.
Khalajzadeh et al. (2011) [58]	A three dimensional CFD simulation tool was used to study the influences of VGHE design parameters on efficiency of heat transfer.	The inlet fluid temperature and pipe diameter had a higher impact on the efficiency of heat transfer, while the depth had a lower impact on the efficiency of heat transfer.
Javed et al. (2011b) [59]	Measured the recovery time needed for the borehole after the test to return to the initial ground temperature.	The recovery time is strongly dependent on the TRT period and the value of heat injection rate throughout the TRT.

Meyer et al. (2011) [60]	Installed a number of residential-size ground source heat pumps in cold climates to study the performance of GSHPs.	The ground source heat pumps were found to be effective in cold climates, and the COP varied between 2.0 and 3.5.
Garber-Slaght et al. (2014) [61]	Installed a residential-size ground source heat pump to study the impacts of extracted heat over a period of three months on the ground thermal properties and any decline in heat pump system efficiency.	The results showed that the surrounding soil temperature is higher than the soil temperature around the ground heat exchanger and the COP of the heat pump was 3.3.
Lhendup et al. (2014) [62]	In-situ thermal responses of borehole heat exchangers were analyzed using slope determination, two variable parameter fitting and the geothermal properties measurement (GPM) model.	The results obtained from GPM model have better agreements with the measured temperatures from boreholes.
Shirazi and Bernier (2014) [63]	Developed a numerical model to study the ground heat transfer in radial and axial directions in the vicinity of the borehole ground heat exchanger. At the same time, an experimental apparatus was constructed in laboratory to validate the obtained results collected from the numerical study.	There was an agreement between the experimental and numerical results which validated the outputs from the numerical model. It was also reported that the experimental apparatus could be used to validate different borehole designs.
Soriano et al. (2015) [64]	Performed the first field tests to estimate the soil thermal response in Guayaquil, Ecuador	Thermal conductivity and resistivity values of the soil were found to be 1.130 W/m-K and 0.33 m-K/W, respectively. The average soil temperature within a depth of 50 m was 29 ºC, lower than daily average daylight temperature in summer, which means the soil could still be used as heat sink to reject the heat in the summer.
Başer et al. (2015) [65]	Carried out a field test to estimate the distribution of undisturbed ground temperature during the period a of heat injection in underground thermal energy storage system.	The undisturbed ground temperature was increased by 7 °C. Four months later, it was noticed that the heat storage was decreased by 60%.
Zhang et al. (2016) [66]	Developed a transient quasi-3D whole time scale line source model, which characterized transient borehole thermal resistance and examined the heat flux profile along the two legs of the U- tube.	The accuracy of predicting the circulating fluid and the outside ground temperatures increased by using the proposed new transient quasi-3D entire time scale line source model. The data collected from the experimental study indicated that the prediction errors for the inlet and outlet fluid temperatures were less than 5%.

Yu et al. (2017) [67]	Investigated the performance of GSHPs installed in 24 buildings in cold climate zones of the United States (US).	The overall performance of the GSHPs used in cold climate regions was slightly better (≈6.1% lower energy consumption and ≈7.2% lower in cost) compared to the national median of energy use and energy cost of typical buildings of the same type nationwide (US).

2.3 Critical Observations

This chapter reviewed various experimental and numerical studies on closed-loop vertical ground heat exchangers (VGHEs). These studies indicate that several parameters such as fluid flow rate, thermal properties of the pipe and grout material, inlet and outlet pipe diameter, configuration of the pipes, etc. have significant impacts on the efficiency of ground source heat pumps (GSHPs). Several studies reported the use of numerical models to simulate the heat transfer process in VGHEs. Numerical models were found to be very useful tools to predict the performance and develop optimum design parameters for VGHEs. According to the studies reviewed in this chapter, several design parameters may be altered to reduce the length of the borehole while increasing the efficiency of the borehole heat exchangers.

Grout material are considered to be one of these parameters that has an effect on the efficiency of VGHEs. In the case of one particular experiment, the thermal resistance between the borehole wall and the heat carrier fluid decreased due to an increase in the thermal conductivity of the grout [17]. Another study found that depending on borehole diameter and soil thermal conductivity, the length of the borehole would decrease when sand is added to cement-sand grout [18]. It was also reported that the thermal conductivity of the grout increases with the increase in soil density and moisture content during both heating and cooling cycles [19]. Under certain geological conditions, groundwater can also function as grout. The presence of natural convection flow in groundwater-filled borehole heat exchangers at deferent heat injection rates during thermal response tests was reported [22].

Borehole configuration also has an impact on the efficiency of ground heat exchangers. The thermal resistance of the double U-Tube VGHEs with spacers was lower than without spacers [20]. Several studies reported that coaxial, double U-Tube, spiral-tube and multi-tube boreholes had superior thermal performance compared to common single U-Tube heat exchangers [33, 36, 39,

41, 52]. The thermal efficiency of coaxial borehole heat exchanger could be improved further by externally insulating the central pipe [33]. Triple-U type was found to produce the highest thermal performance and lowest drilling costs among double-U, triple-U, double-W and spiral [38]. The overall thermal efficiency could be increased by increasing borehole depth [30, 50]. Higher thermal conductivity of the outer pipe would also increase the thermal efficiency of VGHEs [43].

Another parameter that has an impact on the efficiency of the ground heat exchangers is borehole diameter. Larger borehole diameter and/or pipe diameter would lead to an increase in the thermal performance of VGHEs [40, 53].

In addition, the borehole thermal resistance of VGHE could decrease within a range of 9% to 52% due to pipe configurations and characteristics of grout materials [18, 20, 24, 27].

To sum up, this chapter did a comprehensive review on the efficiency of ground heat exchangers (GHE) in heat pump systems. Increasing the efficiency of the GHE may lead to decreased borehole depths and installation costs. Hence, identification and optimization of design and operation parameters that can reduce the borehole depth are among the most important design challenges. To deal with these challenges, various researchers conducted several studies to improve the heat transfer efficiency of GHEs. However, there are still opportunities for engineers to suggest new pipe configurations that can increase the surface area of the pipe and heat transfer rate in GHEs. One of the most attractive solutions to increase the heat transfer rate in VGHEs is to increase the surface area of the pipe configuration which could lead to higher heat exchange capacity of VGHEs. It is well known that heat transfer from a surface can be increased by attaching external fins (i.e. extended surfaces) [2]. However, research activities reported in the literature do not provide any information about the performance of GHEs with external fins. Therefore, this research initiative investigates the impacts of external fins on the heat transfer capacity of VGHEs.

Chapter 3

Methodology

This chapter presents the methodology including the laboratory based thermal response test (TRT) and analysis of the test results using line source theory [14]. The first part describes the principles and procedures of the TRT, and the second part explains how line source theory is applied to determine ground thermal properties.

3.1 Thermal response test (TRT)

Ground source heat pumps (GSHPs) are consisted of two parts: a heat pump, and a vertical ground heat exchanger (VGHE), which are coupled together to provide heating and cooling for residential and commercial buildings. The knowledge of ground thermal properties is considered a prerequisite in order to reach the ideal design for GHEs connected to heat pump systems [68]. Several variables such as the filling inside the borehole (e.g. grout), borehole diameter, pipe size, and pipe configuration have significant impact on the effective ground thermal conductivity and borehole thermal resistance. The values of these two parameters are functionally linked and critical for the thermal performance of GHEs. Since the middle of the 1990s researchers suggested different approaches to measure ground thermal properties in field, and the number of mobile TRTs were built in different countries to carry out these measurements [69]. Today the TRTs are widely used to estimate the ground thermal properties as well as the performance of heat transfer between the GHE and the ground. Various methods are utilized to analyze the inlet, T_{in} (°C), and outlet, T_{out} (°C), fluid temperature data to estimate ground properties.

The primary thermal properties of interest for the performance assessment of GHEs are:

(i) effective ground thermal conductivity, and

(ii) borehole thermal resistance.

- **Effective ground thermal conductivity (λ_{eff})**

The ideal design of VGHEs depends on the value of the effective ground thermal conductivity around the VGHEs. The effective ground thermal conductivity is higher than thermal conductivity of the ground around the borehole. The former is estimated by TRTs, which indicate a mean value for the ground around the vertical ground heat exchanger (influenced by the impacts of groundwater flow, borehole grouting, natural convection in the boreholes, etc.).

- **Borehole thermal resistance ($\mathbf{R_b}$)**

The borehole thermal resistance can be calculated by using steady state heat transfer models, which are designed for this purpose. The borehole thermal resistance is the thermal resistance between heat carrier fluid in the legs of the U-Tube and the borehole wall as shown in Figure 3.1.

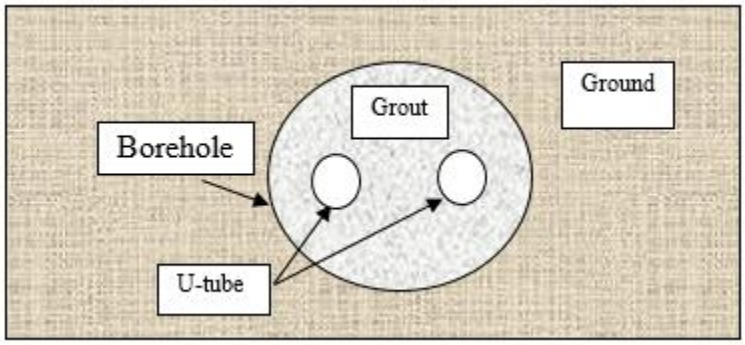

Figure 3.1: Cross section of the borehole

The borehole thermal resistance is defined as:

$$R_b = \frac{(T_f - T_b)}{q} \qquad \textbf{(3.1)}$$

The VGHE consists of three components: the fluid, the pipe, the grout material as shown in Figure 3.2. The borehole thermal resistance can be expressed as shown in the following equation [70, 71, 72, 73]:

$$R_b = R_f + R_p + R_g \qquad \textbf{(3.2)}$$

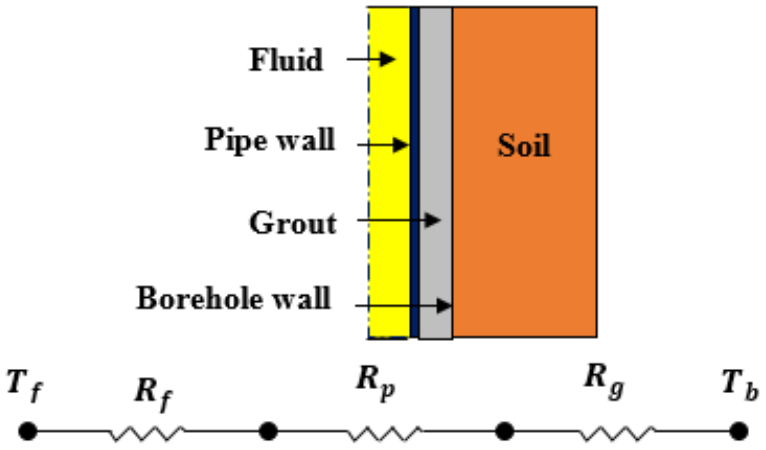

Figure 3.2: Thermal resistance in VGHE [12]

The thermal resistance of the fluid can be calculated by using the following equation [70, 72, 73]:

$$R_f = \frac{1}{2\pi r_i h_i} \quad \textbf{(3.3)}$$

Where, h_i is the convective heat transfer coefficient of the fluid inside the pipe W/ m^2. K, and r_i is the inner radius of the pipe (m).

$$h_i = \frac{0.023 Re^{0.8} Pr^n \lambda_f}{r_i} \quad \textbf{(3.4)}$$

Re is the Reynolds number of the fluid, λ_f is the thermal conductivity of the fluid W/ m. K, P_r is the Prandtl number, n = 0.4 for heating and n = 0.3 for cooling.

The thermal resistance of the grout material was calculated by the equivalent diameter method suggested by Gu and O'Neal (1998) which uses a single concentric cylindrical heat sink instead of U-Tube as shown in Figure 3.3 [70, 74, 75]:

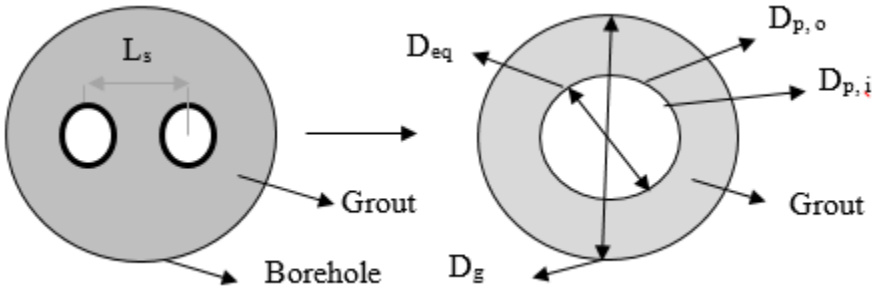

Figure 3.3: Cross section for the equivalent diameter of a VGHE with two legs U- tube

$$D_{eq} = \sqrt{2D_{p,o}L_s} \rightarrow D_{p,o} \leq L_s \leq r_b \quad \textbf{(3.5)}$$

Where, D_{eq} is the equivalent diameter of the pipe (m), $D_{p,o}$ is the outer diameter of the pipe (m), and L_s is the center to center distance between the two legs of the U-Tube (m).

The thermal resistance of the pipe is calculated by using the following equation [15, 72, 75]:

$$R_p = \frac{\ln(\frac{D_{p,o}}{D_{eq}})}{2\pi\lambda_p} \quad \textbf{(3.6)}$$

Where, $D_{eq} = D_{p,i}$ is the inside diameter of the pipe (m), λ_p is the pipe thermal conductivity W/ m. K.

The following equation presents the grout thermal resistance:

$$R_g = \frac{\ln(\frac{D_g}{D_{p,o}})}{2\pi\lambda_g} \quad \textbf{(3.7)}$$

Where D_g is the outside diameter of the grout material m, and λ_g is the grout thermal conductivity W/ m. K. Therefore, the borehole thermal resistance is expressed as:

$$R_b = \frac{1}{2\pi r_i h_i} + \frac{\ln(\frac{D_{p,o}}{D_{eq}})}{2\pi\lambda_p} + \frac{\ln(\frac{D_g}{D_{p,o}})}{2\pi\lambda_g} \quad \textbf{(3.8)}$$

3.1.2 Fundamentals of TRT

TRT is used to determine the heat transfer characteristics between the ground heat exchanger and the ground. Two parameters which define the heat transfer characteristics in this context are: (i) effective ground thermal conductivity, and (ii) borehole thermal resistance [76]. Another important characteristic is the initial ground temperature, which is calculated before the test is started. Figure 3.4 shows the schematic illustration for the experimental apparatus for a TRT.

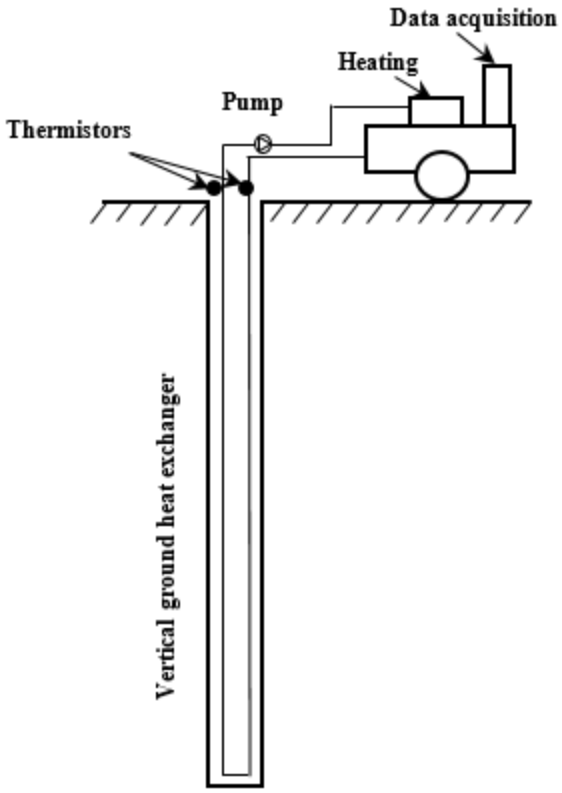

Figure 3.4: Experimental apparatus for a TRT [69]

Eklof and Gehlin (1995) constructed a mobile response test device for TRT at the Lulea University of Technology, Sweden, and in 1996, they also developed a mobile response device to estimate the thermal conductivity of the ground as well as the impact natural convection and flow of the groundwater in the boreholes [14]. Austin (1998) developed a similar experimental apparatus at Oklahoma State University, USA to estimate the ground thermal properties [15]. Sanner et al (1999) performed the field TRT in Germany [16]. In field, TRTs have now become widely utilized in Europe, North America, South America, Asia, and Africa to estimate ground thermal properties for GSHP. Several TRTs were carried out in different parts of the world, including Chile and Argentina [47], Cyprus [48], Saudi Arabia [49], Bulgaria [55], Ecuador [64], Libya [77], and Algeria [78].

TRTs were conducted in the laboratory to characterize thermal properties of GHEs. Beier et al. (2011) built a large horizontal sandbox (length: 18 m, width: 1.8 m, and height: 1.8 m) with a single U-Tube horizontal GHE. Several thermocouples were also placed at specific locations in the sandbox. It was reported that the temperature data that collected during the test were used to

provide independent values for borehole thermal resistance and soil thermal conductivity. These independent values were used to verify models of ground heat exchangers [51]. Shirazi and Bernier (2014) designed and constructed a small experimental apparatus (length: 1.35 m and diameter: 1.4 m) for a single U-Tube VGHE to study transient heat transfer behavior [63]. Blázquez et al. (2017) performed small-scale (length: 1 m and diameter: 0.5 m) laboratory studies to study the impacts of different pipe configurations, including single and double U-Tube (with or without spacers), and spiral pipes on the efficiency of VGHEs [46]. Similar studies were also done by Katsura et al. (2006), Lei and Dai (2013), and Erol and François (2014) [21, 25, 26].

3.1.3 Describing the practical procedures for the TRT

As mentioned in chapter 2 (Section 2.1.1.4), Mogensen (1983) proposed the idea of the TRT [13]. Thereafter, other researchers established the practical procedures to conduct the test in the field [4, 14, 15, 29, 44]. These procedures include estimating the initial ground temperature, measuring the flow rate of heat carrying fluid and heat input rate, and estimating the time duration of the test.

- **Determination of the average initial ground temperature**

The initial average ground temperature has a significant effect in the design of VGHE. An accurate estimation for the average initial soil temperature is needed for the correct design of the VGHE. It is to be noted, the initial ground temperature increases with the increased depth [79, 80]. The average initial ground temperature commonly can be estimated by using three different approaches before the TRT is started.

The first approach is circulating the heat carrier fluid in a close system through the VGHE for about half an hour and without adding heat during the test. The inlet and outlet heat carrier fluid temperatures are recorded at constant intervals, every 30 seconds by the data acquisition system. The average initial ground temperature is calculated by using the inlet and outlet temperatures data collected during 30 minutes. Nevertheless, there is no heat injection by heater during this period, but at the same time some heat will be added into the system by the pump.

The second approach is to insert thermocouples down into the water-filled U-Tube and record the temperatures of water at different depths. An average initial ground temperature is calculated from the collected temperature data [14, 80, 81].

The third approach is to collect the temperatures of soil at different locations and depths after few days of construction of the experimental apparatus. Then, average initial ground temperature is calculated from the collected temperature data.

- **Heat injection rate**

During TRT, the carrier fluid is heated by electricity to generate a constant heat rate, injected to the ground by using heat carrier fluid (e.g. water). This heat rate is very similar to the real value for the operation of GSHP. Gehlin and Hellström (2003) noted that heat transfer rate of 50 W/ m produces the temperature difference at the range of 0.5 °C to 10 °C [82]. It is recommended that the heat injection rates be at a range between 50 W/ m -80 W/ m in the TRT in real life applications, but rates outside these ranges can be used in the laboratory for parametric studies [2, 28]. In this study, the rates of heat injection used were within the range of 25 W/ m -80 W/ m.

- **Flow rate**

Laboratory experiment study for a horizontal sandbox (length: 18 m, width: 1.8 m, depth: 1.8 m) was conducted by Beier et al. (2011) to estimate the ground thermal properties. A constant heat injection rate 1056 W/ m was injected throughout the test with a constant flow rate (V) of 0.197 L/ s, and the TRT was conducted for 50 hours [51]. Shirazi and Bernier (2014) conducted TRT for small scale single U-Tube VGHE to study transient heat transfer in this model. The TRT is contented for 73 hours and the average volumetric flow rate was 0.0114 L/ s throughout the test [63]. Gu and O'Neal (1998) established a small-scale single U-Tube VGHE to estimate the effects of backfills on the performance of U-Tube VGHE at a volumetric flow rate of 0.4 L/ min [83]. The flow rates adopted in this research were within a range of 0.118 to 1.5 L/ min.

- **Measurement duration**

The duration of TRT is a practical concern which is also critical for the reliable determination of ground thermal properties. Kavanaugh (2000, 2001) recommended the time required to obtain

reliable data from the test would be at a range of 36 hours to 48 hours (Ashrae 2011) while Gehlin (1998) recommended the same at a range of 50 to 60 hours [2, 84]. According to their field experiences regarding the time needed for collecting data, Austin et al (1998) recommended that the period of time for the TRT must be minimum 50 hours to estimate reliable ground properties [15]. Beier et al. (2011) needed 52 hours to collect temperature data during TRT from the single U-Tube horizontal GHE within the sandbox to estimate the reliable ground thermal properties [51]. Shirazi and Bernier (2014) conducted TRT to study transient ground heat transfer behavior of the single U-Tube VGHE. The heat was injected for 73 hours into the single U-Tube VGHE, which was inserted in a small-scale sand tank [63]. In this study, the time period used for the TRT within a range of 50 to 60 hours.

- **Waiting period before the test and recovery time**

After the construction of the GHE, it is important to know the time required for the soil to reach a steady state condition. It is recommended that there are two different waiting periods, based on the soil thermal conductivity, to conduct the TRTs after the VGHEs are installed in the ground. A five-day period is suggested as the waiting period for the low-conductivity soil $\lambda < 1.7$ W/ m. K, while three-day period is suggested for high-conductivity soil $\lambda > 1.7$ W/ m. K [2].

Another factor to be considered in the TRT is the recovery time, which represents the period between two tests in the same area. It is very important for the ground temperature to return to a range of -272.85 ºC of the initial ground temperature before another test starts [2]. Javed et al. (2011) recommended that the ground temperature must return to a near range of -273.05 ºC to -272.85 ºC of the initial ground temperature before conducting another test [59]. This study followed the same recommendation (i.e. -272.85 ºC).

3.2 Line source theory

The goal of using the TRT is to estimate the heat transfer between the GHE and the ground, and also the thermal properties of the ground. The rate of the heat transfer of the GHE per unit depth can be calculated by measuring T_{in} and T_{out}, and flow rate of the heat carrier fluid, which circulates into the GHE, as expressed in equation 3.9 [15, 85, 86, 87, 88, 89].

$$q = \frac{C_p \dot{m} (T_{in} - T_{out})}{H} \quad \textbf{(3.9)}$$

Where,

q is the rate of heat transfer of the GHE per unit depth (W/ m), T_{in} and T_{out} are the inlet and outlet fluid temperatures of the GHE (ºC), C_p is the specific heat of the circulating fluid J/ kg. K, $\dot{m}$ is the mass flow rate of the heat carrier fluid in circulation (kg/ s), and H is the borehole depth (m).

Line source model is the analytical solution of the heat transfer problem between the borehole and the vicinity infinite region, as shown in Figure 3.5. To estimate the ground thermal properties, the line source model (LSM) has been used in this research. This approach is commonly used in the practical engineering for Borehole Heat Exchanger (BHE). Line source model is considered one important method for the mathematical models of VGHE in TRT. Ingersoll and Plass (1948) reported that the infinite line source was used in the 40s to calculate the ground temperature change over time for ground loop heat exchangers. Mogensen (1983) carried out the first field study to estimate the thermal conductivity of the ground by using this theory [15, 70, 80, 85].

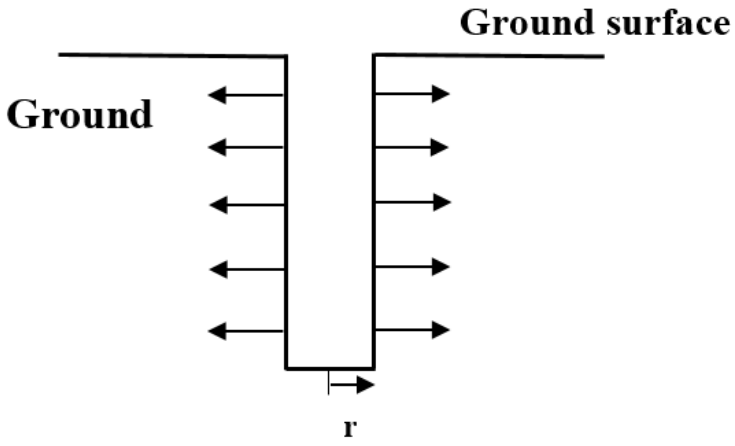

Figure 3.5: Schematic illustration of the line source mode

3.2.1 Mathematical expressions

Temperature at a location of an infinite solid depends on thermal diffusivity(α), as shown in the fundamental equation of heat conduction:

$$\frac{\partial^2 T}{\partial x^2}+\frac{\partial^2 T}{\partial y^2}+\frac{\partial^2 T}{\partial z^2}=\frac{1}{\alpha}\frac{\partial^2 T}{\partial t^2} \qquad \textbf{(3.10)}$$

Where,

T is temperature at a point (x, y, z), and it is a function of time (t) and thermal diffusivity (α).

Thermal diffusivity $(\alpha)=\lambda/\rho c$.

Where,

α is thermal diffusivity (m^2/ s), ρ is the density (kg/ m^3), λ is the thermal conductivity (W/ m. K), and c_p is the specific heat capacity (J/ kg. K).

At point (x, y, z) and at time t in an infinite solid, the temperature goes up as a result of the emission of the amount of instantaneous heat in point $(\acute{x},\acute{y},\acute{z})$. The material initial temperature is assumed to be 0 °C. Equation (3.10) is satisfied by:

$$T=T(r,t)=\frac{Q}{8(\pi\alpha t)^{3/2}}e^{-((x-\acute{x})^2+(y-\acute{y})^2+(z-\acute{z})^2)/4\alpha t} \qquad \textbf{(3.11)}$$

This expression (Eq. 3.11) becomes infinite at $(\acute{x},\acute{y},\acute{z})$ when t=>0. At all the other points it tends to zero. T(r,t) represents the temperature in point (x,y,z) at time t.

Instantaneous line source is crossing through the point $(\acute{x},\acute{y})$ while it is parallel to the z-axis. The temperature is calculated by integrating equation 3.11:

$$T=T(r,t)=\frac{Q}{8(\pi\alpha t)^{\frac{3}{2}}}\int_{-\infty}^{\infty}d\acute{z}\,e^{-\frac{(x-\acute{x})^2+(y-\acute{y})^2+(z-\acute{z})^2}{4\alpha t}}$$

$$=\frac{Q}{4\pi\alpha t}e^{-[(x-\acute{x})^2+(y-\acute{y})^2]/4\alpha t}$$

Where, $r^2=((x-\acute{x})^2+(y-\acute{y})^2$

$$T(r,t)=\frac{Q}{4\pi\alpha t}e^{-r^2/4\alpha t} \qquad \textbf{(3.12)}$$

The above equation expresses line source equation only when $t=0$, so the previous equation can be changed for a continuous line source over a long period of time. If the heat $Q(\acute{t})$ starts to be injected at $t=0$, while the soil temperature is zero, then the temperature at time t will be:

$$T(r,t) = \frac{1}{4\pi\lambda_{eff}} \int_0^t Q(\acute{t}) e^{-r^2/4\alpha(t-\acute{t})} \frac{d\acute{t}}{t-\acute{t}} \quad \textbf{(3.13)}$$

When $Q(\acute{t})$ is constant → $Q(\acute{t}) = q$, then the equation 3.13 become:

$$T(r,t) = \frac{q}{4\pi\lambda_{eff}} \int_0^t e^{-r^2/4\alpha(t-\acute{t})} \frac{d\acute{t}}{t-\acute{t}} \quad \textbf{(3.14)}$$

A new variable is defined as:

$$\beta = \frac{r^2}{4\alpha(t-\acute{t})} = \frac{r^2}{4\alpha}\left(\frac{1}{(t-\acute{t})}\right) \quad \textbf{(3.15)}$$

$\acute{t} = 0 \ \rightarrow \beta = \dfrac{r^2}{4\alpha t}$

$\acute{t} = t \ \rightarrow \beta = \infty$

$$\frac{d\beta}{d\acute{t}} = \frac{\beta}{(t-\acute{t})} = \frac{r^2}{4\alpha}\left(\frac{-(1)(-1)}{(t-\acute{t})^2}\right) = \frac{r^2}{4\alpha(t-\acute{t})^2}$$

$$\frac{\mathrm{d}\beta}{\mathrm{d}\acute{t}} = \frac{\beta}{(\mathrm{t}-\acute{\mathrm{t}})} \rightarrow \frac{\mathrm{d}\beta}{\beta} = \frac{\mathrm{d}\acute{\mathrm{t}}}{(\mathrm{t}-\acute{\mathrm{t}})} \quad \textbf{(3.16)}$$

Substituting (3.15) and (3.16) into the equation (3.14)

$$T(r,t) = \frac{q}{4\pi\lambda_{eff}} \int_{\frac{r^2}{4\pi t}}^{\infty} \frac{e^{-\beta}}{\beta} d\beta \quad \textbf{(3.17)}$$

Where $\int_{\frac{r^2}{4\pi t}}^{\infty} \frac{e^{-\beta}}{\beta}\ d\beta = E_t(\tau) = E_1\left(\frac{1}{4\tau}\right)$ *and* $\tau = \frac{\alpha t}{r^2}$

$$T(r,t) = \frac{q}{4\pi\lambda_{eff}} E_1\left[\frac{r^2}{4\alpha t}\right] \quad \textbf{(3.18)}$$

When the value of $\frac{r^2}{4\alpha t}$ is small

$$E_1\left[\frac{r^2}{4\alpha t}\right] = \gamma + ln\frac{r^2}{4\alpha t} - \frac{r^2}{4\alpha t} + \frac{1}{4}\left[\frac{r^2}{4\alpha t}\right]^2 + O\left(\left[\frac{r^2}{4\alpha t}\right]^3\right) \cong ln\left[\frac{4\alpha t}{r^2}\right] - \gamma \quad \textbf{(3.19)}$$

Where $\gamma = 0.5772$ ... represents Euler's constant.

By putting $ln\left[\frac{4\alpha t}{r^2}\right] - \gamma$ from equation (3.19) into equation (3.18), the equation becomes:

$$T(\mathrm{r},\mathrm{t}) = \frac{q}{4\pi\lambda_{eff}}\left[ln\left[\frac{4\alpha t}{r^2}\right] - \gamma\right] \quad \textbf{(3.20)}$$

The next equation can be used to calculate the borehole temperature for the transient process [14].

$$\mathrm{T_b}(\mathrm{r},\mathrm{t}) = \mathrm{T_o} + \mathrm{T}(\mathrm{r},\mathrm{t}) \quad \textbf{(3.21)}$$

Then by substitute the value of $\mathrm{T}(\mathrm{r},\mathrm{t})$ in equation (3.20), the equation becomes as the following:

$$T_b(r,t) \cong T_o + \frac{q}{4\pi\lambda_{eff}}\left[ln\left(\frac{4\alpha t}{r^2}\right) - \gamma\right] \quad \textbf{(3.22)}$$

As shown in equation (3.21), the borehole wall temperature at time t ($T_b(r,t)$) is a sum of the initial ground temperature (T_o) and the ground temperature at distance r and time t ($\mathrm{T}(\mathrm{r},\mathrm{t})$). Also, there is a relationship between the ground temperature and the heat carrier fluid temperature T_f. The borehole thermal resistance is a function of a constant heat injection, the heat carrier fluid temperature $T_f(t)$, and the borehole wall temperature. It can be defined by using the following equation [90, 91]:

$$T_f(t) - T_b(r,t) = R_b q \quad \textbf{(3.23)}$$

$\mathrm{T_b}(\mathrm{r} = r_b, \mathrm{t})$ is the temperature on the borehole wall at time t (ºC)

$\mathrm{T_f}(t)$= (($\mathrm{T_{in}} + \mathrm{T_{out}}$)/2), where, $\mathrm{T_f}(t)$ denotes the arithmetic mean of the inlet fluid temperature ($\mathrm{T_{in}}$) and outlet fluid temperature ($\mathrm{T_{out}}$) of the borehole (ºC)

The line source temperature at the borehole radius (r_b), including the impact of the borehole thermal resistance (R_b) between the heat carrier fluid and the borehole wall, was used to evaluate the mean fluid temperature, $T_f(t)$. Then the fluid temperature as a function of time could be written as:

$$T_f(t) = \frac{Q}{4\pi\lambda_{eff}H}ln(t) + \frac{Q}{H}\left[\frac{1}{4\pi\lambda_{eff}}\left\{ln\left(\frac{4\alpha}{r_b^2}\right) - \gamma\right\} + R_b\right] + T_o \quad \textbf{(3.24)}$$

Where,

$R_b$is the borehole thermal resistance (m. K/ W), T_o is the initial underground temperature (ºC).

Also the borehole thermal resistance can be expressed by the following equation:

$$R_b = \frac{H}{Q}\left[T_f(t) - T_o\right] - \frac{1}{4\pi\lambda_{eff}}\left[ln(t) + ln\left(\frac{4\alpha}{r_b^2}\right) - \gamma\right] \quad \textbf{(3.25)}$$

It is noticed that the second and third terms on the right hand in the above equation are constant. Then it can be considered that the above equation is similar to the linear slope equation as $y = m.x + b$.

Eklof and Gehlin (1996) assumed that there is a linear relationship between the mean fluid temperature and the logarithm time ln (t) [14, 89, 92]. It is also expressed by using the following equation:

$$T_f(t) = m.ln(t) + b \quad \textbf{(3.26)}$$

$$\text{Slope} = m = \frac{q}{4\pi\lambda_{eff}} \rightarrow \lambda_{eff} = \frac{q}{4\pi m} \quad \textbf{(3.27)}$$

3.3 Discussion summary

This chapter presented the principles and procedures of the thermal response test (TRT), and line source theory used to determine the effective ground thermal conductivity and the borehole thermal resistance. As shown in section 3.1.3, a number of variables must be considered during the TRT such as the initial ground temperature, the flow rate of heat carrying fluid, the heat injection rate, duration of the test, and the waiting period before the test and recovery time. The derivation of the line source theory is explained in section 3.2. The equations in this section are used to find out variables such as the heat injection/extraction rate of VGHE (see equation 3.9), the slope (see equation 3.26), the effective ground thermal conductivity (see equation 3.27), and the borehole thermal resistance (see equation 3.25).

Chapter 4

Small-scale experimental apparatus

This chapter contains the information regarding materials, design, construction and instrumentation of the small-scale test apparatus used in this study to conduct thermal response tests (TRTs).

4.1 Introduction

To evaluate the thermal performance of vertical ground heat exchangers (VGHEs), a small-scale experimental apparatus was designed, constructed, and commissioned in the Laboratory (E-Hut 109) at the University of Victoria. The main objective of this chapter is to describe the small-scale experimental apparatus (Figure 4.1).

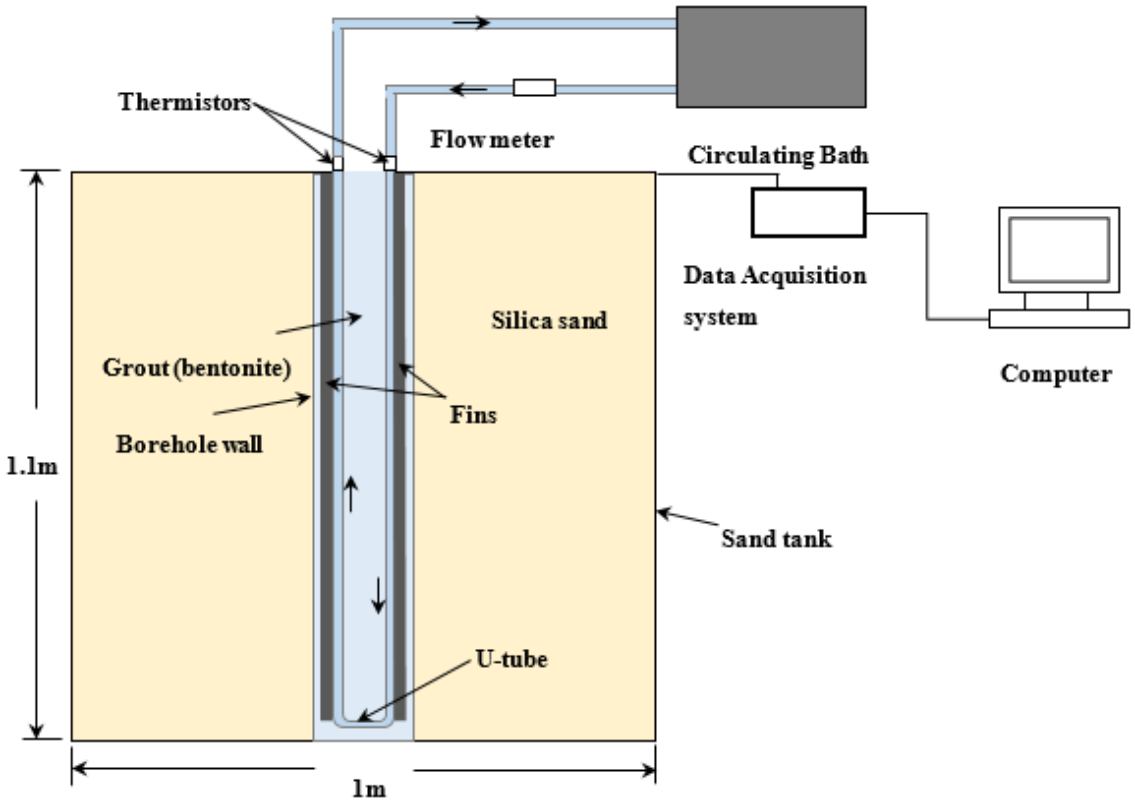

a) Schematic illustration of the experimental setup.

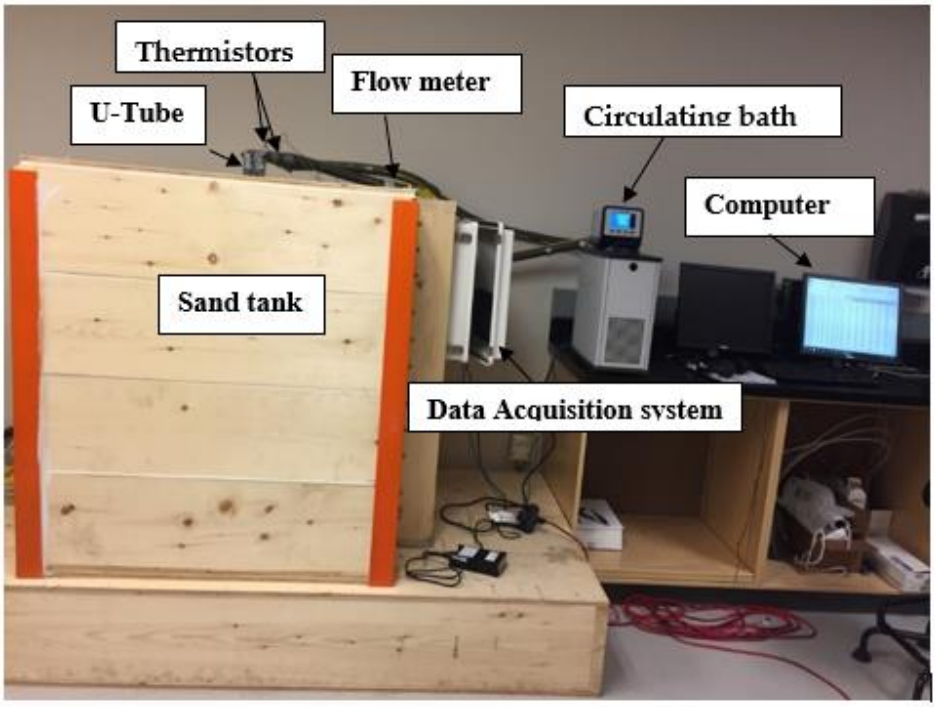

b) Picture of the experimental setup.

Figure 4.1: Small-scale of the experimental apparatus

4.2 Description of the small-scale experimental apparatus

The small-scale experimental apparatus comprises of three main components: (i) a water supply system, (ii) a sand tank, and (iii) a data acquisition system, as shown in Figure 4.1. Further details regarding these three components are provided below.

4.2.1 Water supply system

The water supply system is used to circulate water through the closed system at the specific temperature and flow rate. Major components of water supply system are: (i) circulating bath, (ii) water flow meter, (iii) flow regulation valve, (iv) thermistors, and (v) data logger. Details regarding these components are outlined below.

- **Circulating Bath**

In this study a Circulating Bath (see Figure 4.1b), with a temperature range -20 °C to 135 °C, was used to circulate the carrier fluid (water) in a closed loop between the VGHE and the water

supply system, and add heat to the carrier fluid. The heat carrier fluid flow rate was 13.5 L/ min. The temperature stability of the circulation baths is approximately ±0.01 ºC.

- **Water flow meter**

The water flow rate through the system was measured and modified by the flow meter (Omega FTB-1311) as shown in Figure 4.2. The flow meter used can measure flow rates in the range from 0.118 to 1.5 L/ min with ±1% actual flow accuracy.

Figure 4.2: The water flow rate

- **Flow regulation valve**

Flow regulation valve is used to control the amount of fluid flow rate into the system as shown in Figure 4.2.

- **Thermistors**

Two thermistors (Omega TH-44032-1/4NPT-80; temperature range 0 °C to 75 °C with an accuracy ±0.1 °C) were installed at the inlet and outlet of the VGHE to measure the inlet and outlet water temperatures (see Figure 4.1b). The connecting pipes between the sand tank and the bath were insulated to decrease the heat loss between the connecting pipes and the ambient air, (see Figure 4.1b).

- **Data logger**

A data logger (Omega, OM-62) was used to record the ambient air temperature in the lab during the TRT and recovery time. It can measure the temperature at range of -40 °C to 70 °C and with an accuracy ± 0.5 °C as shown in Figure 4.3.

Figure 4.3: Photo of data logger (MO-62)

4.2.2 Sand tank

The sand tank used in this study consists of: (i) wooden box, (ii) borehole, (iii) grout (bentonite/silica sand), (iv) pipe configuration, (v) spacers, (vi) thermocouples, and (vii) soil (silica sand).

- **Wooden box**

In this study, the sand tank (length: 1.0 m; width: 1.0 m; height: 1.1 m) was constructed with plywood (thickness: 2 cm) and the borehole was inserted in it (see Figure 4.1b).

- **Borehole**

VGHEs are usually consisting of a single U-Tube or double U-Tube inserted into the boreholes. Typically, U-Tube pipe is inserted into the borehole at a depth of 20 m to 300 m, with typical diameters of 76 mm to 150 mm [20, 56, 57]. In this study, a polyvinylchloride (PVC) pipe (length: 1.1 m, inner diameter: 7.6 cm, and outer diameter: 8.2 cm) was inserted from the top at the center of the sand tank, as shown in Figure 4.4.

Figure 4.4: PVC tube (borehole)

- **Grout**

In this study, two different grout materials (bentonite and silica sand) were used to fill the space between the U-tube pipe and the borehole wall (see Figure 4.1a).

- **Pipe configurations**

In this study two different pipe configurations were used: (i) a conventional single U-Tube pipe, and (ii) a novel U-Tube pipe.

1. **Conventional single U-Tube pipe configuration**

The conventional single U-Tube pipe configuration is made with copper, as shown in Figure 4.5a. It consists of two copper pipes (length: 1 m, inner diameter: 12.7 mm, and outer diameter: 16 mm). The thermal conductivity of copper pipe is 400 W/m. K. Figure 4.5b shows the cross section of the conventional single U-Tube pipe configuration.

a) Conventional U-Tube pipe configuration.

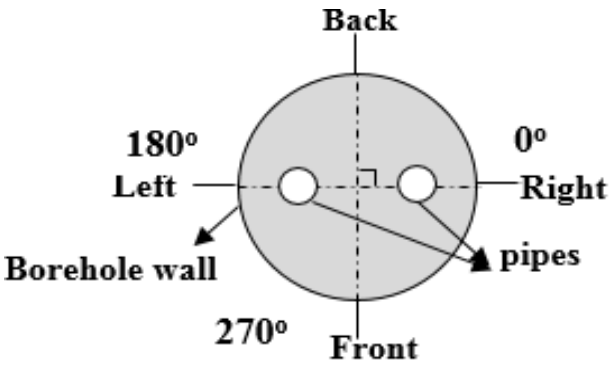

b) Cross section of conventional single U-Tube pipe VGHE

Figure 4.5: Conventional U-Tube pipe configuration VGHE

2. Novel U-Tube pipe configuration

A novel U-Tube pipe configuration is suggested to enhance the heat transfer rate in VGHEs. The novel U-Tube pipe configuration consists of the conventional single U-Tube with two outer fins in two directions on the outer side. The fins are used to enhance heat transfer by conduction through the solid and also by convection from the solid boundaries. The fins are widely used in heat exchanging devices (e.g. air conditioning, refrigeration, heat exchangers in power plants, radiators in cars, and electronic systems). There are many shapes of fins that could be used to enhance the heat transfer rate such as rectangular, trapezoidal, and concave.

According to published literature, several shapes of fins had an impact on thermal efficiency. Moradi and Ahmadikia (2010) carried out numerical and analytical studies to examine the effects of three different shapes of fins (convex, rectangular, and concave) on the thermal efficiency of the fin. The results indicate that the exponential shape had a higher efficiency, followed by the rectangular shape and the convex shape [93]. Torabi et al. (2013) studied the effects of three different fin shapes (concave, rectangular, and trapezoidal) on the efficiency. The results show that the concave shape had a more suitable efficiency, then the trapezoidal shape and the rectangular shape [94]. Based on the obtained results mentioned above, the fins were planned to be designed in concave shape, but then it was decided to change them to trapezoidal shape because the tools in the workshop at the University of Victoria were not suitable for producing fins in concave shape. Another secondary reason to select the trapezoidal shape is its small tip at the end of the fin. This means it can be a good option to increase the fin length without touching the borehole wall, compared to the rectangular fin, which has a wide tip at the end of the fin. However, analytical solutions for the rectangular and trapezoidal shapes are carried out later as shown in Appendix A. The heat transfer rate through the rectangular fin was higher compared to the trapezoidal fin. Appendix A also shows how to calculate the maximum fin length. The optimum fin length was approximately between 0.07 m to 0.12 m (see Appendix A, Figure A.3), and a fin length of 0.08 m was chosen to fit design considerations.

In this study, the fins are made with copper (height: 1 m, length: 8 mm, and width: 4 mm). Figure 4.6a shows the cross section of the trapezoidal shape and figure 4.6b shows the cross section of the novel U-Tube pipe configuration.

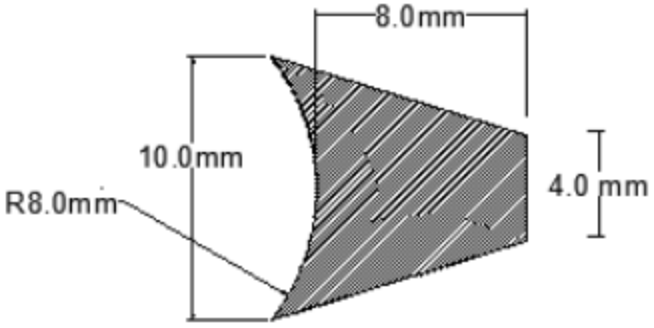

a) Shape and 2-D of the fin.

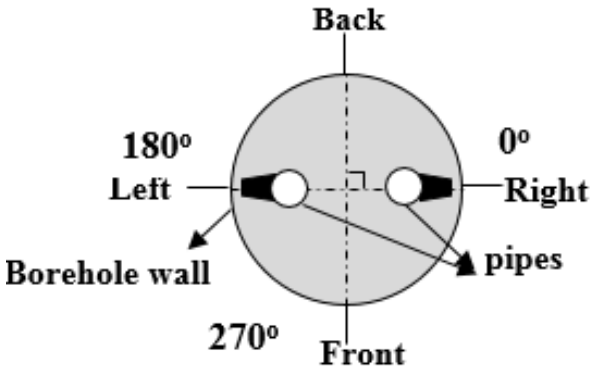

b) Cross section of novel U-Tube pipe configuration.

a) Cross section of novel U-Tube pipe configuration.

Figure 4.6: Novel U-Tube pipe configuration VGHE

- **Spacers**

Figure 4.7 shows that the spacer is placed in the single U-tube configuration and the novel U-Tube pipe configuration to keep the same distance between the two legs of the U-tube and prevent the two legs from having contact.

a) Side view b) Face view

Figure 4.7: Spacer to fix the constant distance between two legs

In order to position the borehole and place the thermocouples inside the sand tank, a wood-frame is fixed on the top of the tank as shown in Figure 4.8.

Figure 4.8: Wood fixed the borehole

- **Thermocouples**

A total of 64 thermocouples (EXPP-K-24, maximum temperature 105 °C, accuracy ± 0.75° C) were installed at the specific locations along the height, length and width inside the tank to measure the sand temperature throughout the test and recovery time (Figure 4.9).

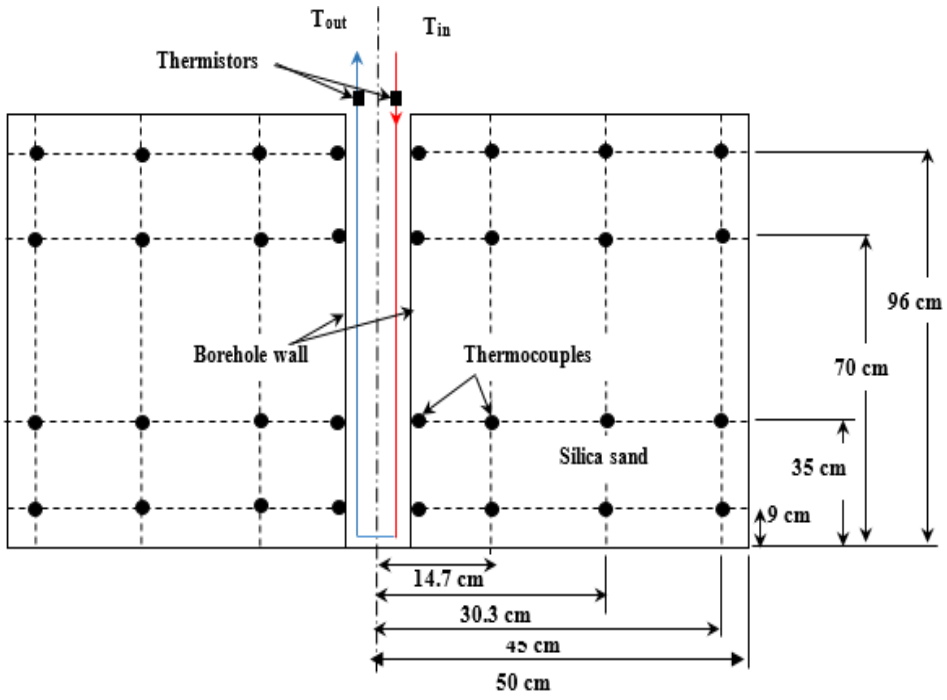

a) Distribution of thermocouples in the sand tank (sectional view)

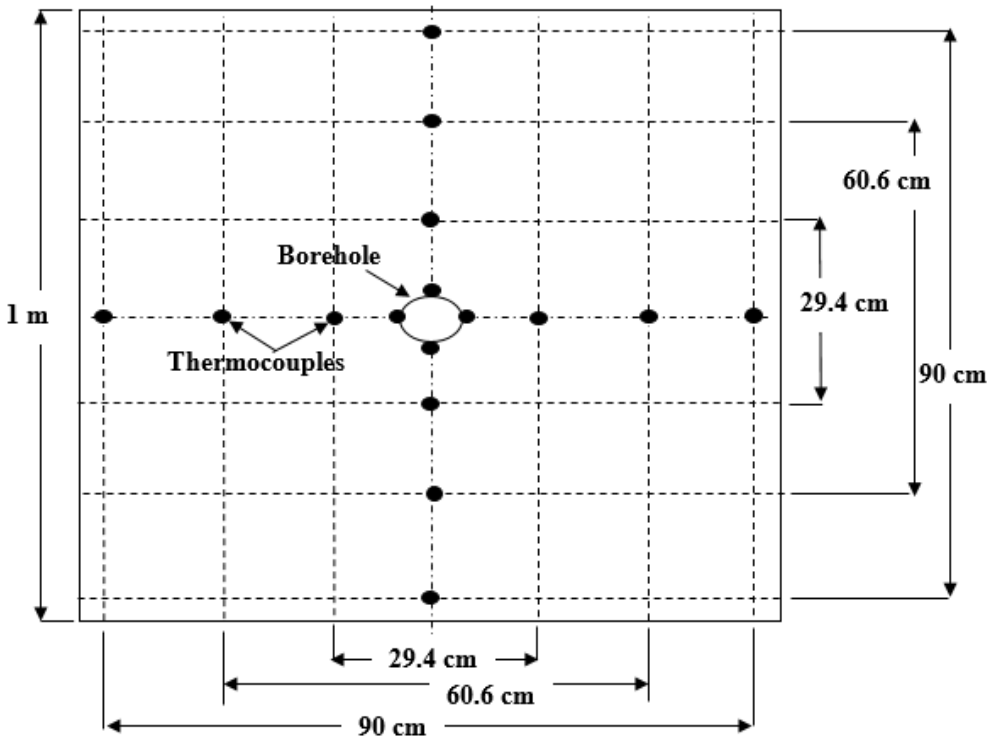

b) Distribution of thermocouples in the sand tank (plan view)

Figure 4.9: Thermocouples in the sand tank

- **Soil (silica sand)**

Soil fills the space between the borehole and the sand tank walls. It is a challenging task to analyze the heat transfer between the legs of the U-Tube and the soil due to the nonhomogeneous nature of the soil in and around the GHE [58]. To study the heat transfer behavior in and around the VGHE, it is very important to use a homogeneous material as soil, such as Ottawa sand type C-109, bentonite, and silica sand that have known thermo-physical properties. Shirazi and Bernier (2014) used the Ottawa sand type C-109 as soil in their research. The thermal conductivity of the Ottawa sand type C-109 is 0.29 W/ m. K and the thermal diffusivity is 0.0198 m^2/ day [63]. Ottawa sand C-109 is a homogeneous graded pure quartz sand with well documented thermal properties. The weight of the Ottawa sand type C-109 required to fill the sand tank was found to be about 6000 kg, which is more than the load carrying capacity of the laboratory wood floor. In order to address this issue, silica sand (1700 kg/ m^3) was used and the weight of silica sand required to fill the sand tank turned out to be only 1500 kg.

4.2.3 Data acquisition system

Campbell scientific data acquisition system (CR1000) was used in this research and it had 80 channel for data recordings (Figure 4.10a). Total number of measurements required in this project was 67 (64 for thermocouples, two for thermistors, and one for water flow meter). To transfer the data, data acquisition system was connected to a personal computer as shown in Figure 4.10b.

a) Data acquisition system b) Data acquisition system connected with a personal computer

Figure 4.10: Photo of data acquisition system

Chapter 5

Performance of conventional and novel single U-Tube pipes

Abstract

A novel U-Tube pipe configuration is suggested to enhance the heat transfer rate in the vertical ground heat exchanger (VGHE). Laboratory experiments are conducted to compare the thermal efficiency of VGHEs with two different pipe configurations: (1) a novel U-Tube pipe configuration (single U-Tube with two outer fins), and (2) a single U-Tube. The results show that the difference between the inlet and outlet temperatures for the novel U-Tube pipe configuration was 0.67 °C after 60 hours, while it was 0.38 °C for the single U-tube after the same amount of time. The borehole thermal resistance for the novel U-Tube pipe configuration was 0.680 m. K/ W, which is 29.2% lower than that of the single U-Tube. The heat exchange rate in the novel U-Tube pipe configuration is increased by 58% compared to the conventional single U-Tube. Measured ground temperatures indicate that compared to single U-Tube pipe configuration, the novel U-Tube pipe configuration has superior heat transfer performance. Based on the experimental results presented in this chapter, it was concluded that increasing the surface area significantly by introducing external fins to the U-tube enhances the heat transfer rate, resulting in increased thermal efficiency of the VGHE.

5.1 Introduction

A ground source heat pump system (GSHP) is an ecofriendly technology utilized for heating and cooling houses and commercial buildings. GSHP technology exploits the constant ground temperature over the year to extract heat from buildings and transfer it into the ground in summer, as well as to extract heat from the ground and transfer it into the buildings in winter [3, 37]. The GSHP system is constructed by connecting a heat pump with a vertical ground heat exchanger (VGHE). Since the second half of the 1990s, TRTs have been used to measure ground thermal

properties (borehole thermal resistance and effective ground thermal conductivity) and characterize the efficiency of VGHEs. Researchers have suggested different approaches to measure ground thermal properties in the field, and a number of mobile experimental apparatuses have been built in different countries to carry out these measurements [69].

The initial capital cost of installing the GSHP systems is a significant consideration in VGHE design. Hence, there are opportunities for designers to do more work in this area and suggest new pipe configurations to increase the heat transfer rate in the VGHEs and thus decrease the depth and cost of borehole installation. During the last decades, several researchers conducted studies to improve the thermal performance of VGHEs by decreasing the thermal resistance between the borehole wall and the ground as much as possible. These studies were based on either numerical or experimental models, the latter includes a small-scale apparatus in the laboratory or a full-scale field investigation.

Gu and O'Neal (1998) built a small-scale single U-Tube VGHE in the laboratory to estimate the effects of backfills (bentonite/masonry sand and bentonite/copper powder) on the heat transfer performance of a single U-Tube VGHE. The single U-Tube copper pipe (inner diameter: 4.8 mm, outer diameter: 6.4 mm, and length: 1.2 m) was inserted in a metal tank. The obtained results showed that backfill materials have an influence on the thermal performance of single U-tube VGHEs [83].

To determine the effects another factor, Pahud and Matthey (2001) conducted TRTs for the double U-Tube VGHEs, with and without spacers, to estimate the influence of these spacers on the borehole thermal resistance. The borehole thermal resistances of double U-Tube VGHEs with and without spacers were 0.141 m. K/ W and 0.143 m. K/ W, respectively [20]. Zeng et al. (2003) suggested an analytical solution considering the influence of fluid axial convective heat transfer on pipe configurations of VGHEs. Two different configurations, single and double U-Tube, of VGHEs were examined by using this method. The results showed that the borehole thermal resistance of double U-Tube VGHE was lower than the single U-Tube VGHE [31].

Esen and Inalli (2009) conducted three TRTs with three different depths (30 m, 60 m, and 90 m) to estimate the thermal performance of the single U-Tube VGHE. The obtained results of the experimental study for the cooling and heating modes show that the borehole heat exchanger with a depth of 90 had the strongest performance, but the optimized depth considering the cost was 60

m with a COP of approximately 3 (see Appendix B) [95]. Javadi et al. (2019) reported that the outlet water temperature in winter and summer increases and decreases with an increase the VGHE depth. Increasing the VGHE depth also leads to increased energy consumption of GSHP and a higher cost. The VGHE depths of 50 to 100 m have been widely used during the last eight years, followed by the depths of 20 to 50 m [96].

To determine the effects of different pipe configurations on the thermal performance of VGHE, Acuña and Palm (2010) proposed a new pipe configuration, coaxial (pipe-in-pipe) VGHE, and it compared with conventional single U-Tube. The outer pipe was in direct contact with the surrounding bedrock. The results showed that the heat transfer performance of the coaxial VGHE was superior to the conventional single U-Tube VGHE [32]. Another field study was conducted by Lee et al. (2011) to estimate the thermal efficiency of two different pipe configurations, the common U-Tube type and a new 3 pipe-type GHEs. The thermal efficiency of the new 3 pipe-type configuration was higher than that of the conventional single U-Tube type [4]. In a study which set out to determine the effects of three different types: (1) coaxial, (2) double U-Tube, and (3) U-Tube VGHEs in Oklahoma City, Beier and Ewbank (2012) found that the best option to reduce the thermal resistance of the borehole was the double U-Tube, followed by the single U-Tube, and finally the coaxial type [34]. In the same year, a field study was performed by Desmedt et al. (2012) to estimate the influence of two different pipe configurations ((1) single U-pipe, and (2) double U-pipe) on the efficiency of the VGHEs. The thermal resistance of the double U-Tube VGHE was 0.162 m. K/ W, 52% lower than the single U-Tube VGHE [35]. To improve the thermal performance of VGHEs, a numerical study was investigated by Haddada and Miyara (2014) to estimate the impacts of pipe numbers inside the borehole on the performance of VGHEs. Four different pipe configurations examined were: (1) U-Tube, (2) multi-tube, (3) three-tube, and (4) four-tube. The heat exchange rate increased between the boreholes and the ground due to an increase in the number of inlet tubes inside the borehole [40].

Kramer and Basu (2014) built experimental apparatus in the laboratory to study the effect of thermal loading on load displacement behavior of the model geothermal pile. The polyvinylchloride (PVC) U-Tube pipe was installed in a sand tank (length: 1.83 m; depth: 1.83 m, width: 1.83 m). The U-Tube pipe consisted of two PVC pipes that had an inner diameter of 12.4 mm with a length of 1.22 m [86]. Shirazi and Bernier (2014) established a small scale experimental

apparatus with a borehole Plexiglas pipe (length: 1.23 m) inserted at the center from the top of the sand tank (length: 1.35 m and diameter: 1.4 m). The TRT was 73 hours for the heat injection and 5 days to let the sand return to its initial ground temperature. It was reported that the borehole thermal resistance for the single U-Tube VGHE was 0.61 m. K/ W [63]. Another small scale VGHE study was conducted by Erol and François (2014) to estimate the effects of backfill materials on the thermal performance of the VGHE. Two parallel pipes were inserted in the 1m length of the VGHE in the sand tank of $1m^3$. Two heat pumps were used to pump the water to pipes at 12 °C, 15 °C inlet and outlet of water temperatures, respectively. The initial temperature of the sand was 20°C [26]. One year later, Cimmino and Bernier (2015) built the experimental setup consisting of a 400 mm tall borehole inserted in center and top of the sand tank (length: 1.35 m, and diameter: 1.4 m). The single U-Tube copper pipe was inserted in the borehole. The objective of this study was to measure the borehole wall temperature at various depths and different times during the TRT. The results showed that the borehole wall temperature increased with an increase in the duration of the TRT [54].

Liu et al. (2015) suggested a new VGHE design with three inlet pipes and one outlet (3I-type) and compared its performance to the single and double U-Tube VGHEs. Experimental results showed that the thermal resistance of the 3I-type was 31% and 15.8% lower than the single and double U-Tubes, respectively [41]. In an analysis of the influences of the different pipe material properties (copper and high density polyethylene pipes) on the performance of VGHEs, Ramadan (2016) found the performance trend remains same for both copper and high density polyethylene pipes in a ground heat exchanger [97]. Another field was conducted by Chang and Kim (2016) to estimate the influence of two different pipe configurations, single U-Tube and double U-Tube, on the thermal performance of VGHEs. The thermal resistance of the single and double U-Tubes was 0.130 m. K/ W and 0.081 m. K/ W, respectively [44]. In a numerical study investigated by Luo et al. (2016) the thermal efficiency of four different pipe configurations (double-U, triple-U, double-W, and spiral) was estimated. The triple U-Tube had a higher thermal efficiency, followed by the double- W, the spiral type, and the double U-Tube. The results also indicated that the double -W type had the lowest economic performance, followed by the spiral type, the double-U type, and the triple-U type [45]. Two years later, another numerical study was investigated by Serageldin et al. (2018) to improve the performance of VGHE by suggestion a novel U-Tube pipe configuration (an oval U-Tube), and it compared a conventional single U-Tube. The results showed that the

thermal resistance of the oval U-Tube was 0.125 m. K/ W, and 15.8% lower than the conventional single U-Tube [98]. A field study was conducted by Bae et al. (2019) to estimate the thermal performance for four different pipe types (High-density Polyethylene (HDPE) type, HDPE-nano type, spiral fin type, and coaxial type). The results showed that the best option to reduce the thermal resistance of the borehole was the spiral fin type (0.181 m. K/ W), followed by the HDPE-nano type (0.181 m. K/ W), HDPE type (0.183 m. K/ W), and a coaxial type (0.306 m. K/ W) [99].

A recent laboratory study was conducted by Li et al. (2018) to estimate the effects of ground stratification on the performance of GHEs. Two U-Tube copper GHEs were installed in a sand tank (depth: 6.25 m, length: 1.5 m, and width 1 m), and the sand tank was filled with sand and clay. The two U-Tube pipe consisted of two copper pipes that had an inner diameter of 5 mm and diameter outer 5.5 mm with a length of 6.25 m. The results showed that an increase in the ground heat injection rates leads to a significant increase in the effects of ground stratification [100]. One year later, Liang et al. (2019) constructed an experimental setup with a small-scale spiral-tube copper pipe VGHE inserted in the metal container (diameter: 0.8 m, and height: 1.1 m) setup to investigate the influences of two parameters ((1) volume flow rate and (2) backfill materials) on the thermal performance of a small-scale spiral-tube VGHE. The results showed that the heat exchange rate in the spiral-tube VGHE in blend added to the sand with different Reynolds numbers (3000 – 8000) enhanced by 20% – 31% compared to the native sand [101]. Researchers proposed that testing times can be significantly reduced by using a radius of influence in the range of 0.5 m to 1.5 m, this provides satisfactory temperature readings to determine thermal properties [102, 103]. In this study, a novel U-Tube pipe configuration (conventional single U-Tube with two outer fins) is proposed to improve the thermal performance of VGHE by increasing the surface area for a higher heat transfer rate. The primary aim of this study is to evaluate the thermal performance of the novel U-Tube pipe configuration and compare it with the conventional single U-Tube pipe configuration. In addition, the ground thermal properties for these two pipe configurations were estimated by using line source theory (see section 3.2). In order to conduct TRTs, a small-scale experimental setup was designed, constructed, and commissioned in the laboratory (see chapter 4).

The conventional single U-Tube pipe consists of two copper pipes that have an inner diameter of 12.7 mm and outer diameter of 16 mm with a length of 1 m (see figure 4.5). The novel U-Tube

pipe configuration consists of two copper pipes that have an inner diameter of 12.7 mm and outer diameter of 16 mm with a length of 1 m. The fins are made of copper and have a cross-section of 8 mm x 4 mm, attached over the full height (1 m) of the U-Tube (see figure 4.6). Figure 5.1 shows the cross-section of the two different pipe configurations. The parameters for the two different pipe configurations of VGHEs are listed in Table 5.1.

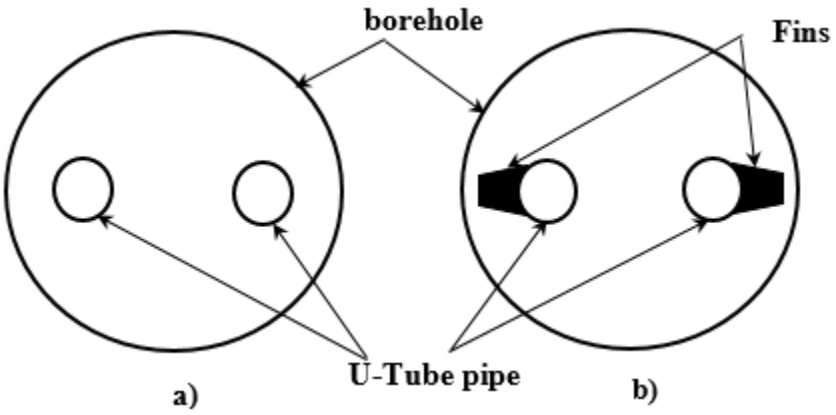

Figure 5.1: Cross-section of the two different pipe configurations: (a) Conventional single U-Tube; (b) Novel U-Tube pipe configuration

A total of 64 thermocouples (EXPP-K-24) are distributed at specific distances inside the sand tank to measure the temperatures at different locations throughout the test and during the recovery time until the sand temperature reached the initial temperature. The thermocouples can measure a maximum temperature of 105 °C with an accuracy ± 0.75 °C. Each direction has 16 thermocouples as shown in Figure 5.2.

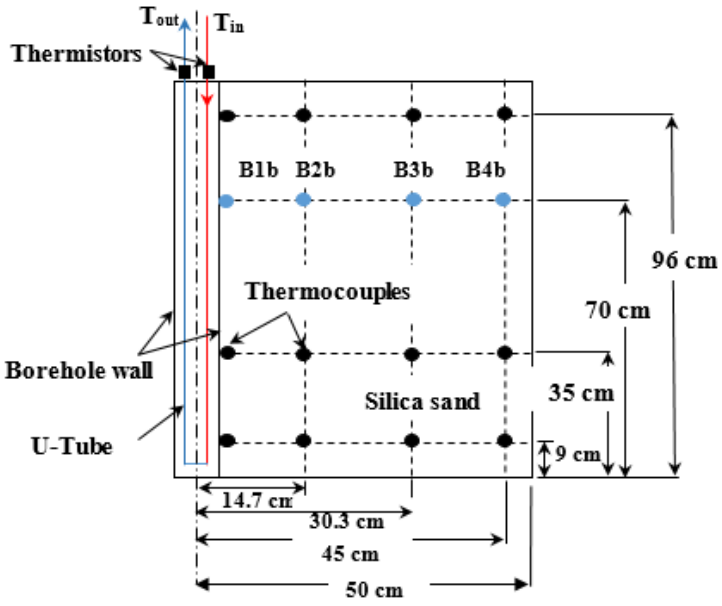

Figure 5.2: Front view for the 16 thermocouples at borehole wall and in silica sand at specific locations on the right side of sand tank

Table 5.1*:* Parameters for the two different pipe configurations of VGHEs

Parameters	Value	Unit
U-Tube pipe outer diameter	16	mm
U-Tube pipe inner diameter	12.7	mm
Space between U-Tube pipes	29	mm
Length of the U-Tube pipe	1.05	m
Thermal conductivity of copper pipe [104]	400	W/ m. K
Fin width	4	mm
Fin length	8	mm
Fin height	1	m
Thermal conductivity of copper fin [104]	400	W/ m. K
Borehole outer diameter (PVC)	82	mm
Borehole inner diameter (PVC)	75	mm
Thermal conductivity borehole wall (PVC) [104]	0.19	W/ m. K
Thermal conductivity bentonite (grout) [105]	0.8	W/ m. K
Thermal conductivity of silica sand (ground/soil) [40]	2.42	W/ m. K
Specific heat of silica sand [40]	750	J/ kg. K
Density of silica sand [40]	1700	Kg/ m^3

5.2 Experimental results

5.2.1 Effective ground thermal conductivity and borehole thermal resistance

Two different approaches can be used to estimate the initial ground temperature before the TRT started [81]. The first approach is to calculate the initial ground temperature with still water in the U-Tube. The inlet and outlet borehole temperatures and the ground temperature at 64 locations in the sand tank are recorded every 1 minute for about 1 hour by using the data acquisition system. The second approach is to circulate the water in a close system through the VGHE for about 1 hour and without adding heat during the test. Nevertheless, there was no heat injection during this period, but at the same time some heat would be added into the system by the pump. Then, the inlet and outlet borehole temperatures and the ground temperatures at the 64 locations in the sand tank were recorded every 1 minute for 1 hour by using the data acquisition system. In this study, the first approach is used to estimate the average initial ground temperature. The U-Tube in the VGHE wall was filled with water for 7 days before the measurement started. The average initial ground temperature was calculated to be 17.58 °C.

After the average initial ground temperature was calculated as shown before by using first approach, the TRT was conducted for 130 hours (60 hours for the heat injection and 70 hours to let the sand return to its initial ground temperature). A constant heat injection rate was used throughout the TRT. The outlet fluid temperature leaving from the circulating bath and entering to the VGHE was set to be 50 °C with a constant volumetric flow rate (V) of 0.730 L/ min. The inlet and outlet fluid temperatures of the borehole were recorded every 5 minutes by using the data acquisition system. As shown in Figure 5.3, the difference between the inlet and outlet temperatures was 0.82 °C after 1hour. Then the temperature difference gradually decreased to 0.52 °C after 30 hours, and it decreased further to 0.4 °C after 60 hours.

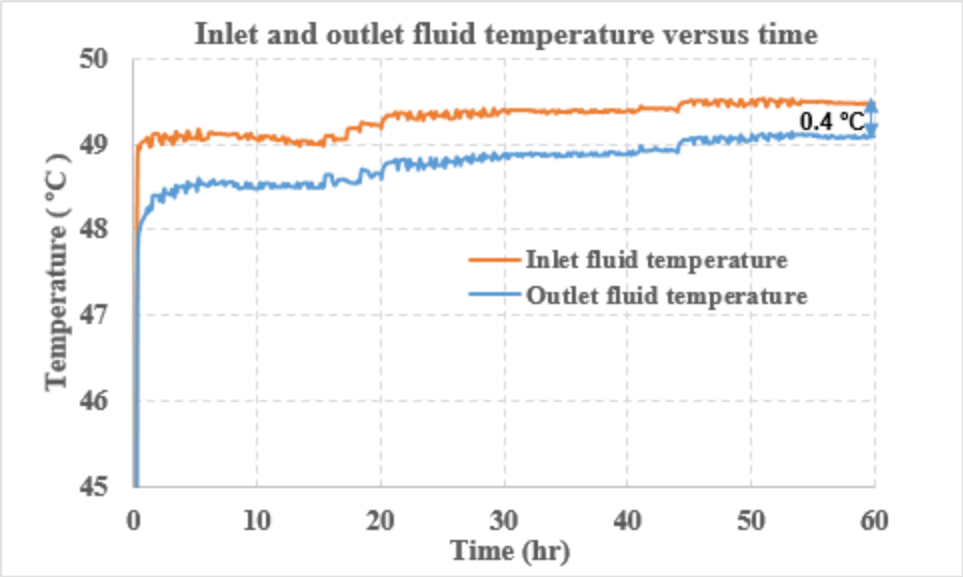

Figure 5.3: Inlet and outlet fluid temperature for the conventional single U-Tube VGHE, during heat injection

As shown in equation 3.2, there is a linear relationship between T_f and $ln(t)$. The slope (m) = 0.6189 was calculated from Figure 5.4, and then substituting 'm' in the equation 3.27, λ_{eff} was calculated as 3.92 W/ m. K.

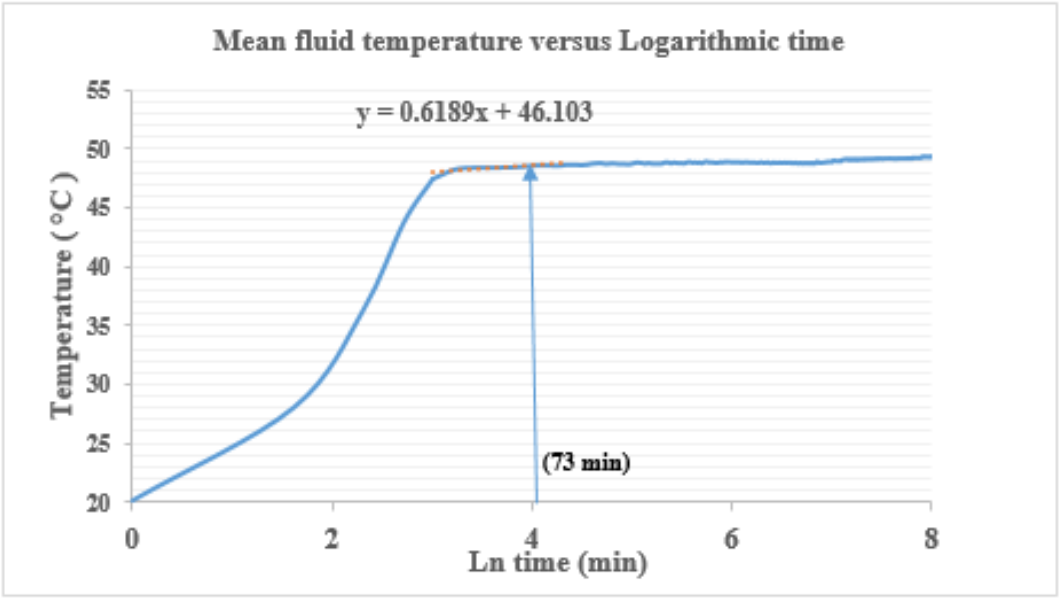

Figure 5.4: Mean fluid temperature plotted versus logarithmic time, conventional single U-Tube VGHE

Using equation 3.9 and from the measured inlet (T_{in}) and outlet (T_{out}) temperatures, the heat exchange rate per unit length (q) of VGHE was calculated. The borehole thermal resistance (R_b) was calculated using the value of λ_{eff} (3.92 W/ m. K) in equation 3.2. The value of borehole thermal resistance (R_b) at t > 5 r^2/ α (i.e. 73 min, see Appendix C; error 10%), was found to be 0.961 m. K/ W. Calculated results are presented in Table 5.2.

Four thermocouples (B1b, B2b, B3b, and B4b) were fixed on the right hand side at borehole wall, 14.70, 30.30, and 45.00 cm from the center of the borehole, at a height of 700 cm from the bottom of the sand tank. The four thermocouples (EXPP-K-24) measure the maximum temperature of 105 ℃ with an accuracy ± 0.75 ℃. Before conducting the test, the initial ground temperature of (B4b, B3b, B2b, B1b) were 17.75 ℃, 17.98 ℃, 18.06 ℃, 18.09 ℃, and they increased after 60 hours during the heat injection to 36.16 ℃, 25.73 ℃, 20.52 ℃, 19.95 ℃, respectively. The ground temperatures of the (B4b, B3b, B2b, and B1b) decreased to 18.2 ℃, 18.28 ℃, 18, and 17.71 ℃ after 70 hours from the end of the test as shown in Figure 5.5. However, the ground temperature changed rapidly and reached to 36.16 ℃ after 60 hours at the borehole wall. It changed slowly away from the borehole at 45 cm from the center of the borehole and reached 19.95 ℃. The ambient temperature was recorded during the TRT and recovery time by using a dada logger (OM 62), and it was confined at a range of 14.64 ℃ to 20.48 ℃. The temperature measurement for the OM-62 was at a range of -40 ℃ to 70 ℃ with an accuracy ±0.5.

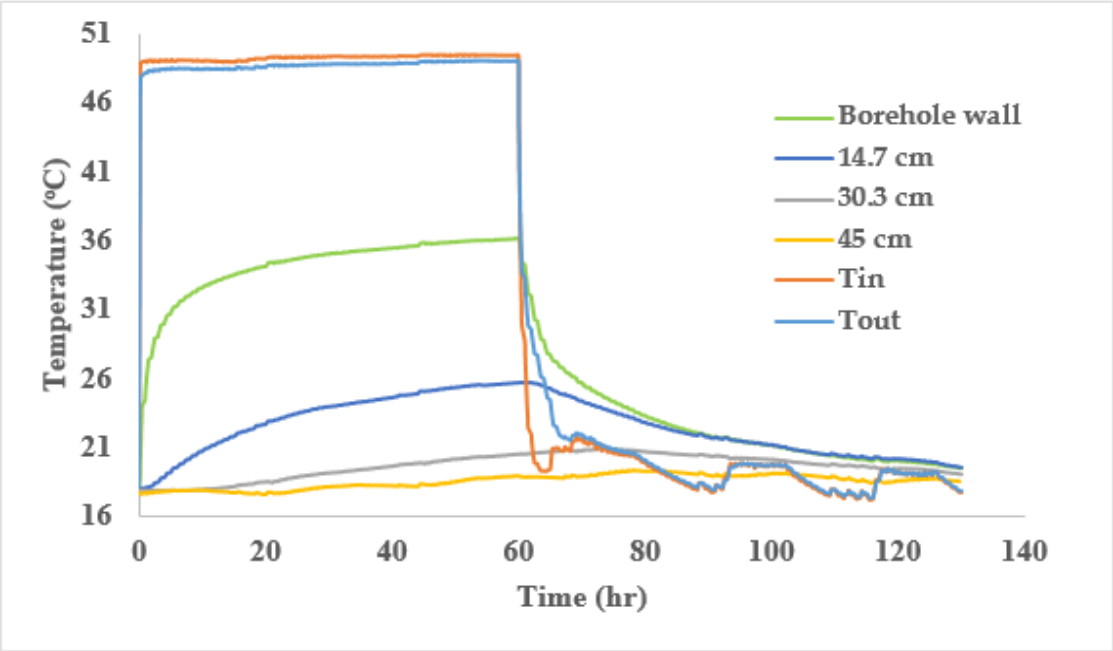

Figure 5.5: Temperature measurement at the inlet and the outlet, borehole wall, and in sand at different locations from the borehole wall, conventional single U-Tube VGHE

Another TRT was performed for the novel U-Tube pipe configuration with the similar boundary conditions used with the conventional single U-Tube. The average initial ground temperature was calculated to be 19.91 °C before the TRT started.

The TRT was conducted for 145 hours (65 hours for the heat injection and 80 hours to let the system return to its initial ground temperature). A constant heat injection rate was used throughout the TRT. The outlet fluid temperature leaving from the bath and entering to the VGHE was set to be 50 °C with a constant volumetric flow rate of 0.703 L/ min. The difference between the inlet and outlet temperatures was 0.97 °C after1 hour. Then the temperature difference gradually decreased to 0.70 °C after 30 hours, and it got to 0.65 °C after 60 hours as shown in Figure 5.6.

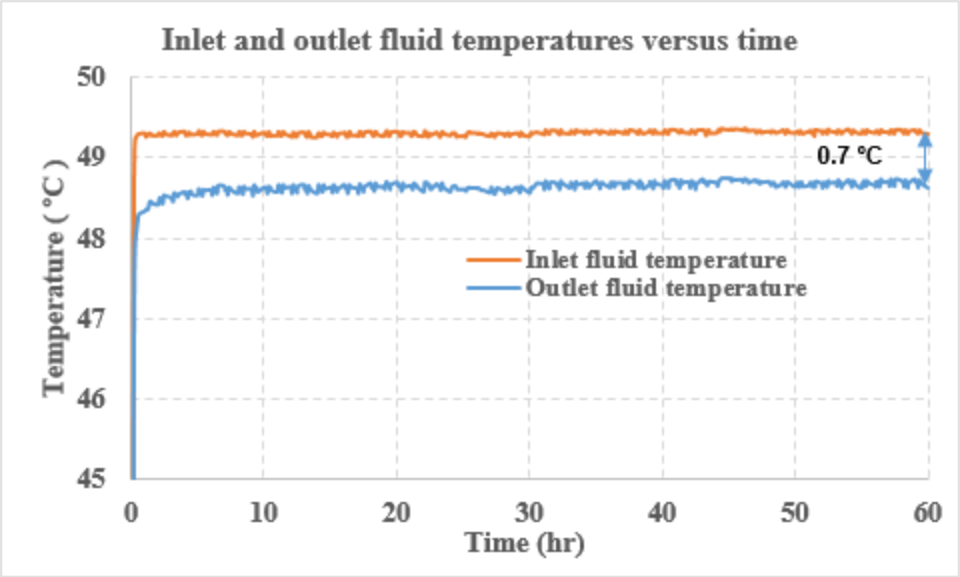

Figure 5. 6: Inlet and outlet fluid temperature for the novel U-Tube pipe VGHE, during heat injection

As shown in equation 3.26, there is a linear relationship between T_f and $ln(t)$. The slope (m) = 0.6642 was calculated from Figure 5.7, and then substituting 'm' in the equation 3.27, (λ_{eff}) was calculated as 4.85 W/ m. K.

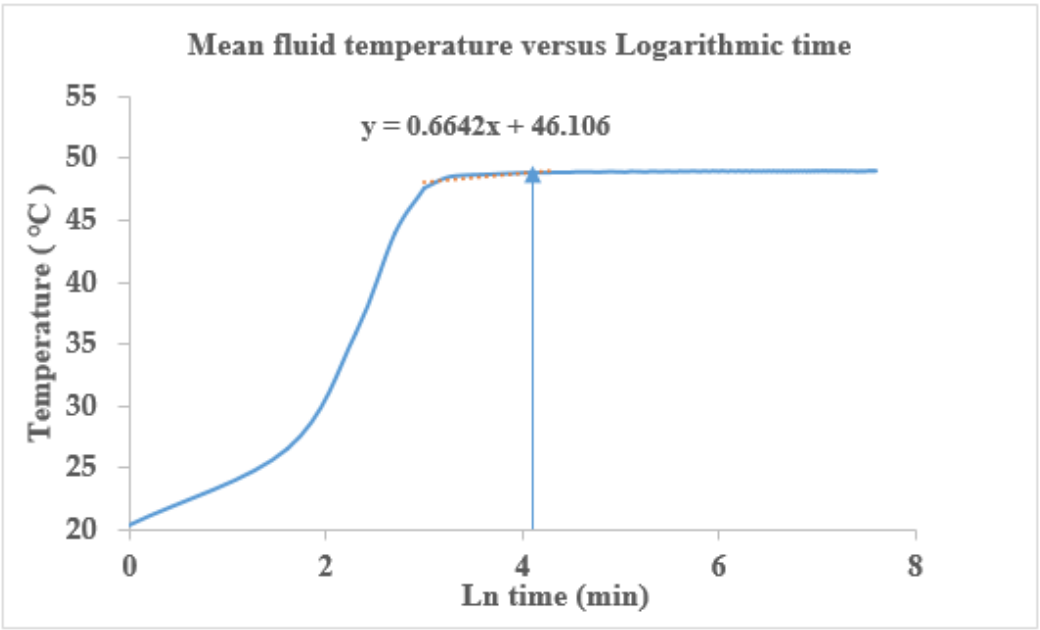

Figure 5.7: Mean fluid temperature plotted versus logarithmic time, novel U-Tube pipe VGHE

Using equation 3.9 and from the measured inlet (T_{in}) and outlet (T_{out}) temperatures, the heat exchange rate per unit length (q) of VGHE was calculated. The value of borehole thermal

resistance (R_b) was calculated using the value of λ_{eff} (4.85 W/ m. K) in equation 3.25. The value of borehole thermal resistance (R_b) at t > 5 r^2/ α (i.e. 73 min, see Appendix C; error 10%), was found to be 0.680 m. K/ W. Calculated results are presented in Table 5.2.

As shown in Figure 5.8 the initial ground temperature of (B4b, B3b, B2b, B1b) were 21.08 °C, 22.02 °C,21.72 °C, 21.09 °C, and they increased after 60 hours during the heat injection to 41.03 °C, 29.28 °C, 23.71 °C, 21.69 °C, respectively. The ground temperatures of the (B4b, B3b, B2b, and B1b) decreased to 20.26 °C, 20.55 °C, 19.74 °C, and 18.5 °C after 80 hours from the end of the test as shown in Figure 5.8. However, the ground temperature changed rapidly and reached to 41.03 °C after 60 hours at the borehole wall. It changed slowly away from the borehole at 45 cm from the center of the borehole and reached 21.69 °C. The ambient temperature was recorded during the TRT and recovery time by using a data logger (OM-62), and it was confined at a range of 14.84 °C to 21.32 °C.

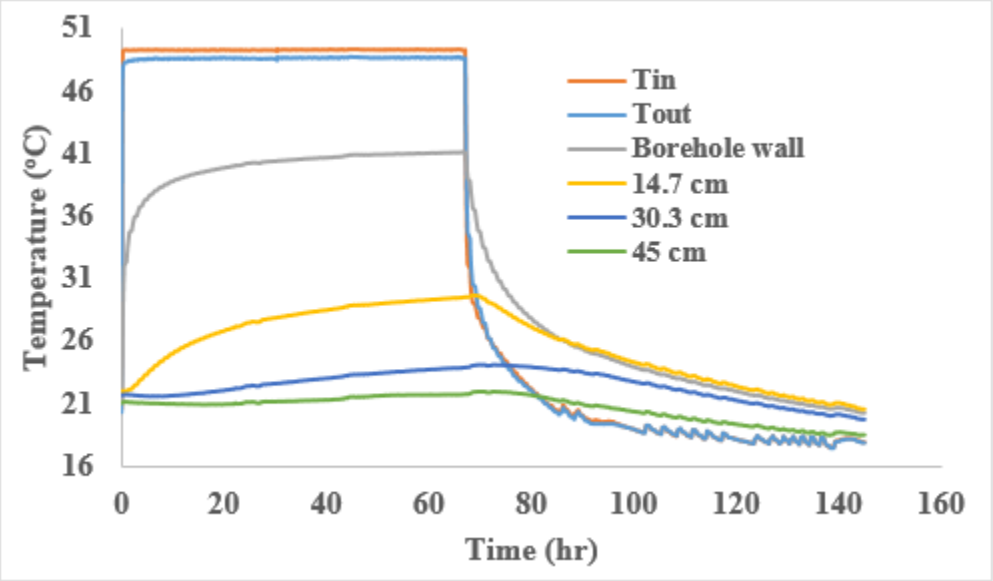

Figure 5.8: Temperature at the inlet and the outlet, borehole wall, and in sand at different locations from the borehole wall, novel U-Tube pipe VGHE

Table 5.2 presents the difference between the inlet and outlet fluid temperatures (ΔT), volumetric flow rate (V), heat injection rate (q), effective ground thermal conductivity (λ_{eff}), and borehole thermal resistance (R_b) for the two different pipe configurations.

Table 5.2: Comparison values of ΔT, V, q, λeff, and Rb for the two pipe configurations

Pipe configurations	**ΔT at 60 hours** ºC	$\boldsymbol{V}$ (L/min)	$\boldsymbol{q\ at\ 60\ hrs}$ (W/ m)	$\boldsymbol{\lambda_{eff}}$ (W/ m .K)	R_b (m. K/ W)
Single U-Tube pipe configuration	0.4	0.730	19.05	3.92	0.961
Novel U-Tube pipe configuration	0.7	0.703	30.09	4.85	0.680

Two TRTs were conducted in the laboratory for the two different pipe configurations under similar boundary conditions to demonstrate the impact of novel U-Tube pipe configuration on the heat transfer rate of the VGHE. The two different pipe configurations are the conventional single U-Tube and the novel pipe configuration (the conventional single U-Tube pipe with fins) as shown in Figure 5.1. The two TRTs are continued for a period of 60 hours. As shown in Figures 5.3 and 5.6, after 60 hours from starting the test, the difference between the inlet and outlet fluid temperatures was 0.4 °C for the conventional single U-Tube pipe VGHE while it was 0.7 °C for novel U-Tube pipe configuration VGHE. The later was increased by 0.29 °C. As would be expected, the borehole thermal resistance also decreased from 0.961 m. K/ W to 0.680 m. K/ W due to the introduction of external fins to the conventional single U-Tube (see table 5.2). The effective ground thermal conductivity was 3.92 W/ m. K for the conventional single U-Tube pipe configuration, and it was 4.85 W/ m. K for the novel U-Tube pipe configuration. The results also indicate that that the heat exchange rate for the novel U-Tube pipe configuration was 30.09 W/ m, i.e. an increase of 11.04 W/ m compared to the conventional single U-Tube (see table 5.2). The results also show that the temperature at the borehole wall increased by 4.87 ºC when the novel U-Tube pipe configuration was used compared to the conventional single U-Tube. With the novel U-Tube pipe configuration, at 45 cm from the center of the borehole and at different depths, the highest temperature increased by 0.54 °C more than the conventional single U-tube pipe configuration as shown in Figures 5.5 and 5.8. Based on the aforementioned observations, it can be concluded that substantial improvement of thermal efficiency of VGHE can be made by the introduction of external fins to the conventional single U-Tube pipe. In practical terms, it means fewer boreholes are required when conventional single U-Tube pipes are replaced by the novel U-Tube pipe configuration with external fins, and this, in turn, will reduce the VGHE installation cost.

5.2.2 Ground temperature

This section discusses the ground temperature behavior at and around the VGHEs during the heat injection and recovery time for the two pipe configurations.

5.2.2.1 Temperature at and around the conventional U-Tube pipe VGHE

As mentioned in section 5.1, the first TRT for a conventional single U-Tube VGHE was conducted for 130 hours (60 hours for the heat injection and 70 hours with no heat injection to let the system return to its initial ground temperature). The ground temperatures were measured by thermocouples at different locations in the sand tank (Figure 5.9).

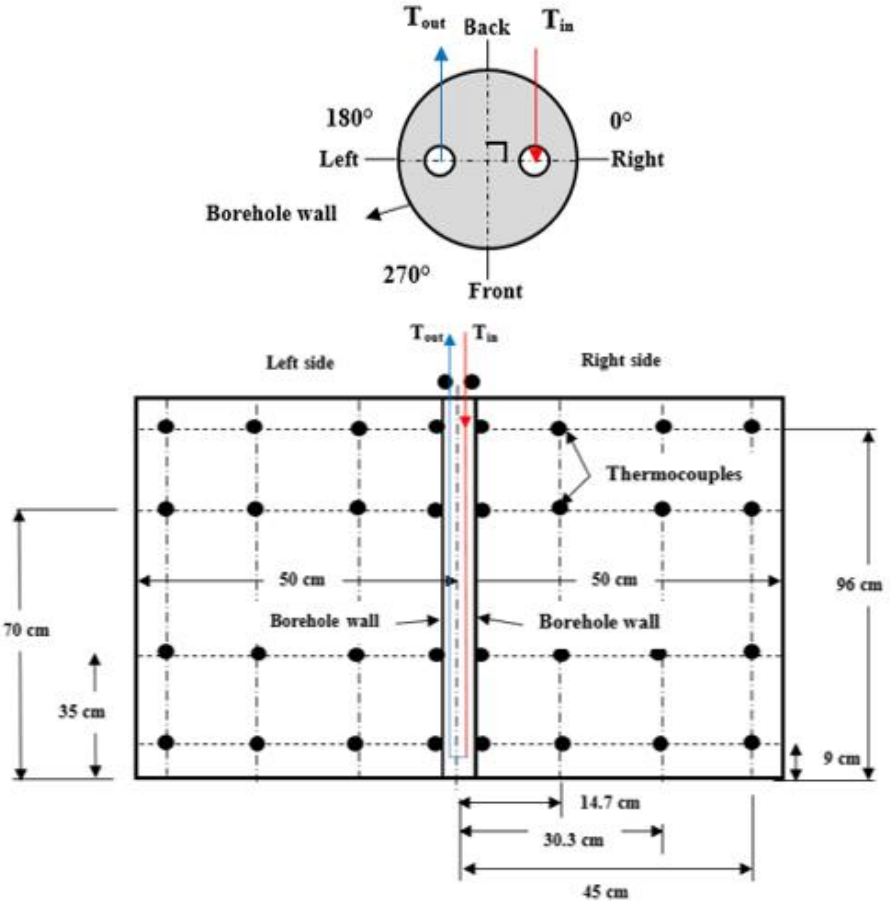

Figure 5.9: Front view for the 32 thermocouples on the right and left sides of sand tank - conventional single U-Tube pipe VGHE

Figures 5.10 and 5.11 show the variation of temperature with time at 64 measurement points inside the sand tank during the TRT and recovery time. Each of these figures consists of two columns, and every column in each figure contains four graphs which represent the temperature

changes at 16 point measurements inside the sand tank during 130 hours. The top row graphs show the change in temperature with depth at the borehole wall, while the two middle row graphs show the change in temperature with depth at horizontal distances of 14.7 cm and 30.3 cm, respectively, from the center of the borehole. The bottom row graphs demonstrate the variation of temperature with depth at horizontal distance 45 cm from the center of the borehole (i.e. close to the sand tank wall). In Figures 5.10 and 5.11, four colors, blue, red, grey, and yellow, represent temperature variation at heights of 96, 70, 35, 9 cm from the bottom of the sand tank, respectively.

In general, it is noticed that ground temperatures continue to go up during 60 hours of heat injection and it did not reach to a steady state level (see Figures 5.10 and 5.11), unlike the fluid temperature (see Figure 5.3).

The top row graphs describe the temperature changes with depth during the period of heat injection and recovery time at the borehole wall. These graphs indicate a rapid rise in temperature during the first hours, followed by a very slow linear increase in temperature, until the end of heat injection (60 hours) period. Immediately after stopping the heat injection, the temperature plummets by about 10 °C in two hours, and thereafter temperature decreased more slowly to the initial temperature (about 18 °C) after about 70 hours of heat rejection.

The temperature variations with the depth at a radial distance 14.7 cm from the center of the borehole show that temperature went up slowly at the beginning of the heat injection, compared to the ground temperature at the borehole wall, and then the temperature increased rapidly until it reached to the highest value at the end of heat injection period. During the recovery time, the temperature declined rapidly and reached close to the initial temperature at the end of heat rejection period. The temperature variations with the depth at 30.3 cm from the center of the borehole in the sand tank showed an initial time lag (about 5 hours) or very slow rate of temperature increase and then there was a gradual increase of temperature until the end of heat injection period (60 hours), however, the rate of temperature increase was much slower than the borehole wall or at a distance of 14.7 cm from the borehole wall. During the recovery time, the temperature started to drop slowly back to the initial ground temperature.

The temperature variations at a distance of 45 cm from the center of the borehole shows that the temperature at this plane changes very slowly and is significantly influenced by the ambient temperature in the laboratory during the test.

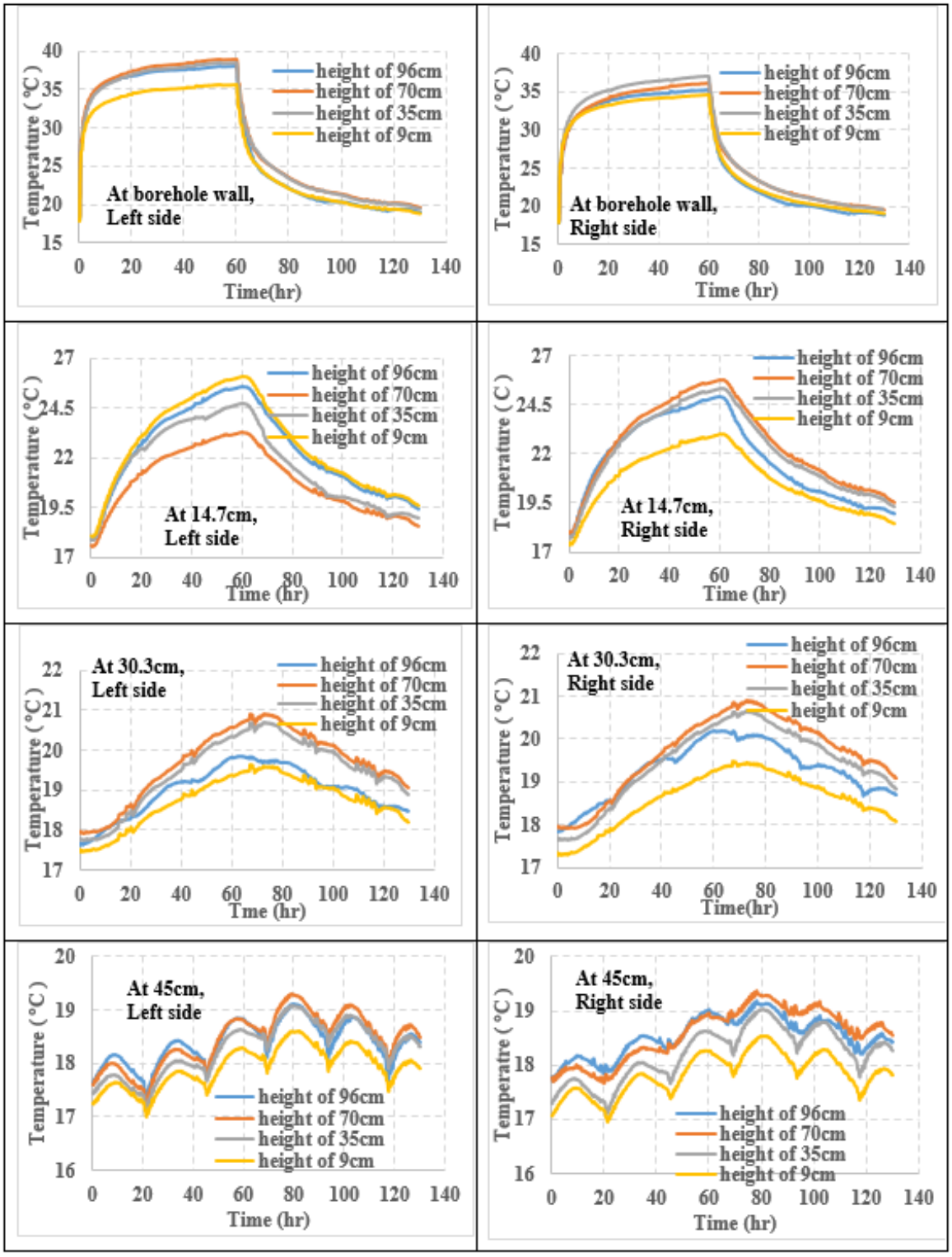

Figure 5.10: Measuring the temperature at different depth on the borehole wall and at specified locations in the sand tank, conventional single U-Tube pipe VGHE

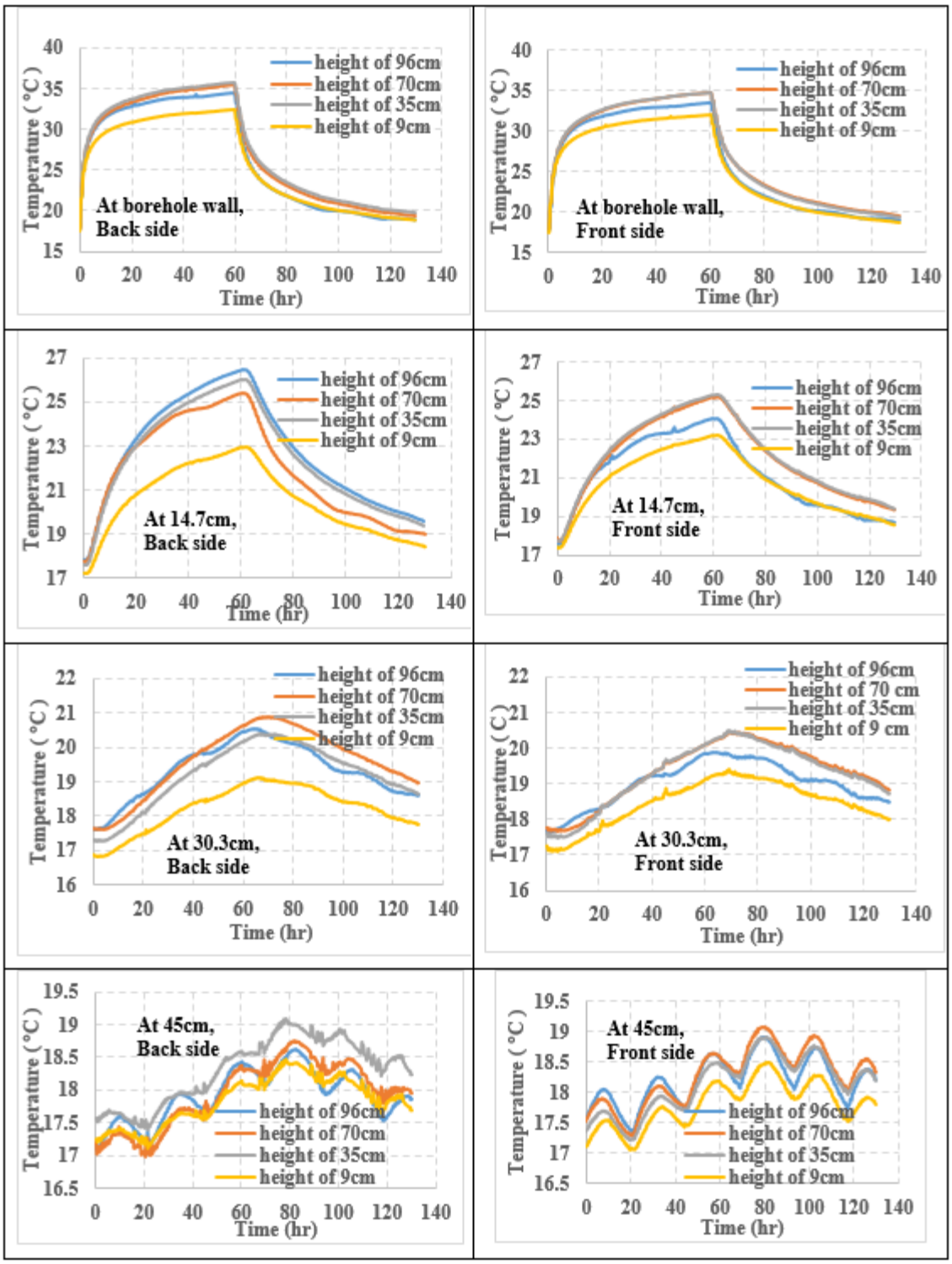

:

Back side (90°) Front side (270°)

Figure 5.11: Measuring the temperature at different depth on the borehole wall and at specified locations in the sand tank, conventional single U-Tube pipe VGHE

5.2.2.2 Temperature measurements at and around the novel U-Tube pipe VGHE

The second TRT for the novel U-Tube pipe VGHE was conducted for 145 hours (65 hours for the heat injection and 80 hours with no heat injection to let the system return to its initial ground temperature). The ground temperatures were measured by thermocouples at different locations in the sand tank as shown in Figure 5.12.

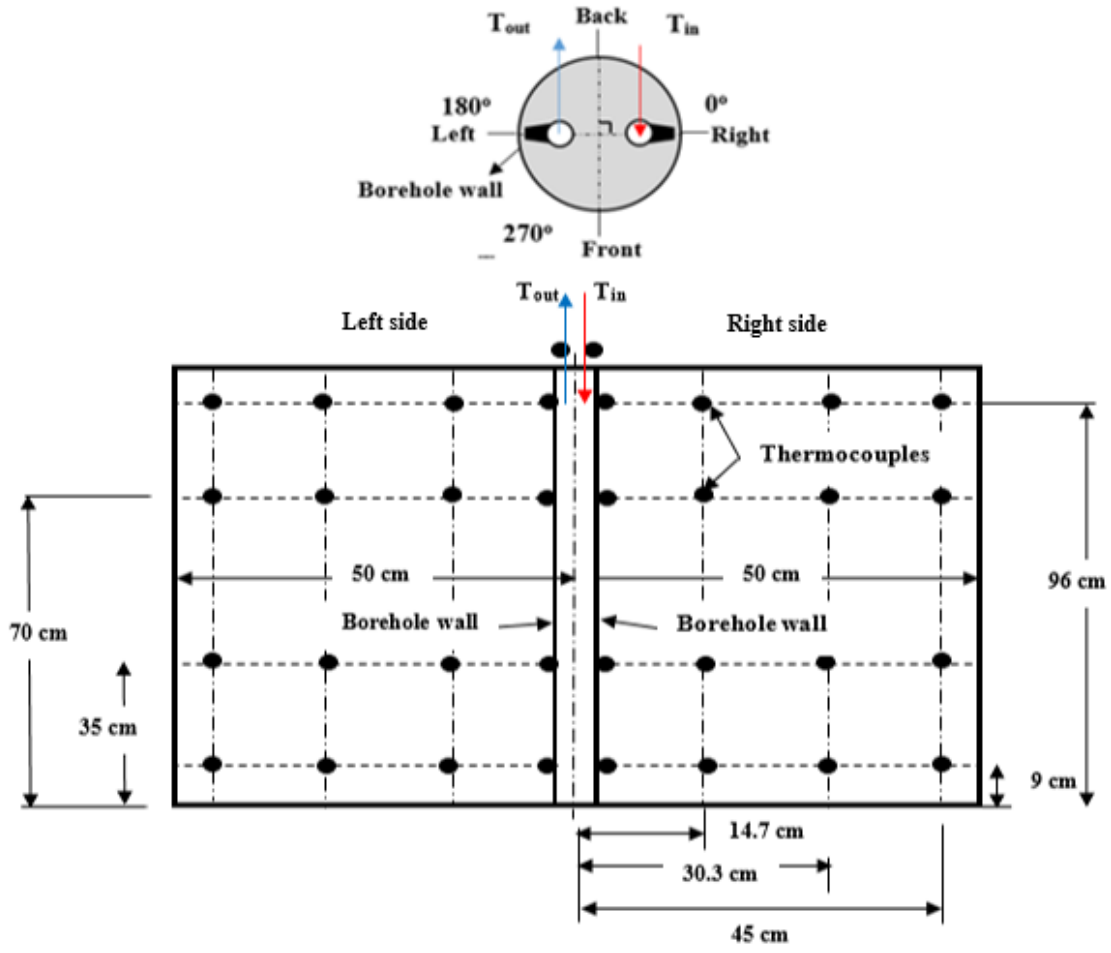

Figure 5.12: Front view for the 32 on the right and left sides of sand tank, novel U-Tube pipe VGHE

Figures 5.13 and 5.14 demonstrate the variation of temperature with time at 64 measurement points inside the sand tank during the TRT and recovery time. Each of these figures consists of two columns, and every column in each figure contains four graphs which represent the temperature changes at 16 point measurements inside the sand tank during 145 hours. The top row

graphs represent the change in temperature with depth at the borehole wall, while the two middle graphs illustrate the change in temperature with depth at horizontal distances of 14.7 cm and 30.3 cm, respectively, from the center of the borehole. The bottom row graphs show the variation of temperature with depth at horizontal distance 45 cm from the center of the borehole (i.e. close to the sand tank wall). Four colors, blue, red, grey, and yellow, represent temperature variation at heights of 96, 70, 35, 9 cm from the bottom of the sand tank, respectively.

In general, it is noticed that ground temperatures continue to go up during 65 hours of heat injection and it did not reach to a steady state level (see Figures 5.13 and 5.14), unlike the fluid temperature (see Figure 5.6). This phenomenon was observed in the case of conventional U-tube pipe too.

The top row graphs describe the temperature changes with depth during the period of heat injection and recovery time at the borehole wall. These graphs indicate a rapid rise in temperature during the first hours, followed by a very slow linear increase in temperature, until the end of heat injection (65 hours) period. Immediately after stopping the heat injection, the temperature plummets by about 12 ℃ in two hours, and thereafter temperature decreased more slowly to the initial temperature (about 20 °C) after about 80 hours of heat rejection.

The temperature variations with depth at horizontal distance 14.7 cm from the center of the borehole show that temperature increased slowly at the beginning of the heat injection, compared to the ground temperature at the borehole wall, and then the temperature increased rapidly until it reached to the maximum value at the end of the heat injection period. During the recovery time, the temperature declined rapidly and reached close to the initial temperature at the end of heat rejection period.

The curves located at 30.3 cm from the center of the borehole and at different depths in the sand tank did not change significantly during the first seven hours, and thereafter the temperature increased slowly until the end of heat injection period.

The temperature variations at a distance of 45 cm from the center of the borehole shows that the temperature at this plane changes very slowly and is significantly influenced by the ambient temperature in the laboratory during the test.

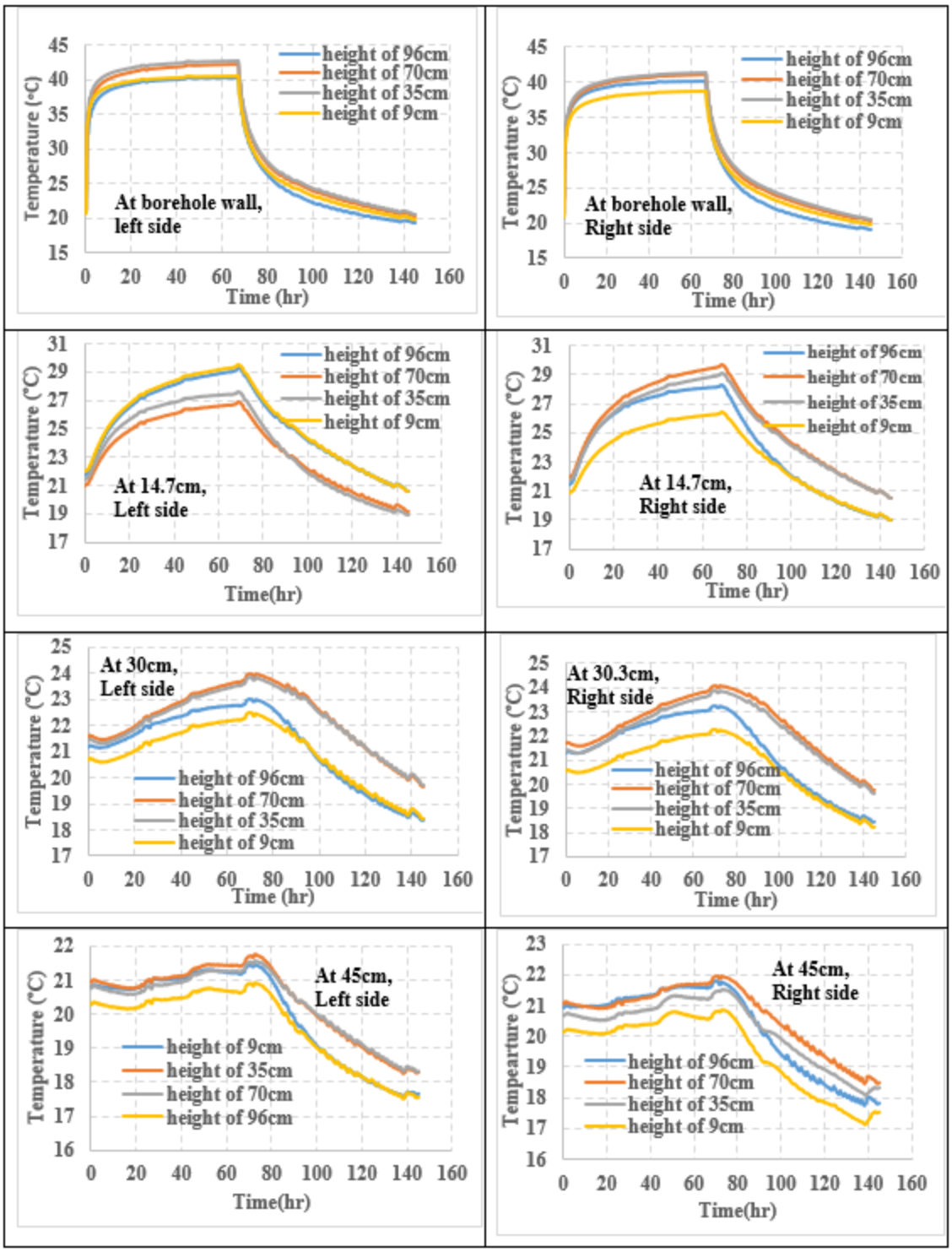

Left side (180°) right side (0°)

Figure 5.13: Measuring the temperature at different depth on the borehole wall and at specified locations in the sand tank, novel U-Tube pipe VGHE

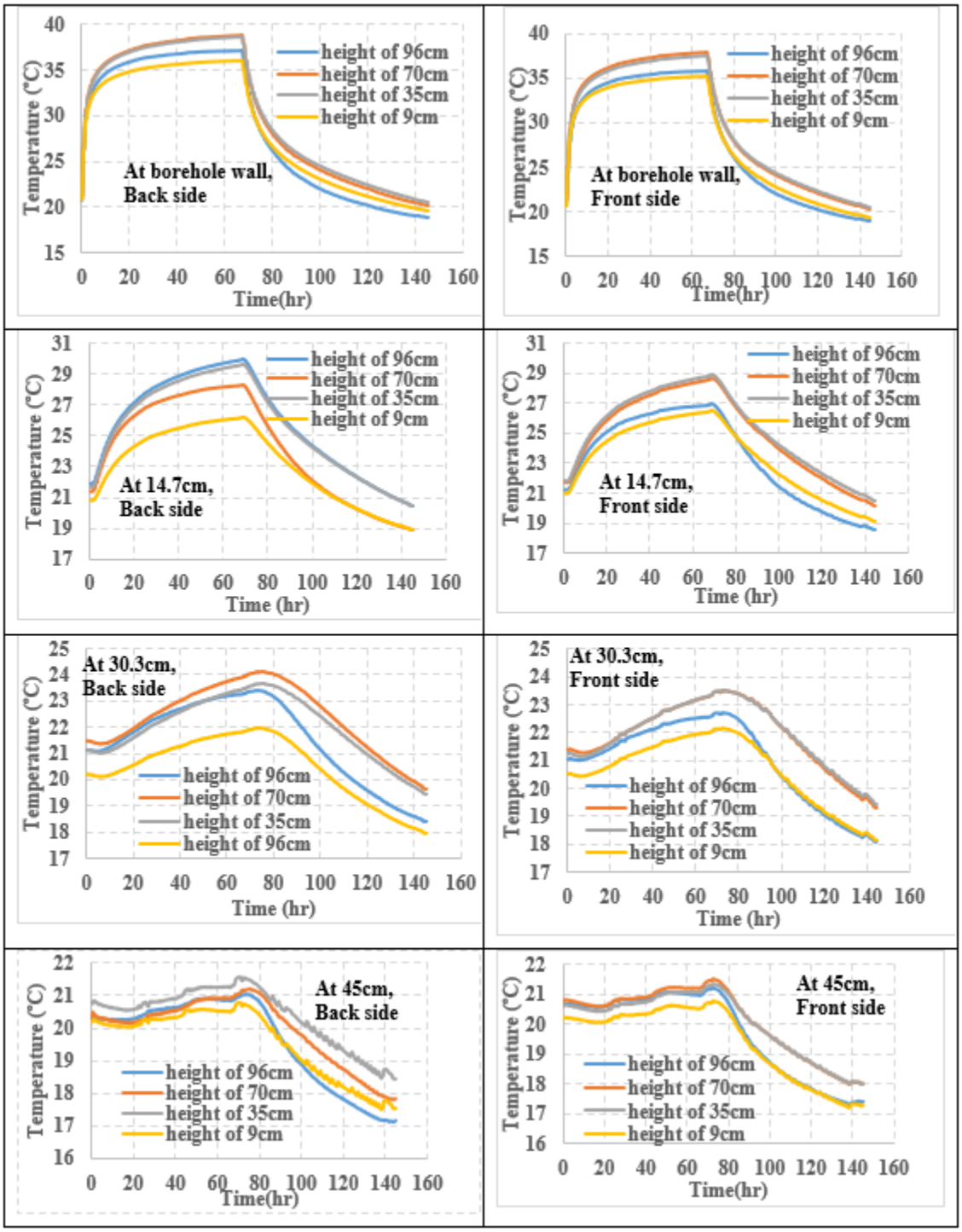

Back side (90°) Front side (270°)

Figure 5.14: Measuring the temperature at different depth on the borehole wall and at specified locations in the sand tank, novel U-Tube pipe VGHE

Aforementioned observations clearly indicate that overall ground temperature variation patterns for conventional U-Tube pipe and novel U-Tube pipe configuration remain same. However, a closer look at the results would show that after 60 hours from starting the test, the average temperatures at the borehole, in the case of conventional U-Tube pipe configuration, were 35.80 °C (right), 37.79 °C (left), 33.72°C (front) and 34.55 °C (back), and the same for the novel U-Tube pipe configuration were 40.07 °C (right), 41.32 °C (left), 36.53°C (front) and 37.56 °C (back). The inlet and outlet fluid temperatures were 49.47°C and 49.09°C for conventional U-Tube pipe configuration, and 49.29 °C and 48.62 °C for novel U-Tube pipe configuration. The fluid flow rates were 0.730 L/ min during the test with the conventional U-Tube pipe, and 0.703 L/ min during the test with the novel U-Tube pipe configuration. These critical observations indicate higher heat injection in the ground when the novel U-Tube pipe configuration was used.

5.3 Summary of observations

The results from the TRTs conducted in the laboratory on a small-scale VGHE with two different pipe configurations, a conventional single U-Tube and the same with external fins, have been presented and examined in this chapter. The main observations are outlined below:

- The difference between the inlet and outlet temperature for the novel U-Tube pipe configuration (i.e. with external fins) was 0.7 °C after 60 hours while the difference between the inlet and outlet temperatures for the conventional single U-Tube pipe configuration was 0.4 °C after 60 hours. Thus, 76.3% increase in temperature difference has been achieved due to the use of novel pipe configuration.
- The effective ground thermal conductivity for the novel U-Tube pipe configuration was 4.85 W/ m. K, a 23.64% increase compared to the conventional single U-Tube pipe configuration.
- The borehole thermal resistance for the novel U-Tube pipe configuration was found to be 0.680 m. K/ W, which is 29.22% lower than that of the same with conventional single U-Tube pipe.
- The increased ground temperatures with the novel U-Tube pipe configuration, compared to single U-Tube pipe configuration, clearly indicate superior heat transfer performance of novel pipe configuration.

- Introduction of external fins to single U-Tube pipe configuration helps to reduce the number of boreholes by about 58%, which will in turn decrease the installation cost.

Chapter 6

Effect of different grout materials and heat injection rate on the performance of VGHE

Abstract

Grout materials are used to increase the heat transfer rate between the heat carrier fluid (water) in the pipes and the ground, and enhance the thermal efficiency of vertical ground heat exchangers (VGHEs). The knowledge of ground thermal properties is considered a prerequisite in order to reach the ideal design for VGHEs. In this study, two different grout materials (bentonite and silica sand) and two different inlet water temperatures (50 °C and 60 °C) are used to evaluate the influence of those parameters on the thermal efficiency of VGHE with novel U-Tube pipe configuration. The results show that the difference between the inlet and outlet water temperatures of VGHE increases with an increase in the inlet water temperature. The differences between the inlet and outlet water temperatures of VGHEs with silica sand are found to be higher than the same with bentonite. The borehole thermal resistance values for the VGHEs with silica sand are lower than the same for with bentonite. The heat exchange rates in the VGHEs with silica sand are higher compared to the VGHEs with bentonite. In addition, the heat exchange rates in VGHEs increase with an increase in the inlet water temperature.

6.1 Introduction

Ground source heat pumps (GSHPs) are utilized to transfer the thermal energy between the ground and buildings for the purpose of heating, cooling, and hot water in the buildings. GSHPs consist of heat pumps and ground heat exchangers (GHEs). A VGHE is used as a device to extract heat in the winter and inject heat in the summer from/ into the ground. This system does not depend on the outside temperature. Several variables such as the filling inside the borehole, borehole diameter, pipe size, pipe configuration, heat injection rate etc. have significant impacts on the

values effective ground thermal conductivity and borehole thermal resistance, the two most important performance parameters for VGHE.

Laboratory studies were conducted by Gu and O'Neal (1998) to estimate the effects of backfills (bentonite/masonry sand and bentonite/copper powder) on the thermal performance of VGHEs. The results showed that backfill materials had an impact on the thermal performance of VGHEs [83]. Researchers conducted laboratory and field studies to estimate the effects of increasing the thermal conductivity of the grout on the borehole thermal resistance. Laboratory and field results indicated that the thermal resistance of grout decreased with an increase in the grout thermal conductivity [17]. Four different types of grout materials were tested to estimate the effects of these different types of grout materials on the borehole thermal resistance of double U-Tube VGHEs. The four different types of grout materials were (1) bentonite, (2) bentonite with spacers, (3) 50% sand and bentonite with spacers, and (4) Quartz sand with spacers. The lowest borehole thermal resistance of double U-Tube VGHE was with quartz sand and spacers, followed by 50% sand and bentonite with spacers, bentonite with spacers, and bentonite without spacers [20]. Esen and Inalli (2009) conducted three TRTs with three different depths (30 m, 60 m, and 90 m) to estimate the thermal performance of the single U-Tube VGHE. The results of the cooling and heating experiments indicated that the thermal performance of the single U-Tube VGHE increased with an increase in borehole depth [50, 106]. Theoretical and experimental studies were used to analyze the impacts of the grout thermal conductivity on two parameters (the borehole thermal resistance and the heat exchange rate) in the VGHE. The results showed there was a significantly more decrease in the total thermal resistance when the thermal conductivity of the grout was changed from 0.75 W/ m. K to 1.5 W/ m. K than when the thermal conductivity of grout was changed from 1.5 W/ m. K to 2.4 W/ m. K. It was also recommended that the thermal conductivity of the grout be larger than the thermal conductivity of the soil to enhance the heat exchange rate of VGHE [73]. Experimental studies were done to estimate the influences of multi-injection-rate on two VGHEs with lengths of 75 m and 150 m. The heat injection rate was in range of 21 W/ m to 83 W/ m. The results indicated that the convective flow in the VGHE increases with an increase in the heat injection rate, followed by a decrease in the borehole thermal resistance from 0.12 m. K/ W to 0.065 m. K/ W [22]. Field studies were conducted to estimate the effects of the two different construction parameters on the borehole thermal resistance of single U-Tube VGHEs. The two different construction parameters were: (i) grout materials (cement and bentonite) and (ii)

additives (silica sand and graphite). The cement grout had a higher thermal efficiency than the bentonite grout. It was also indicated that the graphite had a convincing performance to enhance the thermal efficiency compared to silica sand [4]. Field TRTs were conducted to estimate the effects of different backfill materials on the thermal performance of VGHE. The obtained results indicate that the thermal conductivity of sand–bentonite mixtures increased with an increase in the bentonite percentage in the form of dry mass until it reached to the highest at the range of 10% to 12%. The heat injection and heat extraction rates were enhanced by 31.1% and 22.2% with sand–bentonite backfill material compared to a common sand–clay material [107]. Experimental studies were carried out to estimate the influences of the four different grouting materials on ground thermal properties. However, the four thermal response tests (TRTs) were conducted in same geological area, and every borehole was filled by a different grout mix. The results showed that an increase in the grout thermal conductivity leads to a reduction in the thermal resistance of grout mix [108]. Laboratory studies were carried out to estimate the effects of three different grout materials (silica sand-based, bentonite-based, and homemade admixture containing natural graphite) on the performance of the VGHEs. Laboratory results indicated that homemade admixture containing 5% natural graphite had a higher thermal conductivity, followed by silica sand-based, and the bentonite-based [26]. Shirazi and Bernier (2014) built a small-scale experimental apparatus to run TRTs. A borehole Plexiglas pipe was inserted in the sand tank (length: 1.35 m and diameter: 1.4 m), and a single U-Tube copper pipe was inserted in the borehole. The results indicated that the borehole thermal resistance was 0.61 m. K/ W [63]. Cimmino and Bernier (2015) built a small-scale experimental apparatus to run TRTs in the laboratory. A small-scale borehole (length: 400 mm) was inserted in a sand tank (length: 1.35, and diameter: 1. 4 m), and a single U-Tube copper pipe was inserted in the borehole. In this study, the temperature along the borehole was measured during the TRT and the heat injection rate was calculated [54]. Experimental studies were performed to estimate the influences of two different parameters: (1) two different backfill materials (cement- gravel) and (2) two different heat injection rates (45 W/ m and 90 W/ m) on the thermal performance of VGHEs. The borehole thermal resistance of the VGHEs with gravel and cement was decreased by 9.8% and 8.7%, respectively, as the heat rate was doubled. However, the borehole thermal resistance of the VGHE with cement was higher than that of the VGHE with gravel [28]. Five TRTs were performed to study the effects of multi-rate heat injections on the ground thermal properties of the single U-Tube VGHEs. The heat injection

rate was in a range of - 45 W/ m to 75 W/ m, and the space between the borehole and the single U-Tube was filled by groundwater. The results illustrated that the value of the borehole thermal resistance varied between 0.042 m. K/ W and 0.095 m. K/ W. However, the value of the effective thermal conductivity was between 3.3 W/m. K and 3.4 W/m. K [109]. Li et al. (2018) established an experimental box (6.25 m × 1.5 m × 1 m) to investigate the transient heat transfer performance of double U-Tube GHE in layered ground. Two U-Tubes copper pipes were inserted in the experimental box, which was filled with sand and clay. Then, the experimental results were compared to the numerical results [100]. Field studies were done to evaluate the influences of two different parameters (borehole depths and rock types) on the thermal performance of VGHEs. The two different parameters were rock types (Gneiss, Alluvium, and Granite), and borehole depths (150 m and 200 m). The results showed that the highest ground effective thermal conductivity was with gneiss, followed by alluvial, and granite. The ground effective thermal conductivity increased with the depth increase [30]. A numerical study was investigated to estimate the effects of two parameters (grout thermal conductivity and grout heat capacity) on thermal performance of VGHEs. The results indicated that the grout heat capacity had 5.2% higher compared to the grout thermal conductivity [110]. Laboratory studies were conducted by Li et al. (2019) to estimate the influence of VGHEs in a layered subsurface. The results indicate that using various geological materials resulted in different heat transfer efficiencies of VGHEs because of different temperature distributions [111]. TRTs were performed to evaluate the impacts of two different parameters (heat injection rate and volumetric or recirculation flow rate) on the ground properties of conventional single U-Tube VGHEs. It was reported that the effective thermal conductivity increased with an increase in the heat injection rate. The results also showed the ambient temperature had a higher impact with decrease in recirculation flow rate [89].

The main objective of this study is to estimate the effects of two different grout materials (bentonite and silica sand) and two different heat injection rates (circulating fluid temperatures: 50 °C and 60 °C) on the thermal efficiency of VGHE with novel U-Tube pipe configuration (single U-Tube pipe with two outer fins) as shown in Figure 6.1. Line source theory is used to estimate the effective ground thermal conductivity and the borehole thermal resistance (see section 3.2). Parameters for the pipe configurations, borehole, and grouting materials of the VGHE are listed in Table 5.1.

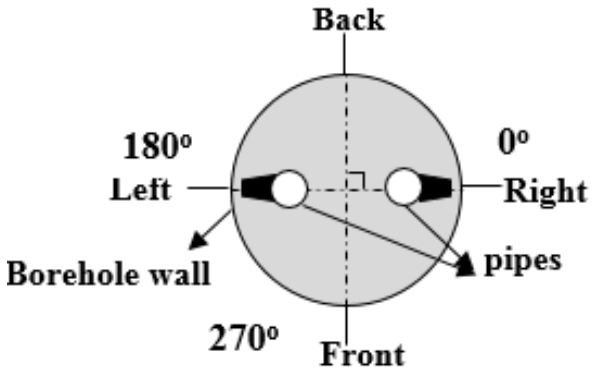

Figure 6.1: Cross section of the novel U-Tube pipe VGHE

6.2 Analysis of experimental results

TRTs are widely used to estimate the thermal properties of GHEs that are coupled with heat pumps for GSHP applications. The principle of the TRT is described in a number of different studies (e.g., see the references [14, 80]). In this research, the circulating bath is used to inject heat to the fluid (water) in a closed circle in and out of the VGHE.

In this study, four TRTs were performed in the laboratory between February 2018 and April, 2018 (see section 4.1). During the first two TRTs, the space between the pipe configuration and the borehole wall was filled with bentonite (VGHE No. 1 and 2), while during the other two TRTs, the space between the pipe configuration and the borehole wall was filled with silica sand (VGHE No. 3 and 4). In addition, TRTs were performed using two different constant inlet water temperatures (50 ºC and 60 ºC) for both grout materials (see Table 6.1).

Table 6.*1*: Test VGHE No., grouting materials of VGHE, and different inlet water temperatures coming from the circulating bath

Test VGHE No.	Grout	Inlet water temperatures coming from the circulating bath
1	bentonite	50 ºC
2	bentonite	60 ºC
3	silica sand	50 ºC
4	silica sand	60 ºC

The average initial ground temperatures were found to be 19.91 ºC and 18.96 ºC for the first two TRTs (VGHE No. 1 and 2) as shown in Table 6.2. As shown in the Figures 6.2 to 6.5, the inlet and outlet water temperatures increased rapidly as soon as the test started. Then water temperatures reached to a constant value within a few hours. During the first two TRTs, borehole with bentonite

(VGHE No. 1 and 2), the inlet and outlet water temperature differences (ΔTs) were within a range of 0.67 °C to 0.83 °C after 50 hours of starting the test, as shown in Figures 6.2 and 6.3. Table 6.2 shows results from the first two TRTs, including the initial ground temperature, water flow rates, and the difference between the inlet and outlet water temperatures.

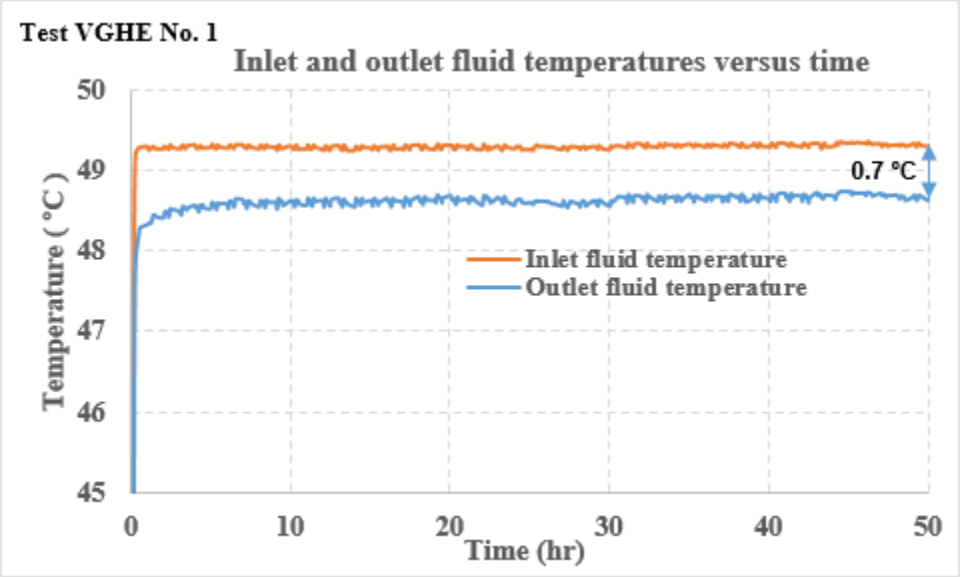

Figure 6.2: Inlet and outlet water temperatures versus time (Inlet water temperature was 50 ºC)

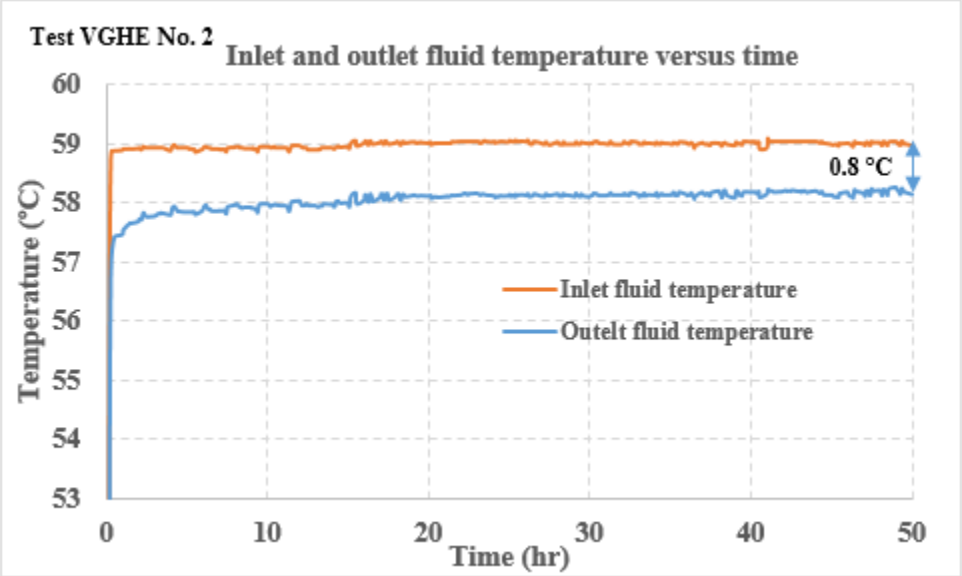

Figure 6.3: Inlet and outlet water temperatures versus time (Inlet water temperature was 60 ºC)

The average initial ground temperatures were found to be 21.09 ºC and 20.99 ºC for the other two TRTs (VGHE No. 3 and 4) as shown in Table 6.2. During other two TRTs for the borehole

with silica sand (VGHE No. 3 and 4), the inlet and outlet water temperature differences (ΔTs) were within a range of 0.69 °C to 0.86 °C after 50 hours from starting the test, as shown in Figures 6.4 and 6.5. Table 6.2 shows results for the other two TRTs, including the average initial ground temperature, water flow rates, and the difference between the inlet and outlet water temperatures.

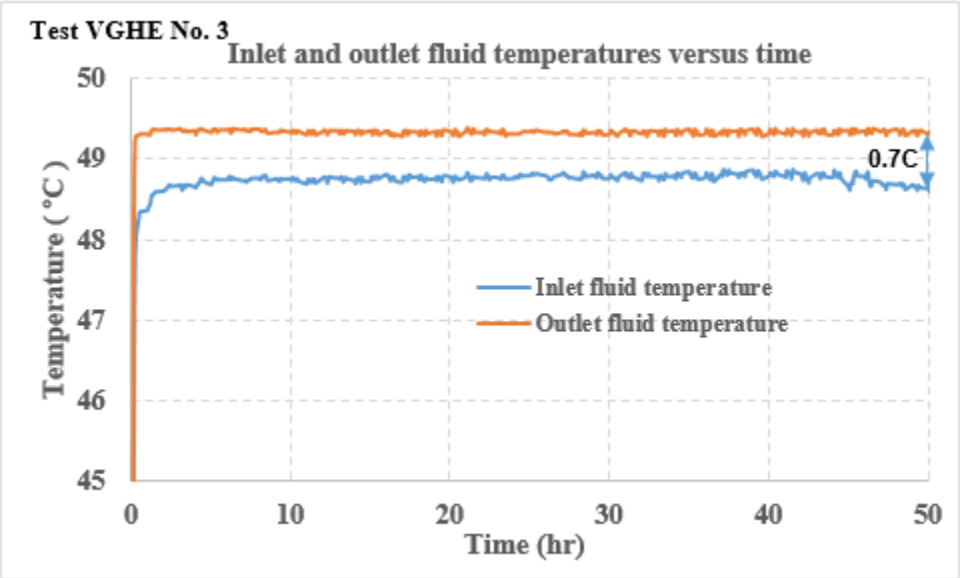

Figure 6.4: Inlet and outlet water temperatures versus time (Inlet water temperature was 50 ºC)

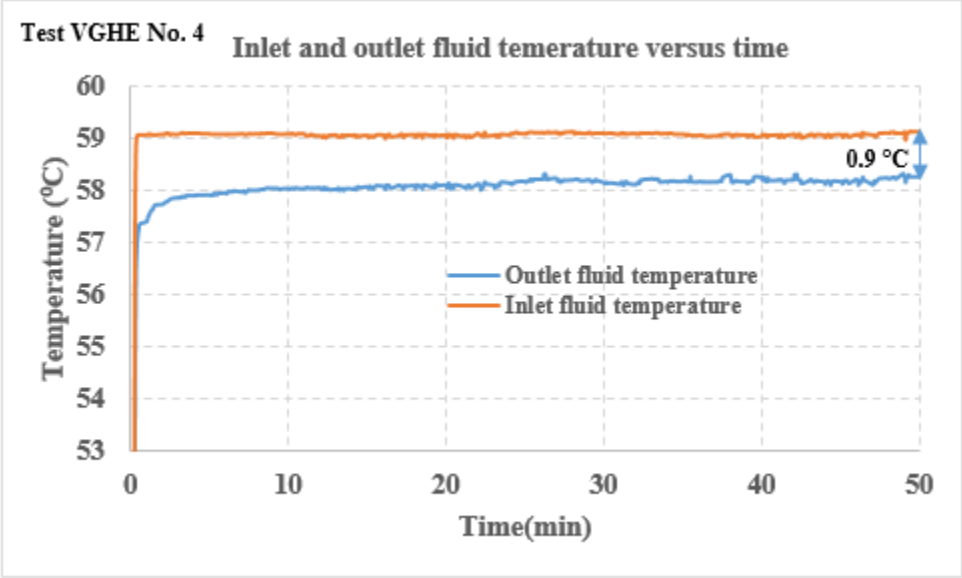

Figure 6.5: Inlet and outlet water temperatures versus (Inlet water temperature was 60 ºC)

The results presented in Figures 6.2 and 6.3 show that during the first two TRTs, with bentonite grout, the differences between the inlet and outlet water temperatures of the VGHE were 0.67°C and 0.83°C for inlet water temperature 50°C and 60 °C, respectively. During the second two TRTs, with silica sand grout, the differences between the inlet and outlet water temperatures of the VGHE were 0.69 °C and 0.86 °C for inlet water temperature 50°C and 60 °C, respectively (see Table 6.2). These observations indicate a highly linear relationship between the heat injection rate, and difference between inlet and outlet water temperature (ΔT) for both bentonite and silica sand grout.

Table 6.2: Conditions of tests and final water temperature difference during TRTs

Test VGHE No.	**TRT starting time (MM DD, YYY)**	**Flow rate $\dot{V}$ $L/\,min$**	**T_o (°C)**	**(ΔT) at 50 hours (°C)**
1	Feb 06, 2018, 14:15	0.684	19.91	0.7
2	Feb 12, 2018, 20:15	0.684	18.96	0.8
3	April 10, 2018, 9:20	0.688	21.09	0.7
4	April 23, 2018, 8:10	0.684	20.99	0.9

6.2.1 Effective ground thermal conductivity and borehole thermal resistance

As shown in equation 3.26, there is a linear relationship between T_f and $ln(t)$. The slope (m) values for first two TRTs (VGHE No. 1 and 2) = 0.6642 and 0.9759 were calculated from Figures 6.6 and 6.7, and then substituting 'm' in the equation 3.27, λ_{eff} were calculated as 4.85 W/ m. K and 5.03 W/ m. K, respectively.

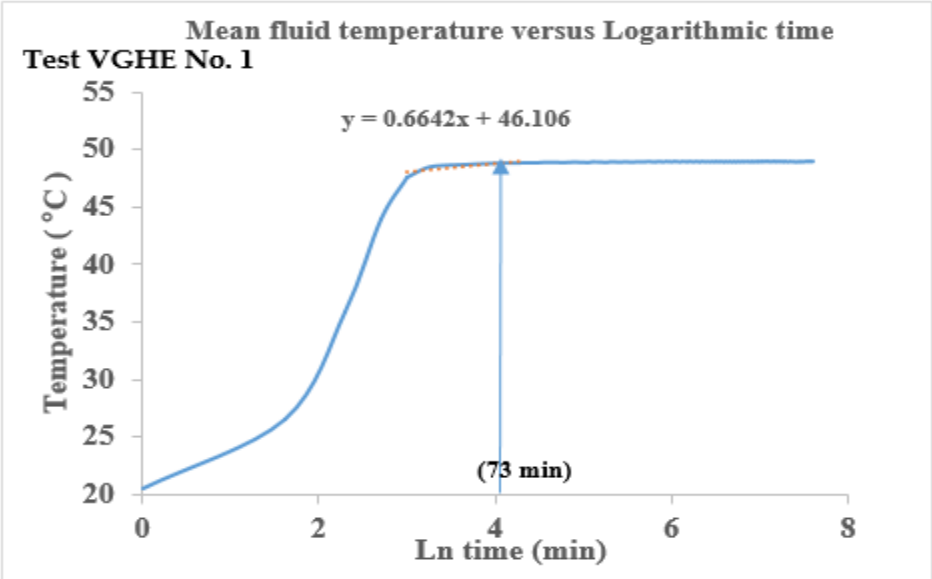

Figure 6.6: Mean fluid temperature versus logarithmic time (Inlet water temperature was 50 ºC)

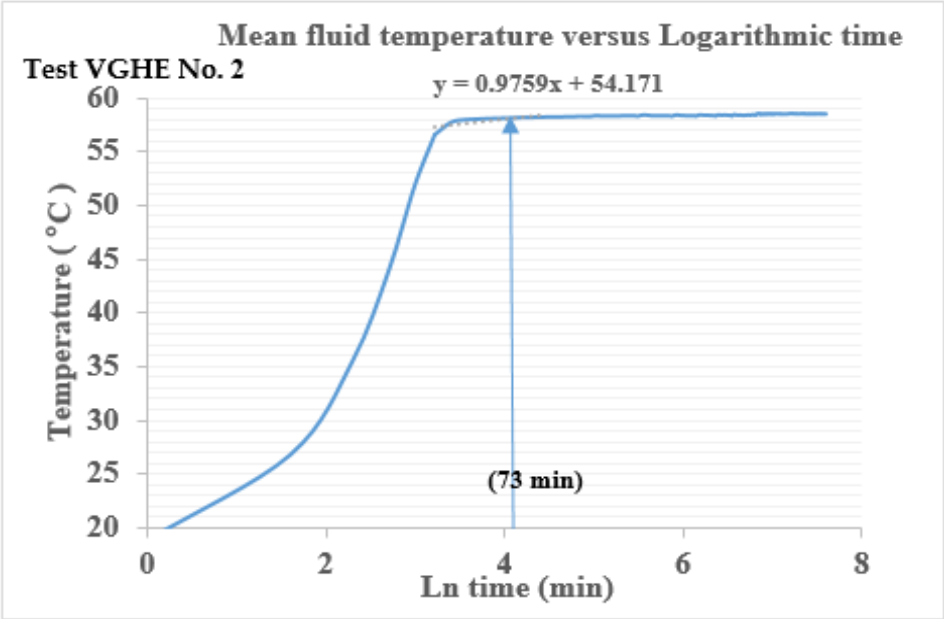

Figure 6.7: Mean fluid temperature versus logarithmic time (Inlet water temperature was 60 ºC)

The values of borehole thermal resistance (R_b) for the first two TRTs were calculated using the values of λ_{eff} (4.85 W/ m. K and 5.03 W/ m. K) in equation 3.25. The values of borehole thermal resistance (R_b) at t > 5 r^2/ α (i.e. 73 min, see Appendix C; error 10%), were found to be 0.680 m. K/ W and 0.597 m. K/ W, respectively, as shown in Table 6.3.

As shown in equation 3.26, there is a linear relationship between T_f and $ln(t)$. The slope (m) values for other two TRTs (VGHE No. 3 and 4) = 0.5494 and 0.8339 were calculated from Figures 6.8- 6.9, and then substituting 'm' in the equation 3.27, λ_{eff} were calculated as 5.90 W/ m. K and 6.60 W/ m. K, respectively.

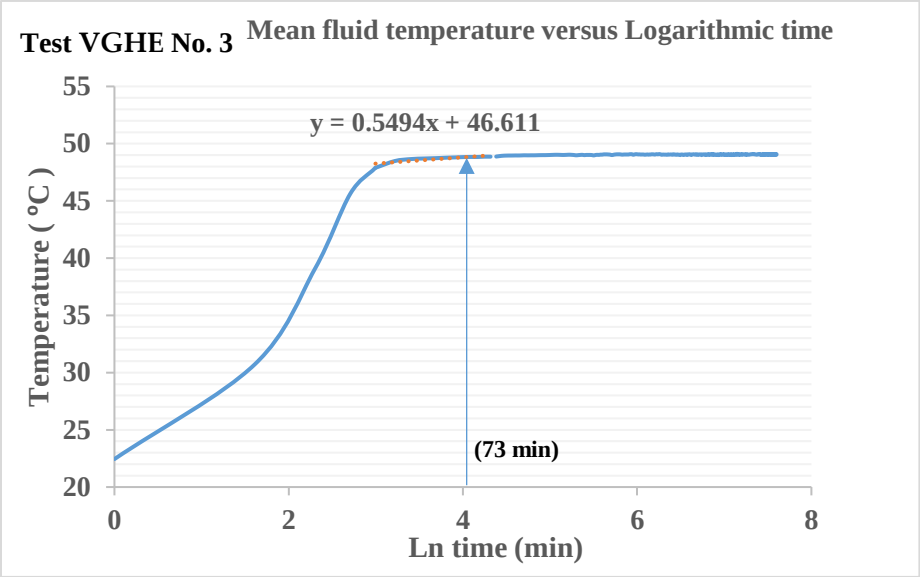

Figure 6.8: Mean fluid temperature versus logarithmic time (Inlet water temperature was 50 ºC)

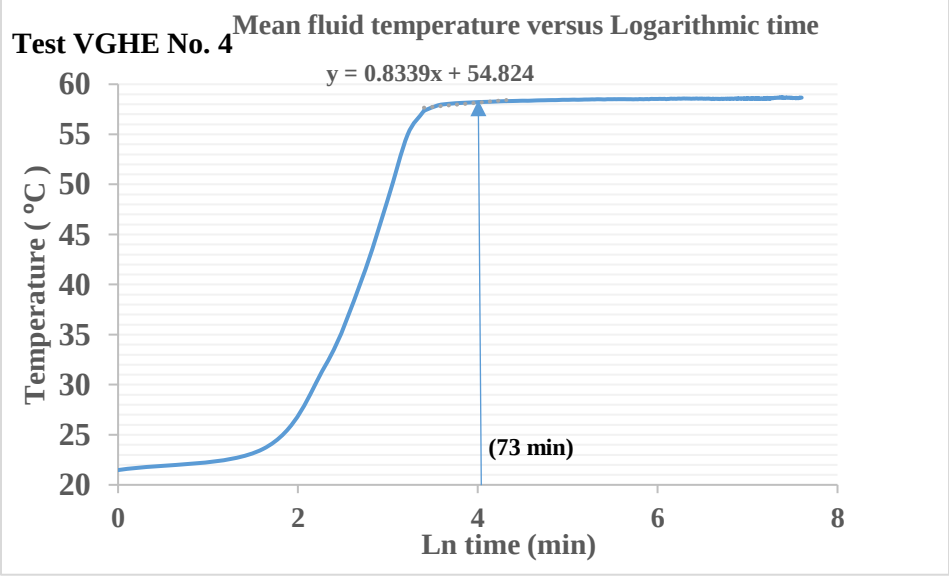

Figure 6. 9: Mean fluid temperature versus logarithmic time (Inlet water temperature was 60 ºC)

The values of borehole thermal resistance (R_b) for the other two TRTs were calculated using the values of λ_{eff} (5.90 W/ m. K and 6.60 W/ m. K) in equation 3.25. The values of borehole

thermal resistance (R_b) at t > 5 r^2/ α (i.e. 73 min, see Appendix C; error 10%), were found to be 0.649 m. K/ W and 0.504 m. K/ W, respectively, as shown in Table 6.3.

Table 6.3: Effective ground thermal conductivity, borehole thermal resistance, and heat injection rate

Test VGHE No.	**TRT starting time (MM DD, YYY)**	λ_{eff} **(W/ m. K)**	R_b **(m. K/ W)**	q (W/m)
1	Feb 06, 2018, 14:15	4.85	0.680	30.35
2	Feb 12, 2018, 20:15	5.03	0.597	37.20
3	April 10, 2018, 9:20	5.90	0.649	30.98
4	April 23, 2018, 8:10	6.60	0.504	38.90

As shown in Figures 6.6- 6.9, four TRTs were performed with two different gout materials (bentonite and silica sand) and two different heat injection rates (circulating fluid temperatures: 50 °C and 60 °C). The obtained results collected during the TRTs for the borehole with bentonite (VGHE No. 1 and 2) show lower effective ground thermal conductivities than those collected during the TRTs for the borehole with silica sand (VGHE No. 3 and 4), as shown in Table 6.3. For example, the effective ground thermal conductivity was compared between a borehole with bentonite (VGHE No. 1) and a borehole with silica sand (VGHE No. 3), all with the same water temperature coming from the circulating bath at 50 °C. It was noticed that the effective ground thermal conductivity for the borehole with bentonite (VGHE No. 1) was 4.85 W/ m. K, while the effective ground thermal conductivity for the borehole with silica sand (VGHE No. 4) was 5.90 W/ m. K. Also the obtained results show that the borehole thermal resistance for the (VGHE No. 1 and 2) with bentonite were higher compared to (VGHE No. 3 and 4) to the same with silica sand, as shown in Table 6.4. For example, the borehole thermal resistance was compared between a borehole with bentonite (VGHE No. 1) and a borehole with silica sand (VGHE No. 3), all with the same water temperature coming from the circulating bath at 50 °C. The borehole thermal resistance for the borehole with bentonite (VGHE No. 1) was 0.680 m. K/ W, while the borehole thermal resistance for the borehole with silica sand (VGHE No. 4) was 0.649 m. K/ W. The lowest borehole thermal resistance (0.504 m. K/ W) was found to be at the borehole with silica sand (VGHE No. 4), and with a water temperature of 60 °C coming from the circulating bath. The heat exchanger rate

for the (VGHE No. 1 and 2) with bentonite silica sand were lower than that for the (VGHE No. 3 and 4) with silica sand (see Table 6.3).

6.3 Summary of observations

In this chapter, four TRTs were conducted in the laboratory to estimate the influence of different grout materials and heat injection rates on the thermal efficiency of VGHEs. Two different inlet water temperature and two different grout materials were used. Line source theory was applied to estimate the effective ground thermal conductivity (λ_{eff}) and the borehole thermal resistance (R_b). The main observations of this investigation are summarized below:

- The heat exchange rate of VGHE is influenced by the circulation water temperature from the bath (i.e. different heat injection rate). Two different inlet water temperatures (50 °C and 60 °C) coming from the circulating bath were used during the first two TRTs (VGHE No. 1 and 2), all with bentonite as grout. Another two TRTs (VGHE No. 3 and 4), used silica sand as grout with the same inlet water temperatures (i.e. 50 °C and 60 °C). The obtained results show that after 50 hours from starting the test, the difference between the inlet and outlet water temperatures of the VGHE were 0.67 °C and 0.83 °C for the first two TRTs, while they were 0.69 °C and 0.86 °C for the other two TRTs, respectively.
- The results show that the effective ground thermal conductivity values obtained from TRTs (VGHE No. 1 and 2), with bentonite as grout, were 4.85 W/ m. K and 5.03 W/ m. K, while the effective ground thermal conductivity values obtained from TRTs (VGHE No. 3 and 4), with silica sand as grout, were found to be 5.90 W/ m. K and 6.6 W/ m. K, respectively. Therefore, the effective ground thermal conductivity values of VGHEs No. 1 and 2, with bentonite as grout, were lower than those for the VGHEs No. 3 and 4, all with silica sand as grout. It is noted that thermal conductivity of bentonite was also lower than silica sand (see Table 5.1).
- The results show that the borehole thermal resistance values for VGHEs No. 1 and 2, with bentonite as grout, were 0.680 m. K/ W and 0.597 m. K/ W , respectively, and the same for VGHEs No. 3 and 4, with silica sand as grout, were 0.649 m. K/ W and 0.504 m. K/ W, respectively. The observations presented in this study confirm the beneficial influence of

using grout materials with higher thermal conductivity or lower thermal resistivity on the overall thermal efficiency of VGHEs.

Chapter 7

Conclusion and scope of future work

This chapter first outlines the conclusions from this study, and then suggests the scope for further research.

7.1 Conclusions

The primary objective of this research is to improve the heat exchange efficiency of vertical ground heat exchanger (VGHE). After conducting a detailed the literature review, thermal response tests (TRTs) were carried in a purpose-built small-scale laboratory test setup, and experimental observations were documented and critically analyzed using line source theory. Conclusions are summarized below:

1. The literature shows that increasing the surface area of the pipe configuration enhances the heat transfer rate in VGHE.
2. Experimental results from this study confirm that a novel U-Tube pipe configuration, created by adding two fins on two directions of the outer side of the conventional single U-Tube pipe, increases the surface area for heat transfer, resulting in increasing the heat transfer rate in the VGHEs.
3. The difference between the inlet and outlet temperatures for the novel U-Tube pipe configuration increased by 0.29 °C after 60 hours, which is 76.3% higher than that of the conventional single U-Tube pipe configuration.
4. The borehole thermal resistance for the novel U-Tube pipe configuration decreased by 0.281 m. K/ W, which is 29.2% lower than that of the conventional single U-Tube pipe configuration.
5. The effective ground thermal conductivity for the novel U-Tube pipe configuration increased by 0.93 W/ m. K, which is 23.6% higher than that of the conventional single U-Tube pipe configuration.

6. The results showed that the heat exchange rate for the novel U-Tube pipe configuration was increased by of 11.04 W/ m, which is 58% higher compared to the conventional single U-Tube.
7. The results indicated that the average ground temperatures at the borehole, in all four directions, for the novel U-Tube pipe configuration were higher than the same for the conventional U-Tube pipe configuration. This mean more heat rejected into the ground when the novel U-Tube pipe configuration was used.
8. Tests conducted in the laboratory, to investigate the effects of two grout materials (bentonite and silica sand) on the thermal efficiency of VGHE, show that the heat exchange rate for the with silica sand (grout) was higher compared to the same with bentonite. Quite naturally, the borehole thermal resistance with bentonite as grout was found to be higher than the same with silica sand.
9. Tests conducted in the laboratory, to investigate the effects two different inlet fluid temperatures on the thermal efficiency of VGHE, show that difference between the inlet and outlet temperatures increased with the increase of inlet fluid temperature coming from the circulation bath.
10. Overall the results obtained from this research indicate that increased surface area of the U-Tube pipe due to external fins enhances the heat transfer rate, resulting in an improvement in the thermal performance of the VGHE, and reduced cost of installation and materials for the ground source heat pump (GSHP).

7.2 Scope of future work

In this research, the concept of external fins to increase the thermal efficiency of vertical ground heat exchanger (VGHE) has been successfully introduced and demonstrated through small-scale laboratory tests. However, further investigations are needed to advance this concept to real life applications as outlined below:

1. Conduct large-scale laboratory and field studies to further characterise the beneficial impacts of single U-tube pipe with external fins on the thermal performance of VGHE.
2. Copper pipe was used in this small-scale laboratory study. Further investigations should be carried out both in laboratory and field using High-density polyethylene (HDPE) U-tube pipe with fins.

3. Different shapes and size of the fins on U-tube pipe and their impacts on the thermal performance of VGHE should be investigated and optimum size and shape of the fins should be determined.

Bibliography

[1] S Self, "Enhancing geothermal heat pump systems with parametric performance analyses," PhD dissertation, University of Ontario Institute of Technology, Oshawa, 2010.

[2] ASHRAE. Heating, Ventilating, and Air-Conditioning Applications; American Society of Heating, Refrigerating and Air-Conditioning Engineers, Inc.: Atlanta, GA, USA, 2011.

[3] K. N. Muraya, "Numerical Modeling of the Transient Thermal Interference of Vertical U-Tube Heat Exchangers," PhD dissertation., Texas A&M University, Texas, 1994.

[4] C. Lee, M. Park, S Min, S. H. Kang, B. Sohn and H. Choi, "Comparison of effective thermal conductivity in closed-loop vertical ground heat exchangers," Applied Thermal Engineering 31, no. 17-18, 3669-3676, (2011).

[5] C. Arson, E. Berns, G. Akrouch, M. Sanchez and J. L. Briaud, “Heat propagation around geothermal piles and implications on energy balance,” Energy Book Series, 1, pp.628-635, 2013.

[6] H. Yang, P. Cui and Z. Fang, “Vertical-borehole ground-coupled heat pumps: A review of models and systems,” Applied energy, 87(1), pp.16-27, 2010.

[7] M. Ozturk, “Energy and exergy analysis of a combined ground source heat pump system. Applied thermal engineering,” 73(1), pp.362-370, 2014.

[8] A. Fashina, M. Mundu, O Akiyode, L. Abdullah, D. Sanni and L. Ounyesiga, “The drivers and barriers of renewable energy applications and development in Uganda: a review,” Clean Technologies, 1(1), pp.9-39, 2019.

[9] O. K. Bishoge, L. Zhang and W. G. Mushi, “The potential renewable energy for sustainable development in Tanzania: A review,” Clean Technologies, 1(1), pp.70-88, 2019.

[10] A. M. Omer, “Ground-source heat pumps systems and applications. Renewable and sustainable energy reviews,” 12(2), pp.344-371, 2008.

[11] I. Sarbu, and C. Sebarchievici, “General review of ground-source heat pump systems for heating and cooling of buildings,” Energy and buildings, 70, pp.441-454, 2014.

[12] P. Monzó, “Comparison of different Line Source Model approaches for analysis of Thermal Response Test in a U-pipe Borehole heat Exchanger,” Master of Science Thesis Energy Technology, KTH School of Industrial Engineering and Management, Stockholm, 2011.

[13] P. Mogensen, “Fluid to duct wall heat transfer in duct system heat storages,” Document-Swedish Council for Building Research, (16), 652-657, 1983.

[14] C. Eklöf and S. Gehlin, “TED-a mobile equipment for thermal response test: testing and evaluation,” Luleå University of Technology, Luleå, 1996.

[15] W. A. Austin III, “Development of an in situ system for measuring ground thermal properties,” Doctoral dissertation, Oklahoma State University, Stillwater, Oklahoma, 1998.

[16] B. Sanner, M. Reuss, E. Mands and J. Müller, “Thermal response test-experiences in Germany,” In Proc. Terrastock, pp. 177-182, 2000.

[17] C. P. Remund, “Borehole thermal resistance: laboratory and field studies,” ASHRAE transactions, 105, p.439, 1999.

[18] M. L. Allan and S. P. Kavanaugh, “Thermal conductivity of cementitious grouts and impact on heat exchanger length design for ground source heat pumps,” Hvac&R Research, 5(2), pp.85-96, 1999.

[19] N. H. Abu-Hamdeh, A. I. Khdair and R. C. Reeder, “A comparison of two methods used to evaluate thermal conductivity for some soils,” International Journal of Heat and Mass Transfer, 44(5), pp.1073-1078, 2001.

[20] D. Pahud and B. Matthey, “Comparison of the thermal performance of double U-pipe borehole heat exchangers measured in situ,” Energy and buildings, 33(5), pp.503-507, 2001.

[21] T. Katsura, K. Nagano, S. Takeda and K. Shimakura, “Heat transfer experiment in the ground with ground water advection,” In Proceedings of 10th Energy Conservation Thermal Energy Storage Conference Ecostock (pp. 2006-5), 2006.

[22] A. M. Gustafsson and L. Westerlund, “Multi-injection rate thermal response test in groundwater filled borehole heat exchanger,” Renewable Energy, 35(5), pp.1061-1070, 2010.

[23] S. Javed, J. D. Spitler and P. Fahlén, “An experimental investigation of the accuracy of thermal response tests used to measure ground thermal properties,” ASHRAE Transactions, 117(1), pp.13-21, 2011.

[24] A. A. Alrtimi, M. Rouainia and D. A. C. Manning, “Thermal enhancement of PFA-based grout for geothermal heat exchangers,” Applied thermal engineering, 54(2), pp.559-564, 2013.

[25] H. Lei and C. Dai, “Comparative experiment of different backfill grouts for concentric ground heat exchangers,” Delta, 37, pp.597-600, 2013.

[26] S. Erol and B. François, “Efficiency of various grouting materials for borehole heat exchangers,” Applied Thermal Engineering, 70(1), pp.788-799, 2014.

[27] J. Luo, J. Rohn, W. Xiang, M. Bayer, A. Priess, L. Wilkmann, H. Steger and R. Zorn, “Experimental investigation of a borehole field by enhanced geothermal response test and numerical analysis of performance of the borehole heat exchangers,” Energy, 84, pp.473-484, 2015.

[28] W. Choi and R. Ooka, “Effect of natural convection on thermal response test conducted in saturated porous formation: Comparison of gravel-backfilled and cement-grouted borehole heat exchangers,” Renewable Energy, 96, pp.891-903, 2016.

[29] J. Luo, J. Tuo, W. Huang, Y. Zhu, Y. Jiao, W. Xiang and J. Rohn, “Influence of groundwater levels on effective thermal conductivity of the ground and heat transfer rate of borehole heat exchangers,” Applied Thermal Engineering, 128, pp.508-516, 2018.

[30] C. Lee, "Thermal performance evaluation of a vertical closed-loop ground heat exchanger according to rock type in Korea.” Energy and Buildings, 183, pp.184-194, 2019.

[31] H. Zeng, N. Diao and Z. Fang, “Heat transfer analysis of boreholes in vertical ground heat exchangers,” International journal of heat and mass transfer, 46(23), pp.4467-4481, 2003.

[32] J. Acuña and B. Palm, “A novel coaxial borehole heat exchanger: description and first distributed thermal response test measurements,” In Proceedings of the World Geothermal Congress (p. 7), 2010.

[33] F. Guillaume, “Analysis of a novel pipe in pipe coaxial borehole heat exchanger,” Master’s thesis, KTH School of Industrial Engineering and Management, Stockholm, 2011.

[34] R. A. Beier and G.vN. Ewbank, “In-Situ Test Thermal Response Tests Interpretations. OG&E Ground Source Heat Exchange Study,” Oklahoma State Univ., Stillwater, Oklahoma City, 2012.

[35] J. Desmedt, J. Van Bael, H. Hoes and N. Robeyn, “Exp`erimental performance of borehole heat exchangers and grouting materials for ground source heat pumps,” International journal of energy research, 36(13), pp.1238-1246, 2012.

[36] J. Acuña, “Distributed thermal response tests: New insights on U-pipe and Coaxial heat exchangers in groundwater-filled boreholes,” Doctoral dissertation, KTH Royal Institute of Technology, Stockholm, 2013.

[37] A. Bidarmaghz, G. Narsilio and I. Johnston, “Numerical modelling of ground heat exchangers with different ground loop configurations for direct geothermal applications,” In Proceedings of the 18th international conference on soil mechanics and geotechnical engineering, Paris, France (pp. 2-6), 2013.

[38] S. Dincer, C. Erdogan, B. B. M. S. ve Ticaret and A. O. Beldesi, “Experimental measurement and long term predictions of a multi-U tube borehole performance for ground source heat pumps,” In Proceedings of the 11th IEA Heat Pump Conference 2014, Montréal, 2014.

[39] J. Haddada and A. Miyara, “Thermal Performance and Characteristics of SpiraL-Tube Ground Heat Exchanger for Ground-Source Heat Pump,” In International Heat Transfer Conference Digital Library. Begel House Inc, 2014.

[40] J. Haddada and A. Miyara, “Performance Investigation of Multiple-Tube Ground Heat Exchangers for Ground-Source Heat Pump,” American Journal of Energy Engineering. Vol. 2, No. 5, pp. 103-107, 2014.

[41] X. Liu, Y. Xiao, K. Inthavong and J. Tu, “Experimental and numerical investigation on a new type of heat exchanger in ground source heat pump system,” Energy efficiency, 8(5), pp.845-857, 2015.

[42] S. Yoon, S. R. Lee, J. Xue, K. Zosseder, G. H. Go and H. Park, “Evaluation of the thermal efficiency and a cost analysis of different types of ground heat exchangers in energy piles,” Energy Conversion and Management, 105, pp.393-402, 2015.

[43] J. Raymond, S. Mercier and L. Nguyen, “Designing coaxial ground heat exchangers with a thermally enhanced outer pipe,” Geothermal Energy, 3(1), p.7, 2015.

[44] K. S. Chang and M. J. Kim, “Thermal performance evaluation of vertical U-loop ground heat exchanger using in-situ thermal response test,” Renewable Energy, 87, pp.585-591, 2016.

[45] J. Luo, H. Zhao, S. Gui, W. Xiang, J. Rohn and P. Blum, “Thermo-economic analysis of four different types of ground heat exchangers in energy piles,” Applied Thermal Engineering, 108, pp.11-19, 2016.

[46] C. Sáez Blázquez, A. Farfan Martin, I. Martin Nieto, P. Carrasco Garcia, L. S. Sánchez Pérez and D. González-Aguilera, “Efficiency analysis of the main components of a vertical closed-loop system in a borehole heat exchanger,” Energies, 10(2), p.201, 2017.

[47] A. Busso, A. Georgiev and P. Roth, “Underground thermal energy storage–first thermal response test in South America,” RIO 3-World Climate and Energy Event, pp.189-196, 2003.

[48] G. Florides and S. Kalogirou, “First in situ determination of the thermal performance of a U-pipe borehole heat exchanger, in Cyprus,” Applied Thermal Engineering, 28(2-3), pp.157-163, 2008.

[49] M. H. Sharqawy, S. A. Said, E. M. Mokheimer, M. A. Habib, H. M. Badr and N. A. Al-Shayea, “First in situ determination of the ground thermal conductivity for boreholeheat exchanger applications in Saudi Arabia,” Renewable Energy, 34(10), pp.2218-2223, 2009.

[50] H. Esen, M. Inalli and Y. Esen, “Temperature distributions in boreholes of a vertical ground-coupled heat pump system. Renewable Energy,” 34(12), pp.2672-2679, 2009.

[51] R. A. Beier, M. D. Smith and J. D. Spitler, “Reference data sets for vertical borehole ground heat exchanger models and thermal response test analysis,” Geothermics, 40(1), pp.79-85, 2011.

[52] J. Acuña, and B. Palm, “Distributed thermal response tests on pipe-in-pipe borehole heat exchangers,” Applied Energy, 109, pp.312-320, 2013.

[53] J. Luo, J. Rohn, M. Bayer and A. Priess, “Thermal efficiency comparison of borehole heat exchangers with different drillhole diameters,” Energies, 6(8), pp.4187-4206, 2013.

[54] M. Cimmino and M. Bernier, “Experimental determination of the g-functions of a small-scale geothermal borehole,” Geothermics, 56, pp.60-71, 2015.

[55] A. G. Georgiev, R. K. Popov and E.T. Toshkov, “In-situ measurements of ground thermal properties around borehole heat exchangers in Plovdiv, Bulgaria,” Bulgarian Chemical Communications, pp.19-26, 2016.

[56] C. Yavuzturk, J. D. Spitler and S. J. Rees, “A transient two-dimensional finite volume model for the simulation of vertical U-tube ground heat exchangers,” ASHRAE transactions, 105(2), pp.465-474, 1999.

[57] Z. Li and M. Zheng, “Development of a numerical model for the simulation of vertical U-tube ground heat exchangers,” Applied Thermal Engineering, 29(5-6), pp.920-924, 2009.

[58] V. Khalajzadeh, G. Heidarinejad and J. Srebric, “Parameters optimization of a vertical ground heat exchanger based on response surface methodology,” Energy and Buildings, 43(6), pp.1288-1294, 2011.

[59] S. Javed, J. Claesson and R. Beier, “Recovery times after thermal response tests on vertical borehole heat exchangers,” In Proceedings of 23rd IIR International Congress of Refrigeration (ICR2011), Prague, Czech Republic, 2011.

[60] J. Meyer, D. Pride, J. O’Toole, C. Craven and V. Spencer, “Ground Source Heat Pumps in Cold Climates,” Alaska Center for Energy and Power Cold Climate Housing Research Center: Fairbanks, AK, USA, 2011.

[61] R. Garber-Slaght, P. R. Daanen and P.A. Roe, “Ground source heat pump effciency in cold climates,” In Proceedings of the Conference Paper Session-Ground Source Heat Pump System, Seattle, WA, USA, 2014.

[62] T. Lhendup, L. Aye and R. J. Fuller, “In-situ measurement of borehole thermal properties in Melbourne,” Applied thermal engineering, 73(1), pp.287-295, 2014.

[63] A. Salim Shirazi and M. Bernier, “A small-scale experimental apparatus to study heat transfer in the vicinity of geothermal boreholes,” HVAC&R Research, 20(7), pp.819-827, 2014.

[64] G. Soriano, R. Villanueva, I. Gonzalez, A. Montero and M. Cornejo, “First in situ measurement of soil thermal response in Guayaquil, Ecuador,” WIT Transactions on Ecology and the Environment, pp.327-336, 2015.

[65] T. Başer, N. Lu and J. S. McCartney, “Operational response of a soil-borehole thermal energy storage system,” Journal of Geotechnical and Geoenvironmental Engineering, 142(4), p.04015097, 2016.

[66] L. Zhang, Q. Zhang and G. Huang, “A transient quasi-3D entire time scale line source model for the fluid and ground temperature prediction of vertical ground heat exchangers (GHEs),” Applied Energy, 170, pp.65-75, 2016.

[67] Y. Yu, R. Miao, L. Miller, H. Yang, G. Olson, “Recent Development and Application of Geothermal Heat Pump Systems in Cold-Climate Regions of the US: A Further Investigation,” Engineering, 9(7), pp.625-648, 2017.

[68] J. D. Spitler and S. E. Gehlin, “Thermal response testing for ground source heat pump systems—An historical review,” Renewable and Sustainable Energy Reviews, 50, pp.1125-1137, 2015.

[69] B. Sanner, G. Hellström, J. Spitler and S. Gehlin, “Thermal response test–current status and world-wide application,” In Proceedings world geothermal congress (Vol. 1436, p. 2005). International Geothermal Association, 2005.

[70] T. R. Young, “Development, verification, and design analysis of the borehole fluid thermal mass model for approximating short term borehole thermal response,” Doctoral dissertation, Oklahoma State University, Oklahoma, 2004.

[71] D. Marcotte and P. Pasquier, “On the estimation of thermal resistance in borehole thermal conductivity test,” Renewable energy, 33(11), pp.2407-2415, 2008.

[72] G. H. Go, S.R. Lee, S. Yoon, H. Park and S. Park, “Estimation and experimental validation of borehole thermal resistance.” KSCE Journal of Civil Engineering, 18(4), pp.992-1000, 2014.

[73] L. Jun, Z. Xu, G. Jun and Y. Jie, “Evaluation of heat exchange rate of GHE in geothermal heat pump systems,” Renewable energy, 34(12), pp.2898-2904, 2009.

[74] Y. Gu, and D. L. O'Neal, “Development of an equivalent diameter expression for vertical U-tubes used in ground-coupled heat pumps. transactions-american society of heating refrigerating and air conditioning engineers”, 104, pp.347-355, 1998.

[75] M. He, “Numerical modelling of geothermal borehole heat exchanger systems,” PhD dissertation, De Montfort University, Leicester, 2012.

[76] M. Marcucci, “Distributed Thermal Response Test on a Grouted U-pipe Borehole Heat Exchanger,” Master’s thesis, KTH School of Industrial Engineering and Management,

Stockholm, 2014.

[77] A. A. Eswiasi, M. A. Muntasser and B. Nordell, First thermal response test in Libya. In International Conference on Thermal Energy Storage: 14/06/2009-17/06/2009. Energi-och Miljötekniska Föreningen/EMTF Förlag, 2009.

[78] M. A. Boukli Hacene, S. Amara and N. E. Chabane Sari, “Analysis of the first thermal response test in Algeria,” Journal of thermal analysis and calorimetry, 107(3), pp.1363-1369, 2012.

[79] P. Eskilson, “Thermal analysis of heat extraction boreholes”, PHD thesis, Lund University, Lund, 1987.

[80] S. Gehlin, “Thermal response test: method development and evaluation,” department of environmental division of water resources engineering, Lulea University, Lulea, 2002.

[81] S. Gehlin and B. Nordell, “Determining undisturbed ground temperature for thermal response test” In ASHRAE Transactions (Vol. 109, No. 1, pp. 151-156), 2003.

[82] S. Gehlin and G. Hellström, “Recent status of in-situ thermal response tests for BTES applications in Sweden,” Proc. Terrastock 2000, pp.159-164, 2000.

[83] Y. Gu and D. L. O'Neal, “Modeling the effect of backfills on U-tube ground coil performance”, Ashrae Transactions, 104, p.356, 1998.

[84] S. Gehlin, “Thermal response test: in situ measurements of thermal properties in hard rock,” Doctoral dissertation, Luleå tekniska universitet, Luleå,1998.

[85] H. J. Witte, G. J. Van Gelder and J. D. Spitler, “In situ measurement of ground thermal conductivity: a Dutch perspective,” Ashrae Transactions, 108(1), pp.263-272, 2002.

[86] C. A. Kramer and P. Basu, “Performance of a model geothermal pile in sand,” In Proc. 8th Int. Conf. on Physical Modelling in Geotechnics, Perth (Gaudin, C. & White, D.(eds)). Leiden: CRC Press/Balkema (pp. 771-777), 2014.

[87] W. Yang, Z. Chen, M. Shi and C. Zhang, “An in situ thermal response test for borehole heat exchangers of the ground-coupled heat pump system,” International Journal of Sustainable Energy, 32(5), pp.489-503, 2013.

[88] T. Zhou, M. Chen, and B. Liang, “Thermal performance of a ground U-shaped tube with twisted tapes in sand/graphite backfill materials,” Experimental Heat Transfer, pp.1-15, 2020.

[89] J. You and C. Lee, “Analysis of effective thermal conductivity stability of geothermal heat exchanger according to ambient environmental conditions,” International Journal of Energy Research, 43(13), 7682-7692, 2019.

[90] P. Zhao, X. Li, Y. Zhang, K. Liu, and M. Lu, “Stratified thermal response test measurement and analysis,’ Energy and Buildings, p.109865, 2020.

[91] S. Yoon and M. J. Kim, “Prediction of ground thermal diffusivity from thermal response tests,” Energy and Buildings, 185, pp.239-246, 2019.

[92] F. Loveridge, C. G. Olgun, T. Brettmann, and W. Powrie, “The thermal behaviour of three different auger pressure grouted piles used as heat exchangers,” Geotechnical and Geological Engineering, 33(2), pp.273-289, 2015.

[93] A. Moradi and H. Ahmadikia, “Analytical solution for different profiles of fin with temperature-dependent thermal conductivity,” Mathematical Problems in Engineering, 2010.

[94] M. Torabi, A. Aziz and K. Zhang, “A comparative study of longitudinal fins of rectangular, trapezoidal and concave parabolic profiles with multiple nonlinearities.” Energy, 51, pp.243-256, 2013.

[95] Esen, H. and Inalli, M., "Thermal response of ground for different depths on vertical ground source heat pump system in Elazığ, Turkey," Journal of the Energy Institute, 82(2), pp.95-101, 2009.

[96] Javadi, H., Ajarostaghi, S.S.M., Rosen, M.A. and Pourfallah, M., "Performance of ground heat exchangers: A comprehensive review of recent advances," Energy, 178, pp.207-233, 2019.

[97] A. S. Ramadan, "Parametric study of vertical ground loop heat exchangers for ground source heat pump systems," Master of Engineering Science, University of Western Ontario, London, Ontario, Canada, 2016.

[98] A. A. Serageldin, Y. Sakata, T. Katsura and K. Nagano, "Thermo-hydraulic performance of the U-tube borehole heat exchanger with a novel oval cross-section: Numerical approach," Energy Conversion and Management, 177, pp.406-415, 2018.

[99] S. M. Bae, Y. Nam, J. M. Choi, K. H. Lee and J. S. Choi, "Analysis on thermal performance of ground heat exchanger according to design type based on thermal response test," Energies, 12 (4), p.651, 2019.

[100] W. Li, X. Li, Y. Peng, Y. Wang and J. Tu, "Experimental and numerical investigations on heat transfer in stratified subsurface materials," Applied Thermal Engineering, 135, pp.228-237, 2018.

[101] B. Liang, M. Chen, B. Fu, and H. Li, "Investigation on the thermal and flow performances of a vertical spiral-tube ground heat exchanger in sand combined with kaolin additive," Energy and Buildings, 190, pp.235-245, 2019.

[102] J. Raymond, R. Therrien, L. Gosselin, and R. Lefebvre, "A review of thermal response test analysis using pumping test concepts," Groundwater, 49(6), pp.932-945, 2011.

[103] C. Zhang, Z. Guo, Y. Liu, X. Cong, and D. Peng, "A review on thermal response test of ground-coupled heat pump systems," Renewable and Sustainable Energy Reviews, 40, pp.851-867, 2014.

[104] A. Salimshirazi, "Transient heat transfer in vertical ground heat exchangers," Doctoral dissertation, École Polytechnique de Montréal, Montreal, 2012.

[105] Geothermal Grout™, Technical Data, Cetco Building Products, www.cetco.com/dpg (Last accessed in January 2018).

[106] A. Eswiasi, and P. Mukhopadhyaya, "Critical Review on Efficiency of Ground Heat Exchangers in Heat Pump Systems," Clean Technologies, 2(2), pp.204-224, 2020.

[107] H. Wang, Y. Cui, and C. Qi, "Effects of sand–bentonite backfill materials on the thermal performance of borehole heat exchangers," Heat transfer engineering, 34(1), pp.37-44, 2013.

[108] R. Borinaga-Treviño, P. Pascual-Muñoz, D. Castro-Fresno and E. Blanco-Fernandez, "Borehole thermal response and thermal resistance of four different grouting materials measured with a TRT," Applied thermal engineering, 53(1), 13-20, 2013.

[109] J. D. Spitler, S. Javed and R. K. Ramstad, "Natural convection in groundwater-filled boreholes used as ground heat exchangers," Applied Energy, 164, 352-365, 2016.

[110] Y. Zhou, Y. Zhang, and Y. Xu, "Influence of grout thermal properties on heat-transfer performance of ground source heat exchangers," Science and Technology for the Built Environment, 24(5), pp.461-469, 2018.

[111] W. Li, X. Li, R. Du, Y. Wang, and J. Tu, "Experimental investigations of the heat load effect on heat transfer of ground heat exchangers in a layered subsurface," Geothermics, 77, pp.75-82, 2019.

[112] G.N. Watson, "A treatise on the theory of Bessel functions." Cambridge university press, 1995.

[113] T.L. Bergman, F.P. Incropera, D.P. DeWitt and A.S Lavine, "Fundamentals of heat and mass transfer." John Wiley & Sons, 2011.

Appendix A

Heat transfer through extended surfaces (fins)

Temperature distribution and heat transfer rate for two types of fin shapes (rectangular and trapezoidal) are shown below:

A.1 Heat transfer through the rectangular fin

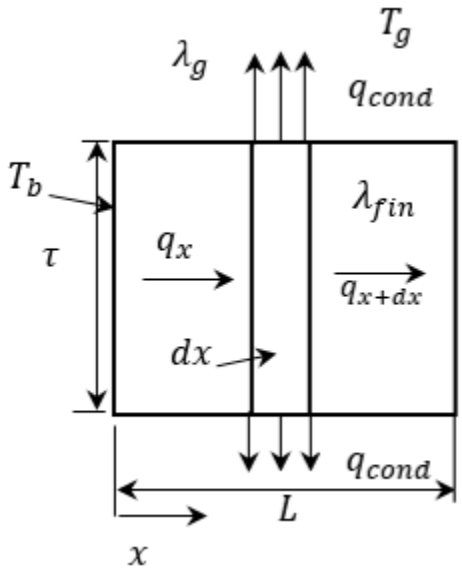

Figure A.1: Top view of rectangular fin.

A_c = Cross-sectional area (m^2)

A_{cond} = Surface area of the element (m^2)

L = Fin length (m)

L_g = Grout thickness (m)

P = Perimeter (m)

q_{cond} = Heat transfer (conduction) from the surface of the element to the surrounding grout (W)

q_{fin} = Conduction heat flow at the base of the fin (W)

q_x = Conduction heat flow rate in the element (W)

q_{x+dx} = Conduction heat flow rate out of the element (W)

T = Temperature of element (ºC)

T_b= Base temperature (ºC)

T_g= Grout temperature (ºC)

T_L= Fin temperature at length L (ºC)

ω = Fin thickness [depth] (m)

τ = Fin width at the base (m)

λ_{fin} = Fin thermal conductivity (W/ m. K)

λ_g = Grout thermal conductivity (W/ m. K)

Heat flow rate into the element is,

$$q_x = -\lambda_{fin}\, A_c \frac{dT}{dx} \tag{A.1}$$

The conduction heat flow rate in and out of the element,

$$q_x = q_{x+dx} + 2\, q_{cond} \tag{A.2}$$

Substituting the value of q_x into q_{x+dx},

$$q_{x+dx} = q_x + \frac{d}{dx}(q_x)dx \tag{A.3}$$

q_{cond}= Conduction heat transfer from the surface of element to the grout,

$$q_{cond} = \frac{\lambda_g}{L} A_{cond}\big(T - T_g\big) = 2\,\frac{\lambda_g}{L_g}\,(P \times dx)\big(T - T_g\big) \tag{A.4}$$

Where A_{cond} is the surface area $(\text{Perimeter}\ (P) \times dx)$ of the element.

Substituting the values of q_{dx} and q_{cond}into equation (A.2),

$$q_x = q_x + \frac{d}{dx}\Big(-\lambda_{fin}\, A_c \frac{dT}{dx}\Big)\, dx + 2\frac{\lambda_g}{L_g}\,(P \times dx)\big(T - T_g\big) \tag{A.5}$$

Equation (A.5) becomes,

$$\frac{d}{dx}\Big(\, A_c \frac{dT}{dx}\Big) - 2\frac{\lambda_g}{\lambda_{fin}\, L_g}\, P\big(T - T_g\big) = 0 \tag{A.6}$$

$$A_c \frac{d^2T}{dx^2} + \frac{dT}{dx}\frac{dA_c}{dx} - 2\frac{\lambda_g}{\lambda_{fin}\, L_g}\, P\big(T - T_g\big) = 0 \tag{A.7}$$

In rectangular fin, A_c is constant, $A_c = \omega\, \tau$

The equation (A.7) becomes,

$$\frac{d^2T}{dx^2} - 2\frac{\lambda_g\, P}{\lambda_{fin}\, L_g\, A_c}\, dT = 0 \tag{A.8}$$

$$\varepsilon^2 = 2\frac{\lambda_g\, P}{\lambda_{fin}\, L_g\, A_c} \rightarrow \varepsilon = \sqrt{2\frac{\lambda_g\, P}{\lambda_{fin}\, L_g\, A_c}} = \sqrt{2\frac{\lambda_g\, \omega}{\lambda_{fin}\, L_g\, \omega\, \tau}} = \sqrt{2\frac{\lambda_g}{\lambda_{fin}\, L_g\, \tau}} \tag{A.9}$$

Let $\theta = T - T_g$, and substituting the value of ε^2 into equation (A.8)

$$\frac{d^2\theta}{dx^2} - \varepsilon^2\,\theta = 0 \qquad \text{(A.10)}$$

Equation (A.10) represents a second order differential equation, and the general solution for this equation is,

$$\theta = C_1\,e^{\varepsilon x} + C_2\,e^{-\varepsilon x} \qquad \text{(A.11)}$$

Where C_1 and C_2 are constants, and these constants can be determined by using boundary conditions.

In this case, the length of the fin is L.

at $x = 0$, $T = T_b$

$$\theta(0) = T_b - T_g \equiv \theta_b \qquad \text{(A.12)}$$

$$\theta_b = C_1 + C_2 \qquad \text{(A.13)}$$

at $x = L$, $T = T_L$

$$2\frac{\lambda_g * A_c}{L_g}\left(T_L - T_g\right) = -\lambda_{fin}\,A_c\left(\frac{dT}{dx}\right)_{x=L} \qquad \text{(A.14)}$$

Dividing the equation A.14 by A_c and substituting the values of $\frac{d\theta}{dx}$ and θ_L instead of $\frac{dT}{dx}$ and $(T_L - T_g)$ respectively.

$$\frac{\lambda_g}{L_g}\theta_L = -\lambda_{fin}\left(\frac{d\theta}{dx}\right)_{x=L} \qquad \text{(A.15)}$$

From equation A.11, $\theta = C_1\,e^{\varepsilon x} + C_2\,e^{-\varepsilon x}$

$$\frac{d\theta}{dx} = \varepsilon\,C_1\,e^{\varepsilon x} - \varepsilon\,C_2\,e^{-\varepsilon x} \qquad \text{(A.16)}$$

$$\left(\frac{d\theta}{dx}\right)_{x=L} = \varepsilon\,C_1\,e^{\varepsilon L} - \varepsilon\,C_2\,e^{-\varepsilon L} \qquad \text{(A.17)}$$

$$\theta_L = C_1\,e^{\varepsilon L} + C_2\,e^{-\varepsilon L} \qquad \text{(A.18)}$$

By substituting the values of $\left(\frac{d\theta}{dx}\right)_{x=L}$ and θ_L into equation A.15,

$$\frac{\lambda_g}{L_g}(C_1\,e^{\varepsilon L} + C_2\,e^{-\varepsilon L}) = -\lambda_{fin}\,(\varepsilon\,C_1\,e^{\varepsilon L} - \varepsilon\,C_2\,e^{-\varepsilon L}) \qquad \text{(A.19)}$$

$$\frac{\lambda_g}{L_g\,\lambda_{fin}\,\varepsilon}(C_1\,e^{\varepsilon L} + C_2\,e^{-\varepsilon L}) + (\,C_1\,e^{\varepsilon L} - \,C_2\,e^{-\varepsilon L}) = 0$$

$$\frac{\lambda_g}{L_g\,\lambda_{fin}\,\varepsilon}C_1\,e^{\varepsilon L} + \frac{\lambda_g}{L_g\,\lambda_{fin}\,\varepsilon}C_2\,e^{-\varepsilon L} + \,C_1\,e^{\varepsilon L} - \,C_2\,e^{-\varepsilon L} = 0$$

$$C_1\left(\frac{\lambda_g}{L_g\,\lambda_f\,\varepsilon}e^{\varepsilon L} + e^{\varepsilon L}\right) + C_2\left(\frac{\lambda_g}{L_g\varepsilon}e^{-\varepsilon L} - e^{-\varepsilon L}\right) = 0$$

$$C_1\left(\frac{\lambda_g}{L_g\,\lambda_{fin}\,\varepsilon}e^{\varepsilon L} + e^{\varepsilon L}\right) = C_2\left(e^{-\varepsilon L} - \frac{\lambda_g}{L_g\,\lambda_{fin}\,\varepsilon}e^{-\varepsilon L}\right)$$

$$C_1 = C_2 \frac{(e^{-\varepsilon L} - \frac{\lambda_g}{L\,\lambda_{fin}\,\varepsilon} e^{-\varepsilon L})}{\left(\frac{\lambda_g}{L_g\,\lambda_{fin}\,\varepsilon} e^{\varepsilon L} + e^{\varepsilon L}\right)}$$

By substituting the value of C_1 into equation A.13,

$$\theta_b = C_2 \frac{(e^{-\varepsilon L} - \frac{\lambda_g}{L_g\,\lambda_{fin}\,\varepsilon} e^{-\varepsilon L})}{\left(\frac{\lambda_g}{L_g \varepsilon} e^{\varepsilon L} + e^{\varepsilon L}\right)} + C_2$$

$$C_2 = \frac{\theta_b}{\left(\frac{\left(e^{-\varepsilon L} - \frac{\lambda_g}{L_g\,\lambda_{fin}\,\varepsilon} e^{-\varepsilon L}\right)}{\left(\frac{\lambda_g}{L_g\,\lambda_{fin}\,\varepsilon} e^{\varepsilon L} + e^{\varepsilon L}\right)} + 1\right)}$$

By substituting the value of C_2 into equation A.13,

$$C_1 = \theta_b\left(1 - \frac{1}{\left(\frac{\left(e^{-\varepsilon L} - \frac{\lambda_g}{L_g\,\lambda_{fin}\,\varepsilon} e^{-\varepsilon L}\right)}{\left(\frac{\lambda_g}{L_g\,\lambda_{fin}\,\varepsilon} e^{\varepsilon L} + e^{\varepsilon L}\right)} + 1\right)}\right)$$

By substituting the values of C_1 and C_2 into equation A.11,

$$\theta = \theta_b\left(1 - \frac{1}{\left(\frac{\left(e^{-\varepsilon L} - \frac{\lambda_g}{L_g\,\lambda_{fin}\,\varepsilon} e^{-\varepsilon L}\right)}{\left(\frac{\lambda_g}{L_g\,\lambda_{fin}\,\varepsilon} e^{\varepsilon L} + e^{\varepsilon L}\right)} + 1\right)}\right) e^{\varepsilon x} + \frac{\theta_b}{\left(\frac{\left(e^{-\varepsilon L} - \frac{\lambda_g}{L_g\,\lambda_{fin}\,\varepsilon} e^{-\varepsilon L}\right)}{\left(\frac{\lambda_g}{L_g\,\lambda_{fin}\,\varepsilon} e^{\varepsilon L} + e^{\varepsilon L}\right)} + 1\right)} e^{-\varepsilon x}$$

$$\frac{\theta}{\theta_b} = \left(1 - \frac{1}{\left(\frac{\left(e^{-\varepsilon L} - \frac{\lambda_g}{L_g\,\lambda_{fin}\,\varepsilon} e^{-\varepsilon L}\right)}{\left(\frac{\lambda_g}{L_g\,\lambda_{fin}\,\varepsilon} e^{\varepsilon L} + e^{\varepsilon L}\right)} + 1\right)}\right) e^{\varepsilon x} + \frac{1}{\left(\frac{\left(e^{-\varepsilon L} - \frac{\lambda_g}{L_g\,\lambda_{fin}\,\varepsilon} e^{-\varepsilon L}\right)}{\left(\frac{\lambda_g}{L_g\,\lambda_{fin}\,\varepsilon} e^{\varepsilon L} + e^{\varepsilon L}\right)} + 1\right)} e^{-\varepsilon x} \quad \text{(A.20)}$$

$$q_{fin} = q_{base} = -\lambda_{fin} A_c \left.\frac{dT}{dx}\right]_{x=0} = -\lambda_{fin} A_c \left.\frac{d\theta}{dx}\right]_{x=0} \quad \text{(A.21)}$$

$$\frac{d\theta}{dx} = \theta_b \varepsilon\left[\left(1 - \frac{1}{\left(\frac{\left(e^{-\varepsilon L} - \frac{\lambda_g}{L\,\lambda_{fin}\,\varepsilon} e^{-\varepsilon L}\right)}{\left(\frac{\lambda_g}{L_g\,\lambda_{fin}\,\varepsilon} e^{\varepsilon L} + e^{\varepsilon L}\right)} + 1\right)}\right) e^{\varepsilon x} - \frac{1}{\left(\frac{\left(e^{-\varepsilon L} - \frac{\lambda_g}{L_g\,\lambda_{fin}\,\varepsilon} e^{-\varepsilon L}\right)}{\left(\frac{\lambda_g}{L_g\,\lambda_{fin}\,\varepsilon} e^{\varepsilon L} + e^{\varepsilon L}\right)} + 1\right)} e^{-\varepsilon x}\right] \quad \text{(A.22)}$$

$$\left(\frac{d\theta}{dx}\right)_{x=0} = \theta_b \varepsilon\left[\left(1 - \frac{1}{\left(\frac{\left(e^{-\varepsilon L} - \frac{\lambda_g}{L_g\,\lambda_{fin}\,\varepsilon} e^{-\varepsilon L}\right)}{\left(\frac{\lambda_g}{L_g\,\lambda_{fin}\,\varepsilon} e^{\varepsilon L} + e^{\varepsilon L}\right)} + 1\right)}\right) e^{\varepsilon x} - \frac{1}{\left(\frac{\left(e^{-\varepsilon L} - \frac{\lambda_g}{L_g\,\lambda_{fin}\,\varepsilon} e^{-\varepsilon L}\right)}{\left(\frac{\lambda_g}{L_g\,\lambda_{fin}\,\varepsilon} e^{\varepsilon L} + e^{\varepsilon L}\right)} + 1\right)} e^{-\varepsilon x}\right]_{x=0}$$

$$\left(\frac{d\theta}{dx}\right)_{x=0} = \theta_b \varepsilon\left[\left(1 - \frac{1}{\left(\frac{\left(e^{-\varepsilon L} - \frac{\lambda_g}{L\,\lambda_{fin}\,\varepsilon} e^{-\varepsilon L}\right)}{\left(\frac{\lambda_g}{L_g\,\lambda_{fin}\,\varepsilon} e^{\varepsilon L} + e^{\varepsilon L}\right)} + 1\right)}\right) - \frac{1}{\left(\frac{\left(e^{-\varepsilon L} - \frac{\lambda_g}{L\,\lambda_{fin}\,\varepsilon} e^{-\varepsilon L}\right)}{\left(\frac{\lambda_g}{L_g\,\lambda_{fin}\,\varepsilon} e^{\varepsilon L} + e^{\varepsilon L}\right)} + 1\right)}\right] \quad \text{(A.23)}$$

From equations A.21 and A.23,

$$q_{fin} = -\lambda_{fin} A_c \theta_b \varepsilon [(1 - \frac{1}{\left(\frac{\left(e^{-\varepsilon L} - \frac{\lambda_g}{L\,\lambda_{fin}\,\varepsilon} e^{-\varepsilon L}\right)}{\left(\frac{\lambda_g}{L_g\,\lambda_{fin}\,\varepsilon} e^{\varepsilon L} + e^{\varepsilon L}\right)} + 1\right)}) - \frac{1}{\left(\frac{\left(e^{-\varepsilon L} - \frac{\lambda_g}{L\,\lambda_{fin}\,\varepsilon} e^{-\varepsilon L}\right)}{\left(\frac{\lambda_g}{L_g\,\lambda_{fin}\,\varepsilon} e^{\varepsilon L} + e^{\varepsilon L}\right)} + 1\right)}] \quad \text{(A.24)}$$

Heat transfer through the rectangular fin (W) =

$$q_{fin} = -\lambda_{fin} (\omega\,\tau) \theta_b \varepsilon [(1 - \frac{1}{\left(\frac{\left(e^{-\varepsilon L} - \frac{\lambda_g}{L_g\,\lambda_{fin}\,\varepsilon} e^{-\varepsilon L}\right)}{\left(\frac{\lambda_g}{L_g\,\lambda_{fin}\,\varepsilon} e^{\varepsilon L} + e^{\varepsilon L}\right)} + 1\right)}) - \frac{1}{\left(\frac{\left(e^{-\varepsilon L} - \frac{\lambda_g}{L_g\,\lambda_{fin}\,\varepsilon} e^{-\varepsilon L}\right)}{\left(\frac{\lambda_g}{L_g\,\lambda_{fin}\,\varepsilon} e^{\varepsilon L} + e^{\varepsilon L}\right)} + 1\right)}] \quad \text{(A.25)}$$

A.2 Heat transfer through the trapezoidal fin

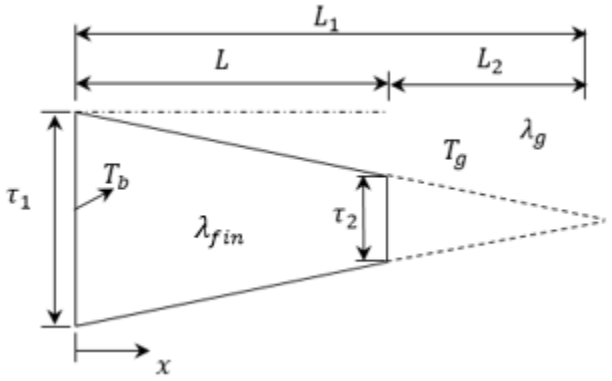

Figure A.2: Top view of trapezoidal fin

A_{cond} = Surface area of the element (m2)

A_x = Cross-section area at distance (m2)

τ = Fin width at the base (m)

L= Fin length (m)

L_2= Length from the end of the fin to the cross point of the two lines (m)

$L_1 = L + L_2$ (m)

L_g = Grout thickness (m)

P = Perimeter (m)

q_{cond} = Heat transfer (conduction) from the surface of the element to the surrounding grout (W)

q_{fin} = Conduction heat flow at the base of the fin (W)

$q_x =$ Conduction heat flow rate in the element (W)

q_{x+dx} = Conduction heat flow rate out the element (W)

T = Temperature of element (ºC)

T_b= Base temperature (ºC)

T_g= Grout temperature (ºC)

T_L= Fin temperature at length L (ºC)

ω = Fin thickness [depth] (m)

τ_1 = Fin width at the base (m)

τ_2 = Fin width at $x = L$ (m)

λ_{fin} = Fin thermal conductivity (W/ m. K)

λ_g = Grout thermal conductivity (W/ m. K)

$A_x = \left(\tau_1 \frac{\omega}{L_1}\right) x$

Heat flow rate into the element is,

$$q_x = -\lambda_{fin}\, A_c \frac{dT}{dx} \qquad \text{(A.26)}$$

The conduction heat flow rate in and out of the element,

$$q_x = q_{x+dx} + 2\, q_{cond} \qquad \text{(A.27)}$$

$$q_{x+dx} = q_x + \frac{d}{dx}(q_x)dx \qquad \text{(A.28)}$$

q_{cond} = Conduction heat transfer from the surface of element to the grout,

From equation (A.27)

$$q_x = q_x + q_{dx} + 2\, q_{cond}$$

$$q_{dx} + 2\, q_{cond} = 0 \qquad \text{(A.29)}$$

Substituting the values of q_{dx} and q_{cond}into equation (A.29),

$$\frac{d}{dx}\left(-\lambda_{fin}\, A_x \frac{dT}{dx}\right) dx + 2\left(\frac{\lambda_g}{L_g} P dx\right) dT = 0 \qquad \text{(A.30)}$$

Dividing the equation A.30 by dx

$$\frac{d}{dx}\left(A_x \frac{dT}{dx}\right) - 2\left(\frac{\lambda_g\, P}{\lambda_{fin}\, L_g}\, dT\right) = 0 \qquad \text{(A.31)}$$

$$A_x \frac{d^2T}{dx^2} + \frac{dT}{dx}\frac{dA_x}{dx} - 2\frac{\lambda_g\, P}{\lambda_{fin}\, L_g}\, dT = 0 \qquad \text{(A.32)}$$

$A_x = \left(\tau_1 \frac{\omega}{L_1}\right) x$, and A_{cond}(conduction area) = perimeter of the fin × length of element, when $\omega >> \tau_x$, $P_x = (\omega + \tau_x) \approx 2\omega$ and is constant.

$$\left(\tau_1 \frac{\omega}{L_1}\right) x\, \frac{d^2T}{dx^2} + \left(\tau_1 \frac{\omega}{L_1}\right) \frac{dT}{dx} - 2\frac{\lambda_g\, 2\omega}{\lambda_{fin}\, L_g}\, dT = 0 \qquad \text{(A.33)}$$

Dividing the equation by $\tau_1 \frac{\omega}{L_1}$

$$x\ \frac{d^2T}{dx^2} + \frac{dT}{dx} - 2\frac{\lambda_g\ L_1}{\lambda_{fin}\,\tau_1\,L_g}\ dT = 0 \qquad \text{(A.34)}$$

Where $\varepsilon = \frac{2\,\lambda_g\ L_1}{\lambda_{fin}\,\tau_1\,L_g}$

Substituting the value of m into equation (A.34),

$$x\ \frac{d^2T}{dx^2} + \frac{dT}{dx} - \varepsilon\ dT = 0 \qquad \text{(A.35)}$$

Let $\theta = T - T_{g,} \rightarrow \frac{dT}{dx} = \frac{d\theta}{dx}$ and $\frac{d^2T}{dx^2} = \frac{d^2\theta}{dx^2}$

$$\frac{d^2\theta}{dx^2} + \frac{1}{x}\frac{d\theta}{dx} - \frac{\varepsilon}{x}\ \theta = 0 \qquad \text{(A.36)}$$

Equation (A.36) is modified Bessel equation, and general solution of homogeneous equations is,

$$\theta = C_1 I_0\left(2\sqrt{\varepsilon x}\right) + C_2 K_0(2\sqrt{\varepsilon x}) \qquad \text{(A.37)}$$

Boundary conditions

At $x = L_1$, $\theta(L_1) = T_b - T_g \equiv \theta_b$

$$\theta_b = C_1 I_0\left(2\sqrt{\varepsilon L_1}\right) + C_2 K_0(2\sqrt{\varepsilon L_1}) \qquad \text{(A.38)}$$

Where

$I_v(x)$ is modified Bessel function of the first kind

$K_v(x)$ is modified Bessel function of the second kind

At $x = L_2$, $\left(\frac{d\theta}{dx}\right)_{x=L_2}$

$$\theta = C_1 I_0\left(2\sqrt{\varepsilon x}\right) + C_2 K_0(2\sqrt{\varepsilon x}) \qquad \text{(A.39)}$$

$$\frac{d\theta}{dx} = C_1 I_0\left(2\sqrt{\varepsilon x}\right)2\frac{\varepsilon}{2\sqrt{\varepsilon x}} + C_2 K_0(2\sqrt{\varepsilon x})2\frac{\varepsilon}{2\sqrt{\varepsilon x}} \qquad \text{(A.40)}$$

$$\left(\frac{d\theta}{dx}\right)_{x=L_2} = C_1 I_0\left(2\sqrt{\varepsilon L_2}\right)2\frac{\varepsilon}{2\sqrt{\varepsilon L_2}} + C_2 K_0(2\sqrt{\varepsilon L_2})2\frac{\varepsilon}{2\sqrt{\varepsilon L_2}} \qquad \text{(A.41)}$$

$$0 = C_1 I_1\left(2\sqrt{\varepsilon L_2}\right)2\sqrt{\varepsilon}\frac{1}{2\sqrt{L_2}} - C_2 K_1(2\sqrt{\varepsilon L_2})2\sqrt{\varepsilon}\frac{1}{2\sqrt{L_2}} \qquad \text{(A.42)}$$

Dividing the equation by $2\sqrt{\varepsilon}\frac{1}{2\sqrt{L_2}}$ and the equation (A.42) become

$$0 = C_1 I_1\left(2\sqrt{\varepsilon L_2}\right) - C_2 K_1(2\sqrt{\varepsilon L_2}) \qquad \text{(A.43)}$$

Equation (A.38) subtract equation (A.43)

$$\theta_b - C_1[I_0\left(2\sqrt{\varepsilon L_1}\right) - I_1\left(2\sqrt{\varepsilon L_2}\right)] = C_2[K_0\left(2\sqrt{\varepsilon L_1}\right) + K_1(2\sqrt{\varepsilon L_2})] \qquad \text{(A.44)}$$

$$C_2 = \frac{\theta_b - C_1[I_0\left(2\sqrt{\varepsilon L_1}\right) - I_1\left(2\sqrt{\varepsilon L_2}\right)]}{[K_0\left(2\sqrt{\varepsilon L_1}\right) + K_1(2\sqrt{\varepsilon L_2})]}$$

By substituting the value of C_2 into equation (A.43)

$$\theta_b = C_1 \frac{I_1\left(2\sqrt{\varepsilon L_2}\right)[K_0\left(2\sqrt{\varepsilon L_1}\right)+K_1(2\sqrt{\varepsilon L_2})]}{K_1(2\sqrt{\varepsilon L_2})} + C_1[I_0\left(2\sqrt{\varepsilon L_1}\right) - I_1\left(2\sqrt{\varepsilon L_2}\right)] \quad \text{(A.45)}$$

$$\theta_b = C_1 \frac{I_1\left(2\sqrt{\varepsilon L_2}\right)K_0\left(2\sqrt{\varepsilon L_1}\right) + K_1\left(2\sqrt{\varepsilon L_2}\right)I_0\left(2\sqrt{\varepsilon L_1}\right)}{K_1\left(2\sqrt{\varepsilon L_2}\right)}$$

$$C_1 = \frac{\theta_b\, K_1\left(2\sqrt{\varepsilon L_2}\right)}{I_1\left(2\sqrt{\varepsilon L_2}\right)K_0\left(2\sqrt{\varepsilon L_1}\right) + K_1\left(2\sqrt{\varepsilon L_2}\right)I_0\left(2\sqrt{\varepsilon L_1}\right)}$$

Substituting the value of C_1 into equation (A.43)

$$0 = \frac{\theta_b\, K_1\left(2\sqrt{\varepsilon L_2}\right)}{I_1\left(2\sqrt{\varepsilon L_2}\right)K_0\left(2\sqrt{\varepsilon L_1}\right) + K_1\left(2\sqrt{\varepsilon L_2}\right)I_0\left(2\sqrt{\varepsilon L_1}\right)} I_1\left(2\sqrt{\varepsilon L_2}\right) - C_2 K_1(2\sqrt{\varepsilon L_2})$$

$$C_2 = \frac{\theta_b\, K_1\left(2\sqrt{\varepsilon L_2}\right)}{I_1\left(2\sqrt{\varepsilon L_2}\right)K_0\left(2\sqrt{\varepsilon L_1}\right) + K_1\left(2\sqrt{\varepsilon L_2}\right)I_0\left(2\sqrt{\varepsilon L_1}\right)K_1(2\sqrt{\varepsilon L_2}} I_1\left(2\sqrt{\varepsilon L_2}\right)$$

$$C_2 = \frac{\theta_b}{I_1\left(2\sqrt{\varepsilon L_2}\right)K_0\left(2\sqrt{\varepsilon L_1}\right)+K_1\left(2\sqrt{\varepsilon L_2}\right)I_0\left(2\sqrt{\varepsilon L_1}\right)} I_1\left(2\sqrt{\varepsilon L_2}\right)$$

Substituting the value of C_1 and C_2 into equation (A.39)

$$\theta = \frac{\theta_b\, K_1\left(2\sqrt{\varepsilon L_2}\right)}{I_1\left(2\sqrt{mL_2}\right)K_0\left(2\sqrt{mL_1}\right) + K_1\left(2\sqrt{\varepsilon L_2}\right)I_0\left(2\sqrt{\varepsilon L_1}\right)} I_0\left(2\sqrt{\varepsilon x}\right) + \frac{\theta_b}{I_1\left(2\sqrt{\varepsilon L_2}\right)K_0\left(2\sqrt{\varepsilon L_1}\right) + K_1\left(2\sqrt{\varepsilon L_2}\right)I_0\left(2\sqrt{\varepsilon L_1}\right)} I_1\left(2\sqrt{\varepsilon L_2}\right)K_0(2\sqrt{\varepsilon x})$$

$$\frac{\theta}{\theta_b} = \frac{K_1\left(2\sqrt{\varepsilon L_2}\right)I_0\left(2\sqrt{\varepsilon x}\right)+I_1\left(2\sqrt{\varepsilon L_2}\right)K_0(2\sqrt{\varepsilon x})}{I_1\left(2\sqrt{\varepsilon L_2}\right)K_0\left(2\sqrt{\varepsilon L_1}\right)+K_1\left(2\sqrt{\varepsilon L_2}\right)I_0\left(2\sqrt{\varepsilon L_1}\right)} \quad \text{(A.46)}$$

$$q_{fin} = (\lambda_{fin} A_{base} \frac{dT}{dx})_{x=L_1} \quad \text{(A.47)}$$

$$A_{base} = \tau_1 \omega,\ \varepsilon = 2\frac{\lambda_g\ L_1}{\lambda_{fin}\tau_1\ L_g}$$

$$\frac{dT}{dx} = \frac{d\theta}{dx} = \left[\frac{d}{dx}\theta_b \frac{K_1\left(2\sqrt{\varepsilon L_2}\right)I_0\left(2\sqrt{\varepsilon x}\right) + I_1\left(2\sqrt{\varepsilon L_2}\right)K_0(2\sqrt{\varepsilon x})}{I_1\left(2\sqrt{\varepsilon L_2}\right)K_0\left(2\sqrt{\varepsilon L_1}\right) + K_1\left(2\sqrt{\varepsilon L_2}\right)I_0\left(2\sqrt{\varepsilon L_1}\right)}\right]_{x=L_1}$$

$$\frac{d\theta}{dx} = \theta_b \frac{1}{I_1\left(2\sqrt{\varepsilon L_2}\right)K_0\left(2\sqrt{\varepsilon L_1}\right) + K_1\left(2\sqrt{\varepsilon L_2}\right)I_0\left(2\sqrt{\varepsilon L_1}\right)}\left[\frac{d}{dx}K_1\left(2\sqrt{\varepsilon L_2}\right)I_0\left(2\sqrt{\varepsilon x}\right) + I_1\left(2\sqrt{\varepsilon L_2}\right)K_0(2\sqrt{\varepsilon x})\right]_{x=L_1}$$

Where $\frac{d}{dx}I_0(x) = +I_1(x), \frac{d}{dx}K_0(x) = -K_1(x)$ [112]

$$\frac{d}{dx}\left[K_1\left(2\sqrt{\varepsilon L_2}\right)I_0\left(2\sqrt{\varepsilon x}\right)\right] = \left[K_1\left(2\sqrt{\varepsilon L_2}\right)I_1\left(2\sqrt{\varepsilon x}\right)\times 2\sqrt{\varepsilon}\,\frac{1}{2\sqrt{x}}\right]_{x=L_1} = K_1\left(2\sqrt{\varepsilon L_2}\right)I_1\left(2\sqrt{\varepsilon L_1}\right)\frac{\sqrt{\varepsilon}}{\sqrt{L_1}}$$

$$\frac{d}{dx}\left[I_1\left(2\sqrt{\varepsilon L_2}\right)K_0\left(2\sqrt{\varepsilon x}\right)\right] = \left[-I_1\left(2\sqrt{\varepsilon L_2}\right)K_1\left(2\sqrt{\varepsilon x}\right)\times 2\varepsilon\,\frac{1}{2\sqrt{x}}\right]_{x=L_1} =$$

$$-I_1\left(2\sqrt{\varepsilon L_2}\right)K_1\left(2\sqrt{L_1}\right)\frac{\sqrt{\varepsilon}}{\sqrt{L_1}}$$

$$\left(\frac{d\theta}{dx}\right)_{x=L_1} = \theta_b\,\frac{K_1\left(2\sqrt{\varepsilon L_2}\right)I_1\left(2\sqrt{\varepsilon L_1}\right)\frac{\sqrt{\varepsilon}}{\sqrt{L_1}} - I_1\left(2\sqrt{\varepsilon L_2}\right)K_1\left(2\sqrt{L_1}\right)\frac{\sqrt{\varepsilon}}{\sqrt{L_1}}}{I_1\left(2\sqrt{\varepsilon L_2}\right)K_0\left(2\sqrt{\varepsilon L_1}\right)+K_1\left(2\sqrt{\varepsilon L_2}\right)I_0\left(2\sqrt{\varepsilon L_1}\right)}$$

$$\left(\frac{d\theta}{dx}\right)_{x=L_1} = \theta_b\,\frac{\sqrt{\varepsilon}}{\sqrt{L_1}}\,\frac{K_1\left(2\sqrt{\varepsilon L_2}\right)I_1\left(2\sqrt{\varepsilon L_1}\right) - I_1\left(2\sqrt{\varepsilon L_2}\right)K_1\left(2\sqrt{\varepsilon L_1}\right)}{I_1\left(2\sqrt{\varepsilon L_2}\right)K_0\left(2\sqrt{\varepsilon L_1}\right)+K_1\left(2\sqrt{\varepsilon L_2}\right)I_0\left(2\sqrt{\varepsilon L_1}\right)}$$

Heat transfer through the trapezoidal fin (W) =

$$q_{fin} = \lambda_{fin}\theta_b\tau_1\omega\,\frac{\sqrt{\varepsilon}}{\sqrt{L_1}}\,\frac{K_1\left(2\sqrt{\varepsilon L_2}\right)I_1\left(2\sqrt{\varepsilon L_1}\right) - I_1\left(2\sqrt{\varepsilon L_2}\right)K_1\left(2\sqrt{\varepsilon L_1}\right)}{I_1\left(2\sqrt{\varepsilon L_2}\right)K_0\left(2\sqrt{\varepsilon L_1}\right)+K_1\left(2\sqrt{\varepsilon L_2}\right)I_0\left(2\sqrt{\varepsilon L_1}\right)} \qquad \text{(A.48)}$$

A.3 Example calculations

A.3.1 Heat transfer for the rectangular fin

Table A.1: Geometrical dimensions and thermal conductivity of rectangular fin and grout

Base temperature (T_b)	49 ºC
Grout temperature (T_g)	20 ºC
Fin thickness (ω)	150 mm
Grout thickness (L_g)	5 mm
Fin length (L)	8 mm
Fin width (τ)	10 mm
Fin thermal conductivity (λ_f)	400 W/ m. K
Grout thermal conductivity (λ_f)	4 W/ m. K

As shown in equation (A.14)

$$\theta_b = T_b - T_g = 49 - 20 = 29\ ^{o}\text{C}$$

$$A_c = \omega\,\tau = 0.15 \times 0.01 = 0.0015\ \text{m}^2$$

$$\varepsilon = \sqrt{2\frac{\lambda_g}{\lambda_f L_g \tau}} = (2 \times 4)/ (400 \times 0.05 \times 0.01) = 20$$

$e^{-\varepsilon L}$	$e^{\varepsilon L}$	$\frac{\lambda_g}{L_g \lambda_f \varepsilon} e^{-\varepsilon L}$	$\frac{\lambda_g}{\lambda_f L \varepsilon} e^{\varepsilon L}$	$\frac{\lambda_g}{\lambda_f L \varepsilon} e^{\varepsilon L} + e^{mL}$	$\frac{\lambda_g}{\lambda_f L \varepsilon} e^{-\varepsilon L} - e^{-\varepsilon L}$
0.8187	1.1735	0.081873	0.117351	1.290862	0.736858

$$[(1 - \frac{1}{\left(\frac{\left(e^{-\varepsilon L} - \frac{\lambda_g}{L_g \lambda_f \varepsilon} e^{-\varepsilon L}\right)}{\left(\frac{\lambda_g}{L_g \lambda_f \varepsilon} e^{\varepsilon L} + e^{\varepsilon L}\right)} + 1\right)}) - \frac{1}{\left(\frac{\left(e^{-\varepsilon L} - \frac{\lambda_g}{L_g \lambda_f \varepsilon} e^{-\varepsilon L}\right)}{\left(\frac{\lambda_g}{L_g \lambda_f \varepsilon} e^{\varepsilon L} + e^{\varepsilon L}\right)} + 1\right)}] = -0.27322$$

As shown in equation (A.25)

$$q_{fin} = -\lambda_f (\omega\, \tau) \theta_b \varepsilon [(1 - \frac{1}{\left(\frac{\left(e^{-\varepsilon L} - \frac{\lambda_g}{L_g \lambda_f \varepsilon} e^{-\varepsilon L}\right)}{\left(\frac{\lambda_g}{L_g \lambda_f \varepsilon} e^{\varepsilon L} + e^{\varepsilon L}\right)} + 1\right)}) - \frac{1}{\left(\frac{\left(e^{-\varepsilon L} - \frac{\lambda_g}{L_g \lambda_f \varepsilon} e^{-\varepsilon L}\right)}{\left(\frac{\lambda_g}{L_g \lambda_f \varepsilon} e^{\varepsilon L} + e^{\varepsilon L}\right)} + 1\right)}]$$

Heat transfer through the rectangular fin =

$$q_{fin} = -400 \times 0.0015 \times 29 \times 20 \times -0.27322 = 95 \text{ W.}$$

A.3.2 Heat transfer for the trapezoidal fin

Table A.2: Geometrical dimensions and thermal conductivity of trapezoidal fin and grout

Base temperature (T_b)	49 ºC
Grout temperature (T_g)	20 ºC
Fin thickness (ω)	150 mm
Grout thickness (L_g)	5 mm
Fin length (L)	8 mm
Fin width at the base (τ_1)	10 mm
Fin width at $x = L$ (τ_2)	4 mm
Fin thermal conductivity (λ_{fin})	400 W/ m. K
Grout thermal conductivity (λ_g)	4 W/ m. K

L_2= 5.333 mm

$L_1 = L + L_2$ = 13.333 mm

$\varepsilon = \frac{2\,\lambda_g\, L_1}{\lambda_{fin}\, \tau_1\, L_g}$ = (2 × 4 × 0.01333)/ (400 × 0.01 × 0.005) = 5.333

Where

$2\sqrt{\varepsilon L_2}$ = 0.337299, $2\sqrt{\varepsilon L_1}$= 0.533332, and $\frac{\sqrt{\varepsilon}}{\sqrt{L_1}}$ = 20

The values of $I_1(2\sqrt{\varepsilon L_2}), K_1(2\sqrt{\varepsilon L_2}), I_0(2\sqrt{\varepsilon L_1}), I_1(2\sqrt{\varepsilon L_1}), K_0(2\sqrt{\varepsilon L_1}), and\ K_1(2\sqrt{\varepsilon L_1})$

From Appendix B (see Table B.5) [113]

$2\sqrt{\varepsilon L_2}$	$I_0(2\sqrt{\varepsilon L_2})$	$I_1(2\sqrt{\varepsilon L_2})$	$K_0(2\sqrt{\varepsilon L_2})$	$K_1(2\sqrt{\varepsilon L_2})$
0.337299		0.119714		4.065881

$2\sqrt{\varepsilon L_1}$	$I_0(2\sqrt{\varepsilon L_1})$	$I_1(2\sqrt{\varepsilon L_1})$	$K_0(2\sqrt{\varepsilon L_1})$	$K_1(2\sqrt{\varepsilon L_1})$
0.533332	0.632001	0.1604	1.4998702	2.668839

$$\theta_b = T_b - T_g = 49 - 20 = 29\ ^{o}\text{C}$$

$$q_{fin} = \lambda_{fin}\theta_b\tau_1\omega\frac{\sqrt{\varepsilon}}{\sqrt{L_1}}\frac{K_1(2\sqrt{\varepsilon L_2})\,I_1(2\sqrt{\varepsilon L_1}) - I_1(2\sqrt{\varepsilon L_2})\,K_1(2\sqrt{\varepsilon L_1})}{I_1(2\sqrt{\varepsilon L_2})\,K_0(2\sqrt{\varepsilon L_1}) + K_1(2\sqrt{\varepsilon L_2})\,I_0(2\sqrt{\varepsilon L_1})} \qquad \text{(A.48)}$$

$$\frac{K_1(2\sqrt{\varepsilon L_2})\,I_1(2\sqrt{\varepsilon L_1}) - I_1(2\sqrt{\varepsilon L_2})\,K_1(2\sqrt{\varepsilon L_1})}{I_1(2\sqrt{\varepsilon L_2})\,K_0(2\sqrt{\varepsilon L_1}) + K_1(2\sqrt{\varepsilon L_2})\,I_0(2\sqrt{\varepsilon L_1})} = 0.0121012$$

Heat transfer through the trapezoidal fin =

$$q_{fin} = 400 \times 0.0015 \times 29 \times 20 \times 0.121012 = 42.1\ \text{W}.$$

A.4 Optimum length of the fin (L)

For the rectangular fin different lengths (see Table A.4) are substituted into the equation (A.25) to find the optimum length to be used.

Table A. 3: Values q_fin of for different fin lengths (L*)*

Fin Length [L] (m)	0.005	0.008	0.048	0.088	0.128	0.168	0.208	0.248	0.288	0.328	0.368	0.408	0.488
q_{fin}(W)	85.3	95.1	205.9	276.1	313.7	324.6	332.2	340.8	346.5	347.3	347.7	347.8	347.9

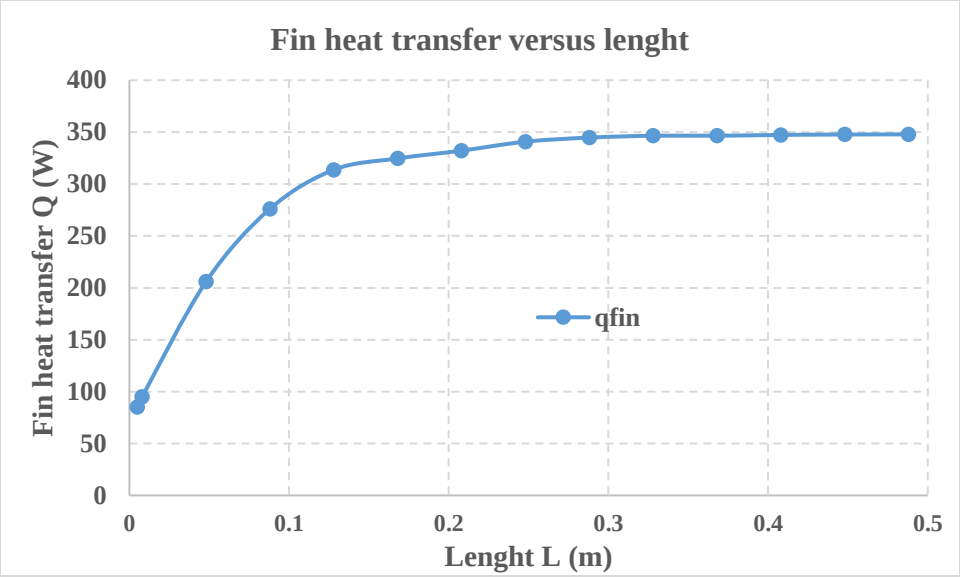

Figure A.3: Heat transfer through the fin as a function of fin length

Based on the observations presented in Figure A.3, an optimum fin length of 0.08 m was chosen for this investigation.

Appendix B

Effects of increasing depth of VGHE on the thermal performance

Esen and Inalli (2009) conducted three TRTs with three different depths (30 m, 60 m, and 90 m) to estimate the thermal performance of the single U-Tube VGHE. The obtained results from the experimental study for the cooling and heating modes show that the borehole heat exchanger with a depth of 90 had the strongest performance, but the optimized depth considering the cost was 60 m with a coefficient of performance (COP) of approximately 3 (see Table B.1 and Figure C.1) [95].

Table B.1: Variation of COP as a function of depth [95]

Depth (m)	Monthly mean value of COP	
	Cooling mode	Heating mode
30	3.37	1.93
60	3.85	2.37
90	4.33	3.03

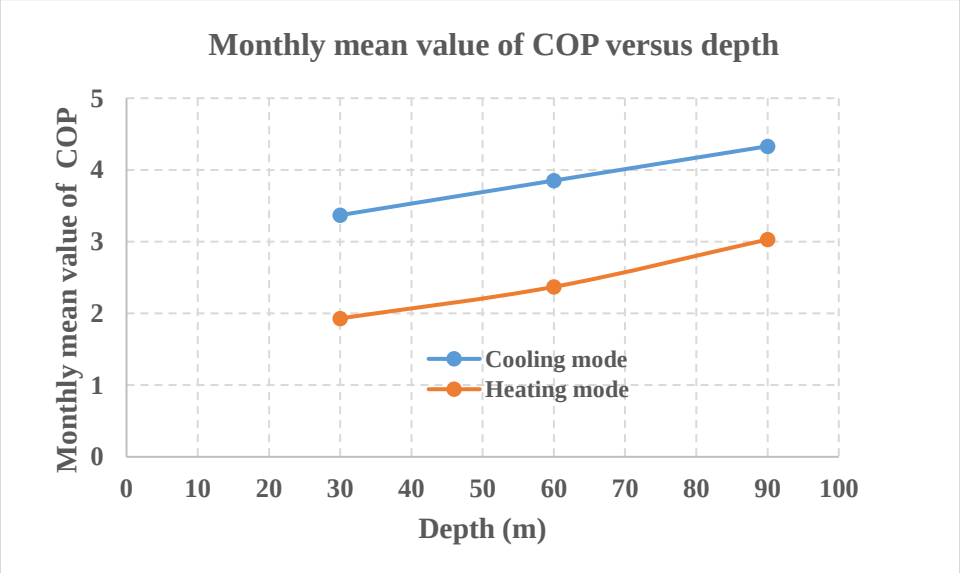

Figure B.1: Variation of COP as a function of depth [95]

The outlet water temperature in winter and summer increases and decreases with an increase the VGHE depth. Increasing the VGHE depth also leads to increased energy consumption of GSHP and a higher cost. The VGHE depths of 50 to 100 m have been widely used during the last eight years, followed by the depths of 20 to 50 m [96].

Appendix C

The time (t) chosen for the calculation of slope on the logarithmic plot was determined based the relationship below:

Table C.1: Borehole radius and material thermal properties of the silica sand

Silica sand	
Density (ρ)	1700 kg/ m^3
Specific heat (C_p)	750 J/ kg. K
Thermal conductivity (λ)	2.42 W/ m. K
Borehole radius (r)	0.041 m

Thermal diffusivity (α) = $\frac{\lambda}{\rho\, C_p} = \frac{2.42}{1700 \times 750} = 1.89804E-06 \frac{m^2}{sec}$

It is reported that the maximum error resulting from using the value of $\frac{\propto \times t}{r^2} \geq 5$ is 10%.

$$t = \frac{5 \times 0.041 \times 0.041}{1.89804E-06 \times 60} \approx 73\ min$$